

# Virus Imprinted Particles



## Inauguraldissertation

zur

Erlangung der Würde eines Doktors der Philosophie  
vorgelegt der  
Philosophisch-Naturwissenschaftlichen Fakultät  
der Universität Basel

von

**Alessandro Cumbo**

aus Italien

Basel, 2013

Genehmigt von der Philosophisch-Naturwissenschaftlichen Fakultät der Universität  
Basel auf Antrag von

Prof. Dr. Wolfgang Meier

Prof. Dr. Thomas R. Ward

Basel, den 17 September 2013

Prof. Dr. Jörg Schibler

Dekan



*A Totò e Carmelina*



# Table of Contents

<b>Abbreviations</b> .....	<b>1</b>
<b>Abstract</b> .....	<b>3</b>
<b>Introduction</b> .....	<b>6</b>
<b>Molecular imprinting: an historical point of view</b> .....	<b>9</b>
Antibody formation theories .....	10
Selective theory .....	11
Instructional theory .....	12
Clonal selection hypothesis .....	13
From natural to synthetic antibody.....	13
<b>Molecular imprinting strategies</b> .....	<b>17</b>
Covalent imprinting .....	17
Non-covalent imprinting.....	18
Semi-covalent imprinting.....	19
<b>Macromolecular imprinting</b> .....	<b>20</b>
Protein-imprinted polymers .....	21
Virus imprinting .....	27
Overview of virus structures and classification .....	27
Virus-imprinted polymers.....	31
<b>Author’s critical view of MIP technology</b> .....	<b>36</b>
<b>Silica nanoparticles - SNPs</b> .....	<b>38</b>
Biosilica and biocompatibility .....	38
<b>References</b> .....	<b>42</b>
<b>Objective of the research</b> .....	<b>48</b>
<b>VIP synthesis and characterization</b> .....	<b>52</b>
<b>Virus imprinted particles – Concept</b> .....	<b>53</b>
Stöber silica nanoparticles.....	54
Model viruses .....	55
VIP synthesis .....	57
Organosilanes .....	58
<b>FESEM characterization</b> .....	<b>62</b>
Characterization of the VIPs <sub>AT</sub> .....	62
Kinetics of VIPs <sub>AT (TYMV)</sub> recognition layer growth.....	64
Characterization of the VIPs <sub>OM</sub> .....	66
Kinetics of the VIPs <sub>OM (TYMV)</sub> recognition layer growth .....	67
FESEM characterization of the VIPs <sub>COM</sub> .....	68
Kinetics of VIPs <sub>COM (TYMV)</sub> recognition layer growth .....	71
<b>Virus removal</b> .....	<b>73</b>
<b>SNPs amino modification and number of imprints</b> .....	<b>77</b>
<b>VIPs<sub>OM (TBSV)</sub> characterization and virus removal</b> .....	<b>79</b>

<b>Conclusion .....</b>	<b>80</b>
<b>References .....</b>	<b>82</b>
<b><i>VIP binding performance .....</i></b>	<b><i>84</i></b>
<b>Quantification techniques.....</b>	<b>85</b>
Sodium dodecyl sulfate polyacrylamide gel electrophoresis (SDS-PAGE) .....	85
Quantitative reverse transcription polymerase chain reaction (qRT-PCR).....	87
Enzyme-linked immunosorbent assay (ELISA) .....	90
<b>Batch rebinding assays .....</b>	<b>91</b>
Time course binding assays for VIPs <sub>AT (TYMV)</sub> and VIPs <sub>OM (TYMV)</sub> .....	91
Recognition layer thickness effect on VIP binding performance.....	95
Particles concentration effect.....	99
BSA concentration effect .....	100
Binding the virus to VIPs: scanning electron microscopy .....	101
Competition assay and matrix effect .....	102
<b>Proof of principle with VIPs<sub>OM (TBSV)</sub> .....</b>	<b>104</b>
<b>Conclusion .....</b>	<b>105</b>
<b>References .....</b>	<b>107</b>
<b><i>Conclusion and future direction .....</i></b>	<b><i>108</i></b>
<b><i>Experimental method .....</i></b>	<b><i>114</i></b>
Solvents, chemicals and kits .....	115
Organosilanes .....	115
Viruses .....	115
Silica nanoparticle synthesis .....	116
Virus imprinted particles – VIPs – synthesis .....	116
Virus removal.....	117
Scanning electron microscopy.....	117
Particles size measurement .....	118
Batch rebinding assay .....	118
Sodium dodecyl sulfate polyacrylamide gel electrophoresis (SDS-PAGE) .....	119
Quantitative reverse transcription polymerase chain reaction (qRT-PCR).....	120
Enzyme-linked immunosorbent assay (ELISA) .....	121
<b>References .....</b>	<b>122</b>
<b><i>Resume and list of contributions.....</i></b>	<b><i>124</i></b>
<b><i>Acknowledgements .....</i></b>	<b><i>128</i></b>

## Abbreviations

Aa	amino acid
APTES	3-aminopropyltriethoxysilane
APTMS	3-aminopropyltrimethoxysilane
AT	APTES and TEOS mixture
BHEAPTES	bis(2-hydroxyethyl)-3-aminopropyltriethoxysilane
BSA	bovine serum albumin
BTES	benzyltriethoxysilane
cDNA	complementary DNA
COM	complex organosilane mixture
CP	capsid protein
DAS-ELISA	double antibody sandwich ELISA
DNA	deoxyribonucleic acid
ds	double stranded
ELISA	enzyme-linked immunosorbent assay
FESEM	field emission scanning electron microscopy
HMTEOS	hydroxymethyltriethoxysilane
HRV	human rhinovirus
HS	human serum
HSA	human serum albumin
IBTES	isobutyltriethoxysilane
IgG	Immunoglobulin G
LOD	limit of detection
LPD	liquid-phase deposition
MIP	molecularly imprinted polymer
MSNP	mesoporous SNP
MW	molecular weight
NIPs	non-imprinted particles
OM	organosilane mixture
ORMOSIL	organically modified silanes
OTES	n-octyltriethoxysilane
pI	isoelectric point
PPOV	parapox ovis virus



PTES	propyltriethoxysilane
QCM	quartz crystal microbalance
qPCR	quantitative polymerase chain reaction
qRT-PCR	quantitative reverse transcription polymerase chain reaction
RNA	ribonucleic acid
s. e. m.	standard error mean
SDS	sodium dodecyl sulfate
SDS-PAGE	sodium dodecyl sulfate polyacrylamide gel electrophoresis
SNPs	silica nanoparticles
SPR	surface plasmon resonance
ss	single stranded
TBSV	tomato bushy stunt virus
TEOS	tetraethylorthosilicate
TMPS	trimethoxypropylsilane
TMV	tobacco mosaic virus
TNV	tobacco necrosis virus
TYMV	turnip yellow mosaic virus
UPTES	ureidopropyltriethoxysilane
VIPs	virus-imprinted particles

## Abstract

Living organisms are capable of identifying and neutralizing exogenous threats. Such a distinguishing feature, developed over millions of years of evolution, is achieved thanks to the immune system, and in particular through the molecular recognition capabilities of antibodies. Besides its importance for immunity, molecular recognition is also crucial to living organisms in other aspects, for example providing them with the possibility of controlling and regulating complex feedback to external and extracellular stimuli (*e.g.* olfactory stimulatory molecules or hormones through G protein-coupled membrane receptors).

Over the past decades, the possibility of creating man-made systems with molecular recognition properties similar to Nature has been a driving force in the design of recognition materials. Among possible target molecules, viruses represent one of the most challenging. Indeed, despite advancement achieved in the design of recognition materials for low molecular weight molecules, a synthetic strategy leading to the production of recognition materials targeting viruses remains challenging. In fact, the main stumbling blocks in the design of materials possessing virus recognition properties are the large size of the target and the fragility of its self-assembled architecture.

The presence of viruses in the environment (*e.g.* water, air and soil) or in biological fluids (*e.g.* blood, milk) is a concern for human health in various industrial sectors including pharmaceuticals, the environment, and agro-food. Different, tedious and energy-consuming strategies are currently applied to detect, inactivate or remove viruses, including quantitative polymerase chain reaction (qPCR), enzyme-linked immuno sorbent assay (ELISA), ultraviolet treatment and nanofiltration. The use of synthetic virus recognition material for the removal and detection of such pathogens could represent a new approach

that will benefit from the robustness of synthetic recognition materials, ease of production, and cost and time efficiency.

Following a surface molecular imprinting approach (*i.e.* template-assisted polymerization of specific monomers), it was developed a synthetic strategy to produce nanoparticulate organic/inorganic hybrids that recognize a major category of viruses (*i.e.* icosahedral non-enveloped) in aqueous environments at concentrations down to the picomolar range. The strategy is based on a sequential process that consists of covalent immobilization of an icosahedral virus at the surface of silica nanoparticles followed by the thickness-controlled growth of a polysilsesquioxane layer at the surface of the particles. A variety of organosilanes, sharing chemical similarities with lateral chains of natural amino acids, were used as building blocks to grow the polysilsesquioxane layer, named the recognition layer. After removing the virus, this procedure allowed the formation of negative, open replica imprints of the virus. The replication-imprinting process described goes beyond simple shape imprinting. Indeed, several experimental sources of evidence have suggested that the viruses were “self-sorting” the building blocks during recognition layer growth. Therefore, the formation of a chemical imprint of the surface of the virus was achieved.

In addition, the developed chemical strategy allows the preservation of the native structure of the 180-subunits viral assembly throughout the organosilanes polycondensation. The so-produced particles, named virus-imprinted particles or VIPs, were characterized by means of scanning electron microscopy. Their molecular recognition performances were tested in a batch rebinding study in aqueous conditions using enzyme-linked immunosorbent assay (ELISA) for virus quantification. Those binding assay results showed that VIPs specifically recognized the template virus. The control of the depth of the imprints provides control of the affinity of the produced VIPs for its target virus. The interaction assays ultimately confirmed that immobilized viruses were self-sorting the

organosilanes during the growth of the recognition layer, thus creating specific binding sites possessing both chemical- and size-recognition properties at the surfaces of the VIPs.

# 1

## Introduction

Molecular imprinting allows the creation of synthetic recognition units through template-assisted polymerization of specific functional monomers that results, after template removal, in a polymer that possesses binding sites for the original template. The produced polymer is named an MIP, which is the acronym for molecularly imprinted polymer.<sup>1</sup>

Historically, polymer scientists were inspired by the early instructional theory on antibody formation as postulated by Linus Pauling (*i.e.* "induced folding" of a polypeptide chain around the target antigen)<sup>2</sup> and by the "key and lock" hypothesis for enzyme – substrate association as theorized by Emil Fischer.<sup>3</sup>

Over the years, different synthetic strategies allowing the design of recognition materials have been developed. Therefore, strategies to produce MIPs were classified according to (i) the method of introducing monomers into the polymer recognition units,<sup>4-6</sup> (ii) the polymerization or polycondensation methods, including the polymer format (*e.g.* bulk, film, surface, beads),<sup>7</sup> and (iii) the kind of functional monomers applied.<sup>8,9</sup>

The use of small molecules as templates for the design of imprinted polymers has been extensively explored using non-covalent interactions between monomers and templates. Examples of templates include drugs,<sup>10</sup> nucleotides,<sup>11</sup> amino acids,<sup>12</sup> pesticides,<sup>13</sup> steroids,<sup>14</sup> and sugars.<sup>15</sup> The design of artificial binding sites for large bio-molecules represents a challenge in molecular imprinting.<sup>16</sup> This specific area, named macromolecular imprinting, targets biological templates with large molecular weights, ranging from proteins to bigger, self-assembled entities such as viruses. Owing to the relevance of the targets and the progress achieved in the field since 2005, the scientific community has significantly investigated macromolecular imprinting.<sup>17</sup>

The large size of bio-macromolecules limits the mass transfer of the template from inside the polymer, resulting in long and tedious template removal

procedures that could, in turn, damage a newly created binding site. The same mass transfer limitation occurs during template rebinding; thus, only the surface imprints of the polymer are accessible to the template. Additionally, it must be taken into account that, owing to the fragile nature of a bio-macromolecule, *i.e.* proteins and multimeric protein complexes, bio-friendly polymerization conditions have to be applied.<sup>18</sup>

Nevertheless, examples of molecularly imprinted materials for bio-molecular recognition were developed for hemoglobin<sup>19,20</sup> and lysozyme<sup>21</sup>. The most convincing examples were developed using surface imprinting approaches, whereby the imprints were limited to the polymer surface.<sup>20</sup> The imprinting of even bigger bio-molecular entities, such as viruses, is of great interest, with possible applications in purification, diagnostics and therapy. A few examples of MIPs specifically designed to target viruses were reported for picornaviruses,<sup>22</sup> tobacco mosaic virus<sup>23</sup> and the human rhinovirus.<sup>24</sup> Nevertheless, the performances of the materials produced are still fairly limited and virus imprinting remains a great challenge when the intent of the design is 'artificial antibodies' that bind viral particles.

## Molecular imprinting: an historical point of view

The first report in which polymer selective binding properties were attributed to a templating effect during polymerization was described by Polyakov in 1931.<sup>25</sup> Indeed, he described the enhanced adsorption of benzene and toluene on silica particles prepared in the presence of these molecules. In 1940, Pauling formulated the instructional theory on antibody formation (explained below). In order to experimentally prove his concept, one of Pauling's students, Dickey, reported on the selective adsorption of a dye (methyl orange) on inorganic silica prepared in the presence of the dye.<sup>26</sup> Despite these pioneering reports, the molecular imprinting concept was taken in consideration only in 1972, after the Wulff<sup>27</sup> and Klotz<sup>28</sup> parallel reports on the template selective binding of imprinted organic polymers. Later on, in the 80s and at the beginning of the 90s, Mosbach laid the foundation of the molecular imprinting technology as it is known today.<sup>10,29-31</sup> Indeed, by producing a methacrylic-based, imprinted polymer using theophylline and diazepam as template molecules, template selective binding in human serum was shown.<sup>10</sup>

Altogether, these milestone studies represented the early beginning of the molecularly imprinted polymer technology. From the 1993 Mosbach paper, indeed, more and more researchers were involved in the field of MIP technology and they produced more than 8400 peer-reviewed papers by 2012.<sup>7,32</sup>

A short overview of the early antibody formation theories, which are historically at the basis of molecular imprinting, follows here. Indeed, the instructional theory on antibody formation, as proposed by Pauling in 1940 and revealed as incorrect, represented the initial molecular imprinting concept that was further developed in material science.



## Antibody formation theories

The early theories of antibody formation, proposed in the first half of the 20<sup>th</sup> century, indirectly led to unexpected further progress in material sciences, initiating the field of MIP technology. Antibodies (Fig. 1.1) are a class of glycoproteins present in the extracellular environment and mainly involved in the humoral immunity of vertebrates (also named antibody-mediated immunity).<sup>33</sup> Antibodies possess selective recognition properties directed against a specific part of foreign substances and infectious agents (*e.g.* bacteria and viruses).

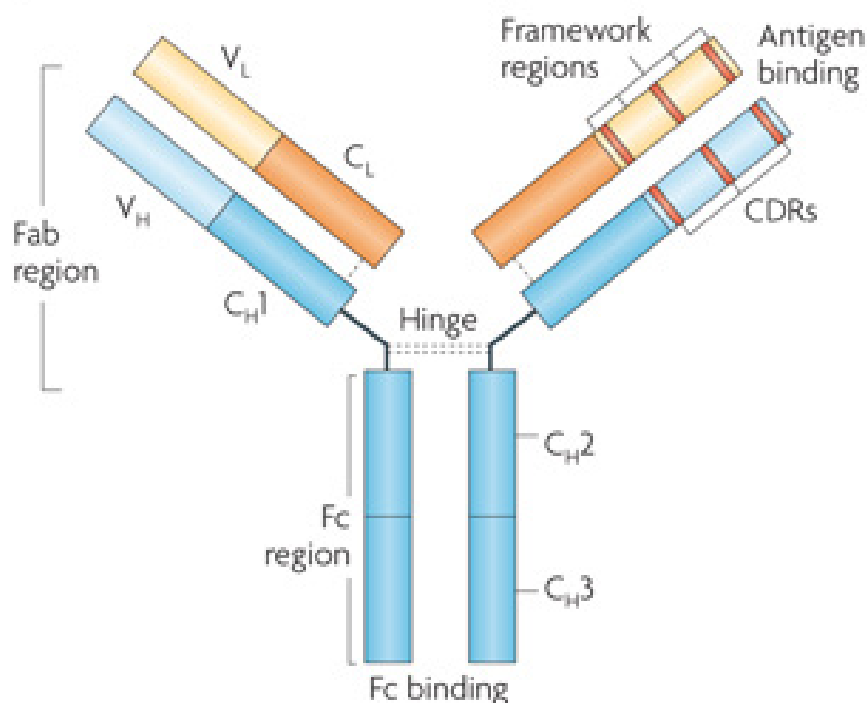


**Figure 1.1 | General antibody structure.** An antibody comprises two identical light chains and two identical heavy chains, associated by non-covalent and covalent bonding (disulfide bridges). Both light and heavy chains consist of two distinct regions: constant (C<sub>L</sub>: constant light chain; C<sub>H</sub>: constant heavy chain) and variable (V<sub>L</sub>: variable light chain; V<sub>H</sub>: variable heavy chain). The constant region of the heavy chain delineates the antibody class. The combination of the light and heavy variable regions forms the antigen binding sites. CDRs: complementarity-determining regions; Fab: fragment, antigen binding; Fc: fragment, crystallisable. [Reproduced with permission from ref. 34. Copyright 2010, the Nature publishing group]

Recognition of such foreign substances by antibodies leads to their identification and further neutralization by the immune system. Antigen is the term applied to the entire molecule as recognized by antibodies. The specific antibody binding portion of the antigen is named the epitope.<sup>33</sup> In an attempt to explain the initial experimental evidence on the role and formation of an antibody, two independent theories were confronted: (i) the instructional theory, which postulated the active involvement of the antigen during antibody formation; and (ii) the selective theory, which assumed that the antigen reacts with an already existing repertoire of antibodies.

### Selective theory

The first promoter of the selective theory of antibody formation was Paul Ehrlich, proposing the “side-chain theory” at the beginning of the 20<sup>th</sup> century.<sup>35</sup> By using Fischer’s “key and lock” theory,<sup>36</sup> Ehrlich proposed that a particular kind of cell (later identified to be the lymphocyte B cell) could, upon antigen stimulus, expose at its surface a class of side-chains responsible of binding and neutralizing the foreign antigen.<sup>37</sup> In addition, he claimed that these side-chains would, eventually, be released and freely circulate in the extracellular fluid as antibodies. Thus, he primarily described what he named the “magic bullet” (*magische Kugel*): a compound able to selectively target and destroy a disease-causing agent.<sup>38</sup>

Afterward, in 1935, the findings of Karl Landsteiner<sup>39-41</sup> slowed the progress of the selective theory. Indeed, by using azoproteins as the antigen (from horse serum), modified with different aliphatic chains and thus creating a series of unnatural compounds, he was able to induce an immune response and antibody production in rabbit. According to the selective theory, the direct consequence of these results would have been that a finite repertoire of existing antibodies would have recognized an infinite number of antigens, particularly unnatural

antigens. Landsteiner's results were thus in conflict with the selective theory, which temporarily lost the support of the scientific community.

### Instructional theory

To fill this conceptual gap, in 1940 Pauling proposed his instructional theory on the formation of antibodies.<sup>2</sup> He hypothesized that linear polypeptide chains would assume a final, tertiary conformation in the presence of an antigen, thus forming a complementary antibody specifically recognizing the template antigen (Fig 1.2).

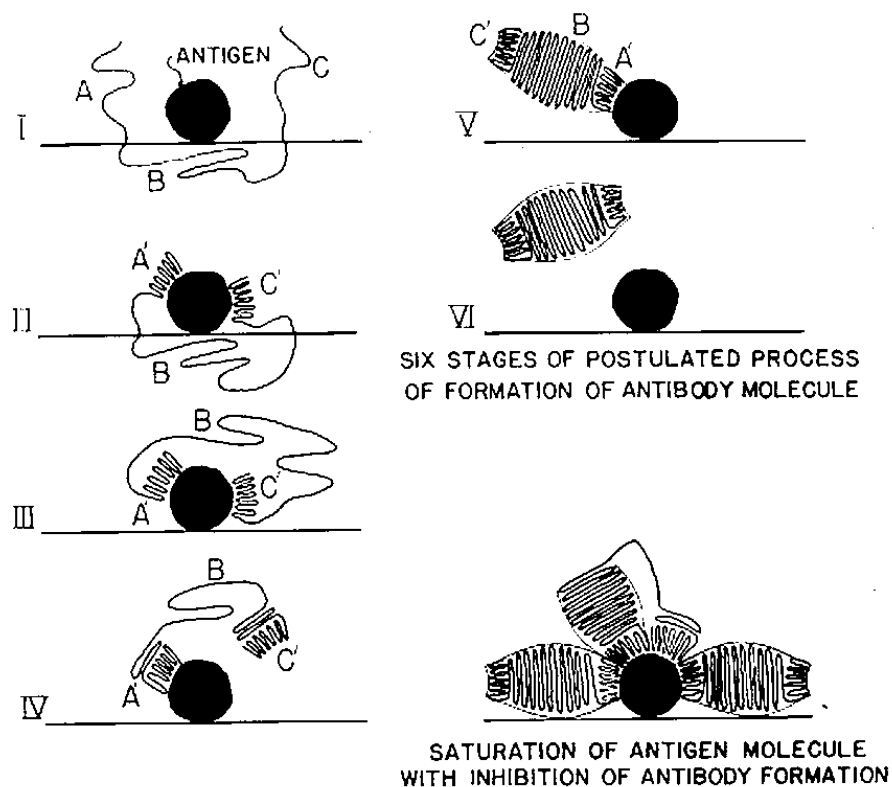


**Figure 1.2 | Instructional theory concept.** (I) Polypeptide chain consisting of three parts: A and C could interchange between different conformational stable states (templating by the antigen, black circle); in the B region only one folding is favorable over the other. (II) A and C fold in the presence of the antigen. (III) The B part is consequently liberated and (IV) A'/C' assume their stable, folded configuration. (V) The B region folds into its stable configuration, forming the final antibody, (VI) which will dissociate from the antigen over time. [Reproduced with permission from ref. 2. Copyright 1940, the American Chemical Society.]

However, Pauling's theory was lacking in some of the important aspects of the experimental results: the possibility for the same linear antibody to discriminate between "self" and "non-self"; and the possibility of memory, as the secondary immune responses to an antigen are greater and faster than the primary.<sup>42</sup>

### **Clonal selection hypothesis**

The selective theory, as accepted today, was formulated in 1956 by Frank Macfarlane Burnet.<sup>43</sup> He further developed a theory based on the early conceptualization by Ehrlich and on the 1955 hypothesis of Niels Kaj Jerne on natural antibody selection.<sup>44</sup> The concept introduced by Burnet, namely the clonal selection hypothesis, includes the presence of two classes of cells responsible for both early and future responses to the antigen (memory cells). Once in the presence of the antigen, the cells capable of producing the antibody that possesses the higher affinity for the antigen are reinforced in their reproduction (clonal selection) in order to ensure a sufficient amount of antibody available to combat the infection. The discovery of Gustav Nossal,<sup>45</sup> in 1958, that B cells produce one single kind of antibody was the first evidence of the clonal selection hypothesis. Further discoveries on the genetic mechanisms (variable, diverse and joining (V(D)J) recombination)<sup>46</sup> leading to the formation of an unlimited number of antibodies starting from a limited number of genes, finally corroborated the selective theory. Indeed, thanks to a somatic gene recombination process, different gene portions (variable, diverse and joining) that code for the different portions of the antibody are randomly rearranged to produce a large antibody repertoire to be screened for antigen selection. The repertoire is estimated to have  $10^{11}$  possible combinations.<sup>47</sup>

### **From natural to synthetic antibody**

Despite Pauling's theory being shown as incorrect, it paved the way to a new concept in synthetic recognition material design, which has been further

investigated and developed and has led to what is today known as the molecularly imprinted polymers (MIPs) technology. Pauling wrote:

*"...all antibody molecules contain the same polypeptide chains as normal globulin, and differ from normal globulin only in the configuration of the chain; that is, in the way that the chain is coiled in the molecule. [...] Let us assume that the globulin molecule consists of a single polypeptide chain, containing several hundred amino-acid residues [...] In stage I there are shown an antigen molecule held at a place of globulin production and a globulin molecule with its two ends [...] with the extended configuration. At stage II each of the ends has assumed a stable coiled configuration. These stable configurations are not, however, identical with those assumed in the absence of the antigen. The atoms and groups which form the surface of the antigen will attract certain complementary parts of the globulin chain (a negatively-charged group, for example, attracting a positively-charged group) and repel other parts; as a result of these interactions the configurations of the chain ends which are stable in the presence of the antigen and which are accordingly assumed in the presence of the antigen will be such that there is attraction between the coiled globulin chain ends and the antigen, due to their complementarity in structure." <sup>2</sup>*

This hypothesis has inspired scientists to pursue analogous synthetic approaches aiming at obtaining man-made binding sites by chemical means (Fig. 1.3). Indeed, the MIP concept originates with the ability of the template (the antigen in Pauling's theory) to organize a pool of functionalized monomers (the linearized, single polypeptide chain of Pauling's theory) driven by the non-covalent interactions established by the monomers and the template itself.

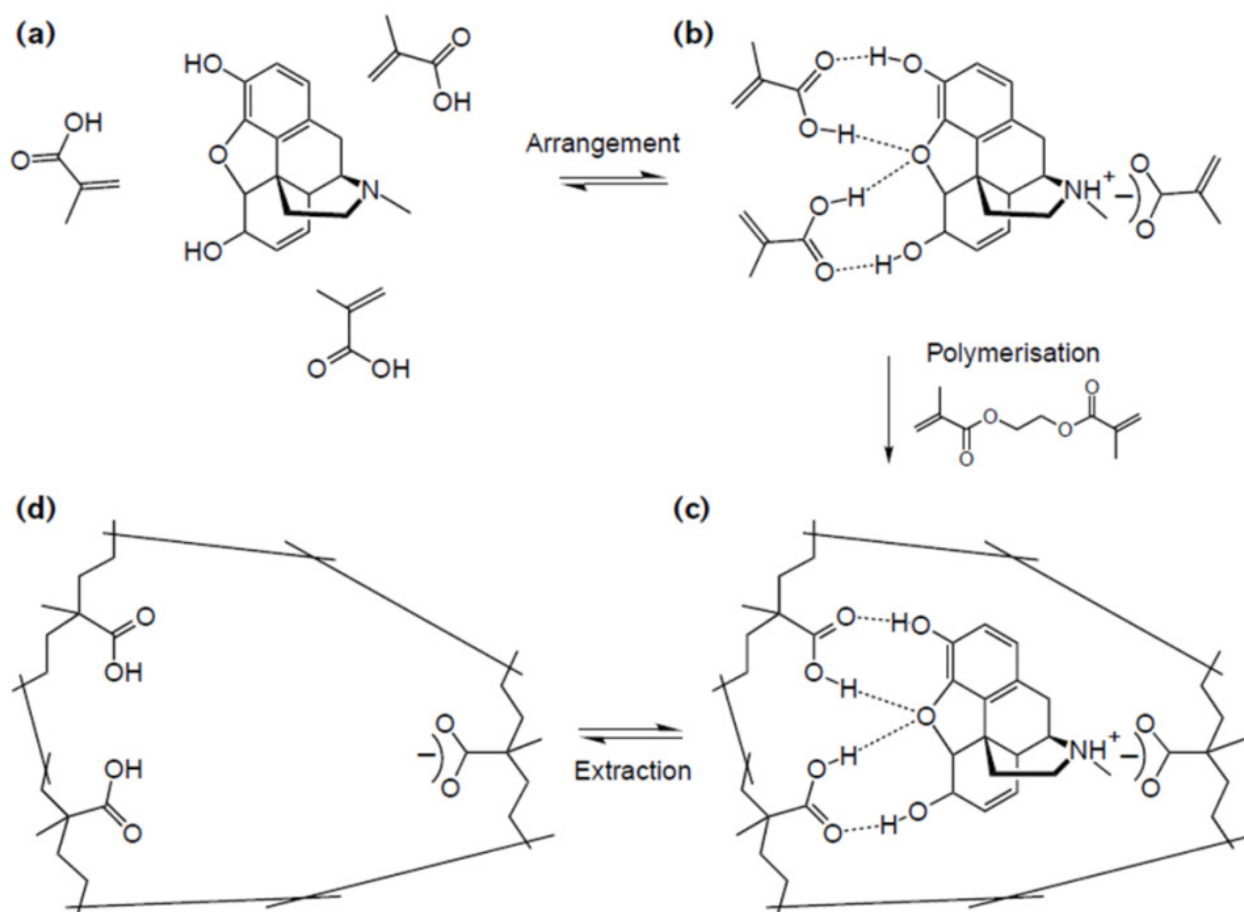


**Figure 1.3** | MIPs synthesized following a non-covalent approach. (a) Morphine as the template and methacrylic acid as monomers. (b) Template-monomers pre-polymerization complex is (c) polymerized using ethylene glycol dimethacrylate as cross-linker. (d) The final imprinted polymer is obtained after template extraction. [Reproduced with permission from ref. 48. Copyright 1999, Elsevier.]

The current definition of molecular imprinting, which considers the accumulated experimental findings, was proposed by Whitcombe in 2006:

*"The construction of ligand selective recognition sites in synthetic polymers where a template (atom, ion, molecule, complex or a molecular, ionic or macromolecular assembly, including micro-organisms) is employed in order to facilitate recognition site formation during the covalent assembly of the bulk phase by a polymerization or polycondensation process, with subsequent removal of some or all of the template being necessary for recognition to occur in the spaces vacated by the templating species"*<sup>7</sup>

(A literature overview of the different synthetic strategies and templates used is reported in the following section).

## Molecular imprinting strategies

Several synthetic strategies leading to the formation of imprinted polymers were developed over the years. With respect to the interactions established between template and monomer during the pre-polymerization step, the main developed strategies are the covalent, the non-covalent, and the semi-covalent approach.

### Covalent imprinting

The covalent imprinting strategy is based on the use of a monomer-bearing template, prepared through the formation of a covalent bond between the template and one or more specific monomers (Fig 1.4). Once the polymer is formed and the template cleaved out, template rebinding occurs through the same covalent bond.<sup>49</sup> Classical examples of the chemical bond applied in this approach are boronate ester,<sup>50</sup> ketal/acetal<sup>51</sup> and Schiff's base.<sup>52</sup>

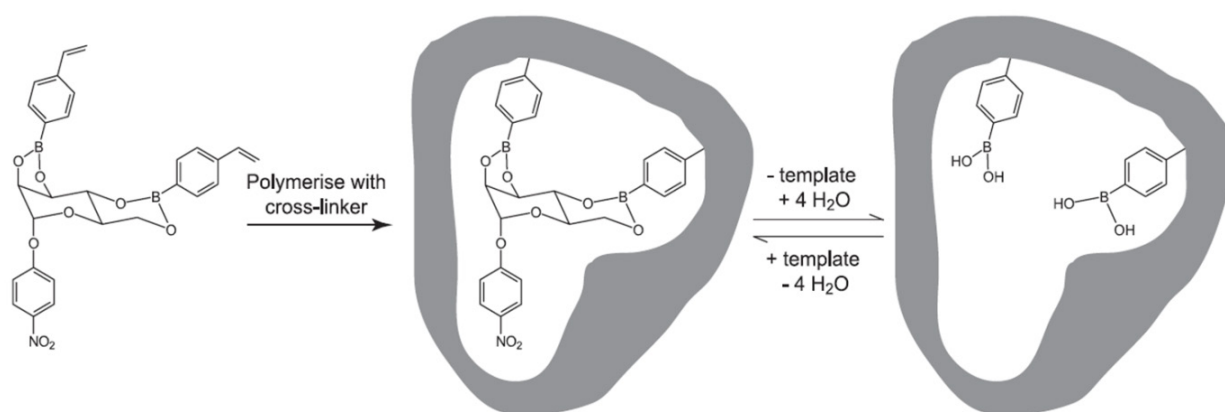


**Figure 1.4 | Covalent imprinting using a boronate ester.** The template monomer complex was prepared by condensation of 4-vinylbenzeneboronic acid with 4-nitrophenyl- $\alpha$ -D-mannopyranoside to produce the 4-nitrophenyl- $\alpha$ -D-mannopyranoside-2,3:4,6-di-O-(4-vinylphenylboronate). After polymerization, the template is removed by the hydrolysis of the boronate ester groups. [Reproduced with permission from ref. 53. Copyright 2005, Elsevier.]

Owing to the structural – chemical functionalities required in the template in order to synthesize the monomer-bearing template, a limited spectrum of



template molecules could be used with this approach. Nevertheless, two main advantages result. Indeed, owing to the stoichiometric amount of monomer applied, it yields imprinted polymers possessing a homogenous binding site distribution. Secondly, for the same reason, it may help in reducing unspecific binding on the produced imprinted polymer.<sup>53</sup>

### **Non-covalent imprinting**

The non-covalent imprinting approach relies on non-covalent interactions that establish between templates and monomers before polymerization (example given in fig 1.3).<sup>54</sup> The forces involved in this imprinting method are generally hydrogen bonds, ion pairs, dipole – dipole, hydrophobic interactions and van der Waals forces. This variety of interaction forces allows the non-covalent imprinting method to be versatile for a variety of template molecules.<sup>53</sup> The possibility of using a mixture of monomers, bearing different chemical functionalities that target the template chemical functionalities, will result in a final synthetic binding site possessing multiple interaction points, having a higher affinity for the template than the single template-monomer interaction.<sup>53</sup> It has to be added that this approach provides binding sites with a chemical imprint of the template. Finally, the non-covalent nature of the interactions, as compared with the covalent approach, allows for easy reversibility of template binding, especially during the template removal step, after polymer synthesis.

This approach was first proposed as proof of concept by Mosbach.<sup>30</sup> The synthetic method as published included the use of different acrylic monomers with rhodanile blue and safranin O as templates, yielding a bulk polymer that was crushed to 300 – 500  $\mu\text{m}$ -size particles and washed in order to remove the template. By loading the produced polymer in a chromatographic column, the authors showed preferential binding of each template for the corresponding imprinted polymer.<sup>30</sup>

Together with its above-mentioned beneficial aspects, non-covalent imprinting has a major drawback. Indeed, the presence of an excess of monomers not associated with the template could produce non-imprinted surfaces that are potentially available to non-specific binding.<sup>55</sup>

### Semi-covalent imprinting

The semi-covalent approach combines the use of the monomer-bearing template during the polymer formation of the covalent approach with a non-covalent template-polymer rebinding of the non-covalent approach.<sup>55</sup> Although several examples of imprinted polymers are reported in the literature, targeting *p*-aminophenylalanine ethyl ester,<sup>56</sup> testosterone methacrylate,<sup>14</sup> 4-nitrophenol<sup>57</sup> and bisphenol-A<sup>58</sup>, a major drawback of the technique, as with the covalent approach, resides in the structural – chemical moieties needed in the template molecule in order to create the monomer-bearing template. Thus, the spectrum of possible template molecules that could be used with this approach is limited.<sup>55</sup> An alternative approach, which includes the use of a sacrificial spacer between the template and monomer (lost during template removal), was proposed by Whitcombe for the imprinting of cholesterol.<sup>59</sup>

All of these synthetic strategies, including the different templates and the monomers used in the selected examples, represent major achievements in the ongoing development of MIPs for the design of plastic antibodies. The developed approaches<sup>7,60</sup> were, and still are, challenged by the macromolecular imprinting of large biological templates, which requires "bio-friendly" polymerization conditions and a surface imprinting approach in order to make all created binding sites available for rebinding, avoiding mass transfer limitation.

## Macromolecular imprinting

Great interest from the scientific community lies in the possibility of producing plastic antibodies for biological molecules.<sup>16,18,61</sup> Such synthetic materials could, indeed, find application as drug delivery systems,<sup>62</sup> sensing devices,<sup>63</sup> artificial enzyme-mimic catalysts<sup>64</sup> and high affinity materials for purification<sup>65,66</sup> in the pharmaceutical, agro-food, and environmental industries.

Imprinting of large biological templates requires synthetic strategy optimization in order to face a series of problem intrinsically related with the nature of bio-molecules, namely size, complexity, solubility and conformational flexibility.<sup>16</sup> Indeed, the large size of biological macromolecules limits their diffusion into the imprinted polymer (for both template removal and rebinding). This necessitates the modification of the polymer format, moving from bulk polymers that entrap the template molecules and need to be crushed in order to increase the available imprint sites, to films and surface imprinted polymer.<sup>67</sup>

Furthermore, as opposed to small molecules, biological templates possess a larger surface with an enormous number of potential interaction sites.<sup>18</sup> This requires the use of complex monomer mixtures in order to provide a variety of chemical functionalities available for establishing a wide range of non-covalent interactions with the template. The use of complex monomer mixtures may result in unwanted side reactions (*e.g.* self-polymerization) that should be taken into account, otherwise this may increase unspecific binding, owing to the formation of a non-imprinted surface on the polymer.<sup>16,54</sup>

The solvent of choice is indubitably water. Indeed, a vast majority of proteins unfold once dissolved in non-aqueous solvents, thus losing their function. Furthermore, imprinting in non-physiological conditions would cause conformational changes, aggregation or complete denaturation of bio-molecules, leading to the imprint of the protein in a non-native conformation.<sup>16</sup> The

restriction of the solvent to water also constrains the choice of monomers to water-soluble molecules.<sup>68</sup>

## Protein-imprinted polymers

Despite the aforementioned challenges to the macromolecular imprinting of biological templates, several examples are reported in the literature.<sup>16,68,69</sup> The principal model proteins used as templates include: hemoglobin, bovine serum albumin and lysozyme.<sup>68</sup> A variety of functional monomers were applied, resulting in the formation of polymers of differing natures, comprising hydrogels,<sup>70-73</sup> acrylates<sup>74</sup> and sol-gels.<sup>75</sup>

Using lysozyme as a template, Matsunaga *et al.*<sup>70</sup> produced imprinted hydrogel films on a vinyl, pre-modified surface of an SPR (surface plasmon resonance) chip. SPR is a label-free detection system based on the measurement of refractive index changes occurring at the sensor surface with a binding event (within 300 nm from the sensor surface). The authors observed preferential binding of the template (lysozyme) on the imprinted polymer as compared to a series of reference, non-template proteins (RNase A, cytochrome C, myoglobin and lactalbumin).

Sol-gels have been extensively used as an enzyme encapsulation matrix in order to overcome limitations associated with the use of free enzymes, including the difficulty of separation of enzyme from a reaction mixture, poor stability, and limited reuse.<sup>76,77</sup> Indeed, the mild polycondensation conditions needed for the formation of siloxane or polysilsesquioxane are compatible with proteins in their native conformation.<sup>16</sup> The study of Mosbach's group, in 1985, was the first successful report of siloxane protein imprinting.<sup>31</sup> A transferrin glycoprotein was imprinted on the surface of porous silica beads using a mixture of silanes that included a new boronate-silane functional monomer designed for interaction with

the carbohydrate group of the protein. Imprinted beads were shown to preferentially bind the template rather than the control protein (BSA).

More recently, Shiomi *et al.*<sup>20</sup> reported on a new approach, based on covalent immobilization of the template protein (hemoglobin) on porous silica nanoparticles followed by the polycondensation of 3-aminopropyltrimethoxysilane (APTMS) and trimethoxypropylsilane (TMPS). The imprinted particles resulted in preferential binding of the template protein as compared with the non-modified silica. Nevertheless, authors have also reported on the strong, unspecific binding of a series of non-template proteins used as control, including  $\beta$ -amylase, cytochrome C and myoglobin.

From the point of view of the polymer format, several elegant approaches have been developed. By using a liquid-phase deposition (LPD) approach, Tatemichi *et al.* prepared an imprinted polymer film for pepsin (Fig. 1.5).<sup>78</sup>

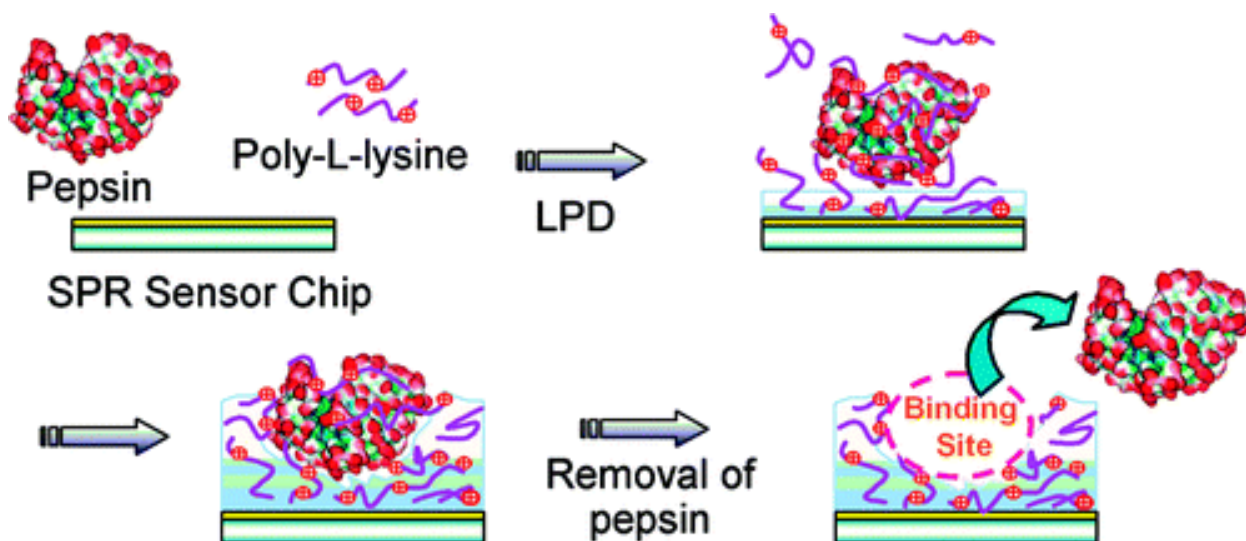


**Figure 1.5 | Scheme of pepsin imprinting LPD process.** The template protein (pepsin) in complex with poly-L-lysine is deposited on an SPR chip gold surface by using a titanium oxide-LPD process. [Reproduced with permission from ref. 78. Copyright 2007, the American Chemical Society.]

Briefly, LPD deposition occurs in solution in a two-step reaction: first, a metal fluoride is hydrolyzed to form a metal oxide, thus releasing a fluoride ion; the produced fluoride ion is then reacted with boronic acid, resulting in an acceleration of the metal hydrolysis reaction. As a result, a metal oxide film is homogeneously deposited on various kinds of surfaces.<sup>79</sup> By using titanium oxide-LPD, pepsin-poly-L-lysine complexes were co-deposited with titanium oxide on SPR sensor chip surfaces, producing a pepsin-imprinted organic-inorganic hybrid film (Fig. 1.5). The binding study demonstrated that the film was specific for its template.

By combining protein immobilization and micro-contact printing techniques, Lin *et al.* uses lysozyme, ribonuclease A and myoglobin as a mold to stamp them onto a 3-(trimethoxysilyl)-propyl methacrylate-grafted glass slide in the presence of monomers and crosslinker.<sup>80</sup> Once the photopolymerization completed, the cover glass was removed to obtain a protein surface-imprinted polymer film (Fig. 1.6).

Although the micro-contact approach seems to be promising, a series of fundamental difficulties associated with the technique have been found. Indeed, without considering the nanometer precision device needed to perform such micro-contact printing, which already, in and of itself, limits the widespread application of the procedure, the fact that the protein closely approaches the cross-linker in the monomer solution deprives the imprinting method of any form of control of the size of the imprints. Indeed, owing to cross-linker monomer surface irregularities, an inhomogeneous binding site size distribution is expected, resulting in binding sites possessing variable affinities for the template.

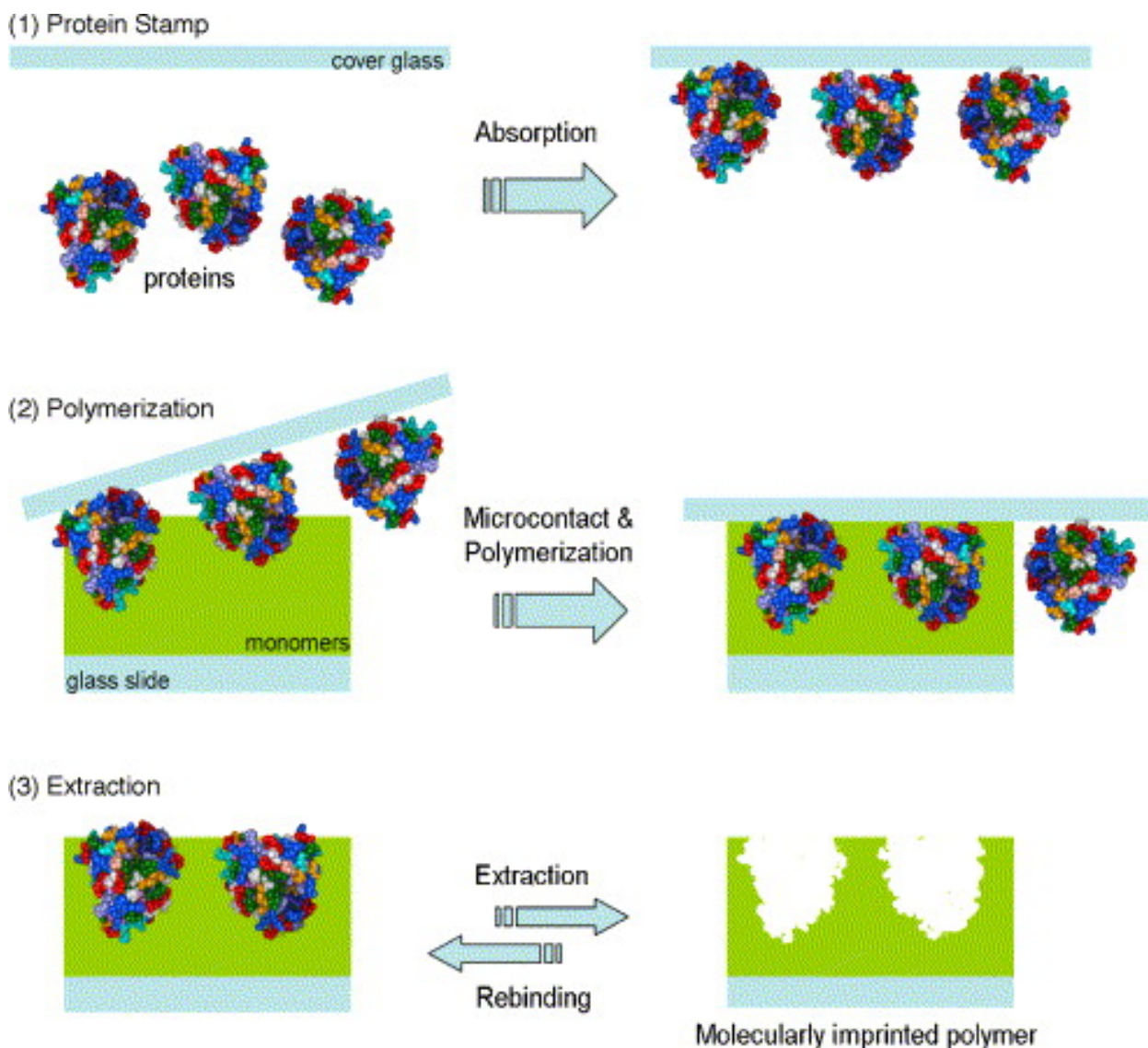


**Figure 1.6 | Scheme of micro-contact molecular imprinting process.** The template protein (myoglobin) is first absorbed on glass, thus creating the protein stamp. The stamp is then placed in contact with monomers and polymerization proceeds. The removal of the cover glass yields a molecularly imprinted thin film. [Reproduced with permission from ref. 80. Copyright 2004, Elsevier.]

An additional approach, fluoropolymer-based surface imprinting, was proposed by Ratner's group, by using a disaccharide (trehalose) as a functional monomer.<sup>81,82</sup> This approach was developed for a number of proteins, including bovine serum albumin, immunoglobulin-G, fibrinogen, lysozyme and ribonuclease-A. The template protein was at first adsorbed on a mica surface. A layer of the disaccharide was then applied and coated with a fluoropolymer layer applied by

plasma deposition. The removal of the mica surface and a sodium hydroxide/sodium hypochlorite treatment was performed to dissolve and extract the protein. The final imprinted polymers showed to unspecifically adsorb all of the protein assayed ( $^{125}\text{I}$ -labelled BSA, IgG and fibrinogen). Nevertheless, the portion of eluted protein, after washing, varied according to the imprint present in the polymers.

The ability to inhibit a given enzymatic activity associated with a pathological condition is a powerful tool that can provide a specific therapy for that condition.<sup>83</sup> Indeed, enzyme inhibitors represent a part of the potential drugs available for use in treating a series of diseases, including cancer, cardiovascular-, neurological-, infectious- and metabolic diseases.<sup>84</sup> Proof of concept of the use of a molecularly imprinted polymer as an enzyme inhibitor was made by Haupt, using trypsin as a model enzyme (Fig. 1.7).<sup>85</sup>

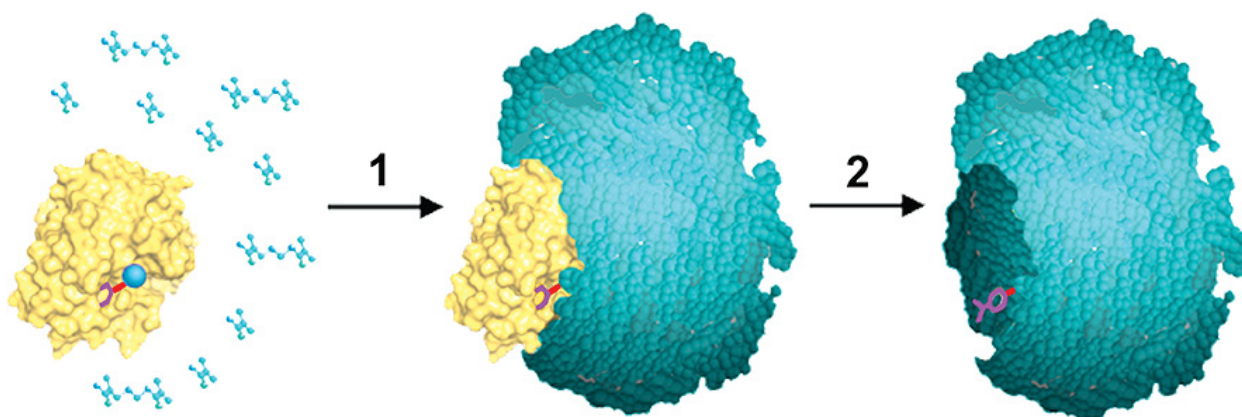


**Figure 1.7 | Strategy for artificial trypsin-inhibitor synthesis produced by molecular imprinting.** The modified, natural trypsin inhibitor, N-methacryloyl-4-aminobenzamidine (red with blue sphere), interacts with the enzyme (yellow). Its methacryloyl moiety can then polymerize with the monomers to create a single-enzyme imprinted polymer. [Reproduced with permission from ref. 85. Copyright 2009, the American Chemical Society.]

The modification of a natural trypsin inhibitor (benzamidine) with a methacryloyl group allows its use as a polymerizable monomer in the creation of a polymer possessing a surface that is complementary to that of the enzyme. Thanks to



this strategy, the imprinted polymer showed a 3-fold greater inhibition effect than the free, low molecular weight inhibitor benzamidine. Indeed, the imprinted polymer (created with the methacryloyl group bearing benzamidine) provided an additional series of contact points between the inhibitor and the enzymes. Therefore, the affinity of the final polymer for the trypsin increased in comparison with that of the free inhibitor.

## Virus imprinting

Within this PhD project, viruses were chosen as biological entities to template the formation of specific recognition units on silica nanoparticle (SNP) surfaces. Before reviewing the state of the art on virus molecularly imprinted polymers, a brief overview of virus characteristics is given in order to provide the non-expert reader with a minimal understanding of viral morphology.

## Overview of virus structures and classification

Viruses<sup>86</sup> are the simplest infective pathogenic agents known to propagate in all living organisms, spanning from protozoa to plants, from bacteria to mammals. As obligatory parasites, they benefit from the cell's protein synthesis machinery in order to complete their life cycles, producing new viral progeny. Viruses are essentially made of a nucleic acid core (DNA or RNA, single or double stranded) encapsulated by a self-assembly of proteins, the capsid protein(s).<sup>87</sup> A number of viruses possess an additional host cell-derived lipid bilayer carrying specific viral glycoproteins. This lipid stratum, named the envelope, forms the outermost layer of many animal viruses (Fig. 1.8).<sup>88</sup>

Originally, viruses were classified according to their morphology (*i.e.* shape, nucleic acid, presence of envelop and dimensions) within the classical Linnaean hierarchical system, *i.e.* phylum, class, order, family, genus and species. With the advancement of molecular biology, a new classification system, based on viral genetics, was developed. The Baltimore classification groups viruses into seven classes according to their genome and method of replication.<sup>89</sup> Table 1.1 reports a list of viruses that includes their Baltimore classification, morphology and family.

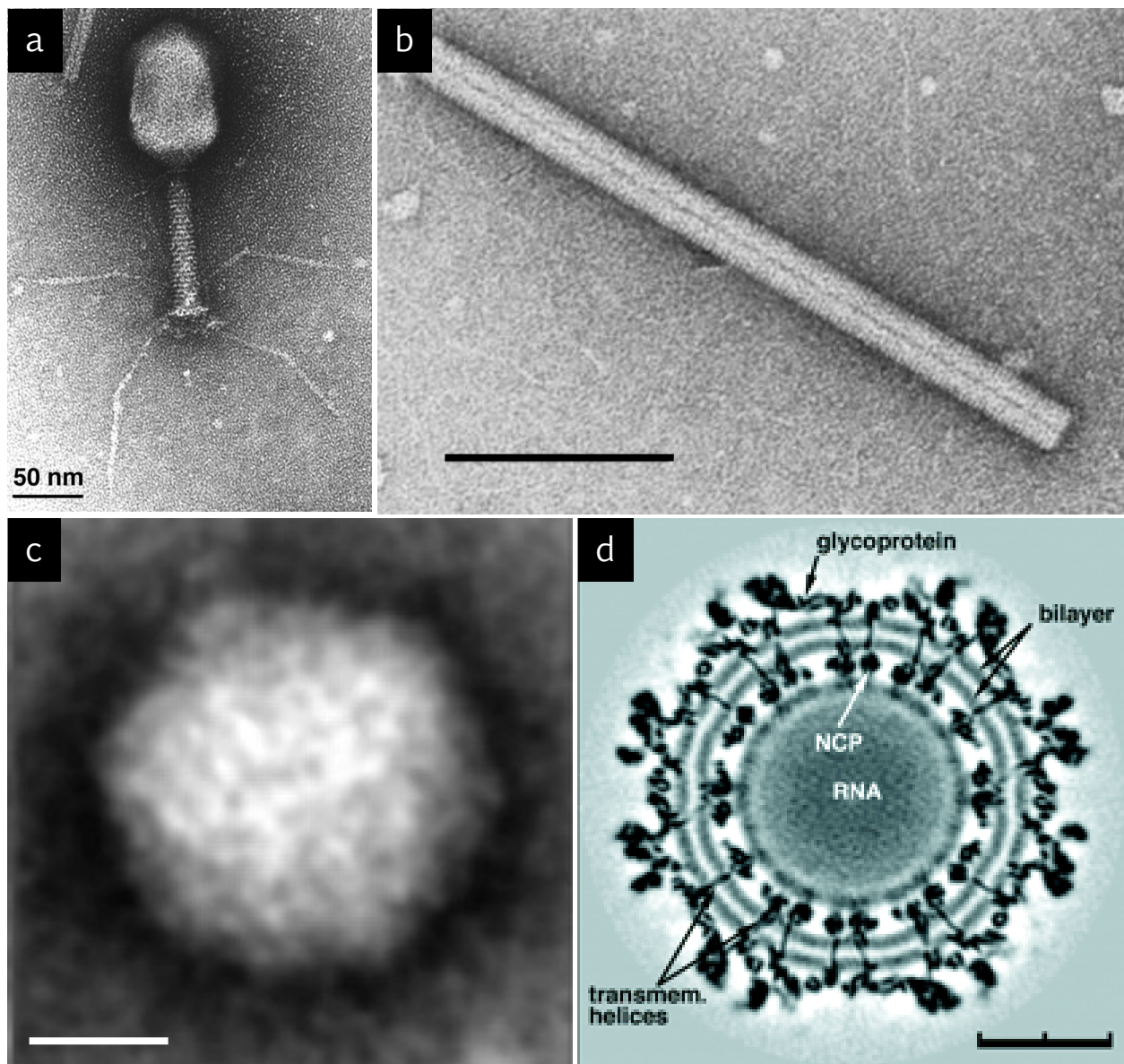


**Figure 1.8** | Representative electron micrographs of viral morphological variability. (a) Bacteriophage T4 with a prolate icosahedral head, tail and long tail fibers [Reproduced with permission from ref. 90. Copyright 2003, the American Society for Microbiology.]; (b) Rod-shaped tobacco mosaic virus (scale bar: 100 nm) [Reproduced with permission from ref. 91. Copyright 1955, the National Academy of Sciences]; (c) Non-enveloped icosahedral *Heterocapsa circularisquama* RNA virus (scale bar: 10 nm) [Reproduced with permission from ref. 92. Copyright 2011, the Society for General Microbiology.]; (d) Cross section of enveloped icosahedral Sindbis virus (scale bar: 20 nm; NCP: nucleocapsid) [Reproduced with permission from ref. 93. Copyright 2002, the American Society for Microbiology.]

Viruses are widespread in the environment. Their simple structures, and their rapidity and efficiency of propagation make these parasites the most contagious

and variant pathogenic agent known. Indeed, all living organisms, spanning from bacteria to plants, insects and mammals, are infected by viruses.<sup>94</sup>

Pathogenic human viruses that pose significant health, social and economic difficulties worldwide include human immunodeficiency virus (HIV),<sup>95</sup> hepatitis viruses,<sup>96</sup> human papillomavirus (HPV),<sup>97</sup> enteroviruses,<sup>98</sup> dengue<sup>99</sup> and influenza viruses.<sup>100</sup> Moreover, the incidence and outbreaks of emerging and re-emerging infectious viral diseases have increased recently, owing to the progressively increasing social complexity of our modern world, including population growth and travel frequency.<sup>101</sup> Therefore, detection of a viral pathogenic agent is a persistent issue in fields ranging from clinical diagnostics to agro-food to water borne pathogens. Thus, new technological approaches to detection and/or removal of viruses are required.

	Morphology	Symmetry	Nucleic acid	Group	Examples
Adenoviridae	Non-enveloped	Icosahedral	dsDNA	I	Adenovirus, Infectious canine hepatitis virus
Papovaviridae	Non-enveloped	Icosahedral	dsDNA circular	I	Papillomavirus, Polyomaviridae, Simian vacuolating virus
Parvoviridae	Non-enveloped	Icosahedral	ssDNA	II	Parvovirus B19, Canine parvovirus
Herpesviridae	Enveloped	Icosahedral	dsDNA	I	Herpes simplex virus, Varicella-zoster virus, Cytomegalovirus, Epstein-Barr virus
Poxviridae	Complex coats	Complex	dsDNA	I	Smallpox virus, Cow pox virus, Sheep pox virus, Vaccinia virus
Hepadnaviridae	Enveloped	Icosahedral	dsDNA circular	VII	Hepatitis B virus
Anelloviridae	Non-enveloped	Icosahedral	ssDNA circular	II	Torque teno virus
Reoviridae	Non-enveloped	Icosahedral	dsRNA	III	Reovirus, Rotavirus
Picornaviridae	Non-enveloped	Icosahedral	ssRNA	IV	Enterovirus, Rhinovirus, Hepatovirus, Cardiovirus, Aphthovirus, Poliovirus, Parechovirus, Erbovirus, Kobuvirus, Teschovirus, Coxsackie
Caliciviridae	Non-enveloped	Icosahedral	ssRNA	IV	Norwalk virus
Togaviridae	Enveloped	Icosahedral	ssRNA	IV	Rubella virus, Alphavirus
Arenaviridae	Enveloped	Complex	ss(-)RNA	V	Lymphocytic choriomeningitis virus
Flaviviridae	Enveloped	Icosahedral	ssRNA	IV	Dengue virus, Hepatitis C virus, Yellow fever virus
Orthomyxoviridae	Enveloped	Helical	ss(-)RNA	V	Influenzavirus A, Influenzavirus B, Influenzavirus C, Isavirus, Thogotovirus
Paramyxoviridae	Enveloped	Helical	ss(-)RNA	V	Measles virus, Mumps virus, Respiratory syncytial virus, Rinderpest virus, Canine distemper virus
Bunyaviridae	Enveloped	Helical	ss(-)RNA	V	California encephalitis virus, Hantavirus
Filoviridae	Enveloped	Helical	ss(-)RNA	V	Ebola virus, Marburg virus
Coronaviridae	Enveloped	Helical	ssRNA	IV	Corona virus
Astroviridae	Non-enveloped	Icosahedral	ssRNA	IV	Astrovirus
Bornaviridae	Enveloped	Helical	ss(-)RNA	V	Borna disease virus
Arteriviridae	Enveloped	Icosahedral	ssRNA	IV	Arterivirus, Equine arteritis virus
Hepeviridae	Non-enveloped	Icosahedral	ssRNA	IV	Hepatitis E virus

**Table 1.1 | Examples of viruses according to Baltimore groups and morphological classification.** ds: double strand; ss: single strand; (-) negative polarity of the nucleic acid strand, which need to be retrotranscribed in order to produce a suitable positive strand for protein synthesis.

## Virus-imprinted polymers

For the reasons mentioned in the previous paragraph, imprinted polymers for virus recognition could provide a new solution offering the advantages of material robustness and ease of production. Owing to the complex, fragile self-assembled viral structure, there is a higher hurdle to overcome by the synthetic strategies leading to the formation of virus-imprinted polymers compared to protein imprinting. Nevertheless, different strategies have been developed to molecularly imprint viruses.

Dickert developed a series of virus-imprinted polymers used as recognition elements in a sensor device. By using a soft lithography stamping approach (Fig. 1.9), virus imprinted polymers were produced on mass-sensitive quartz crystal microbalance (QCM) sensor chips.

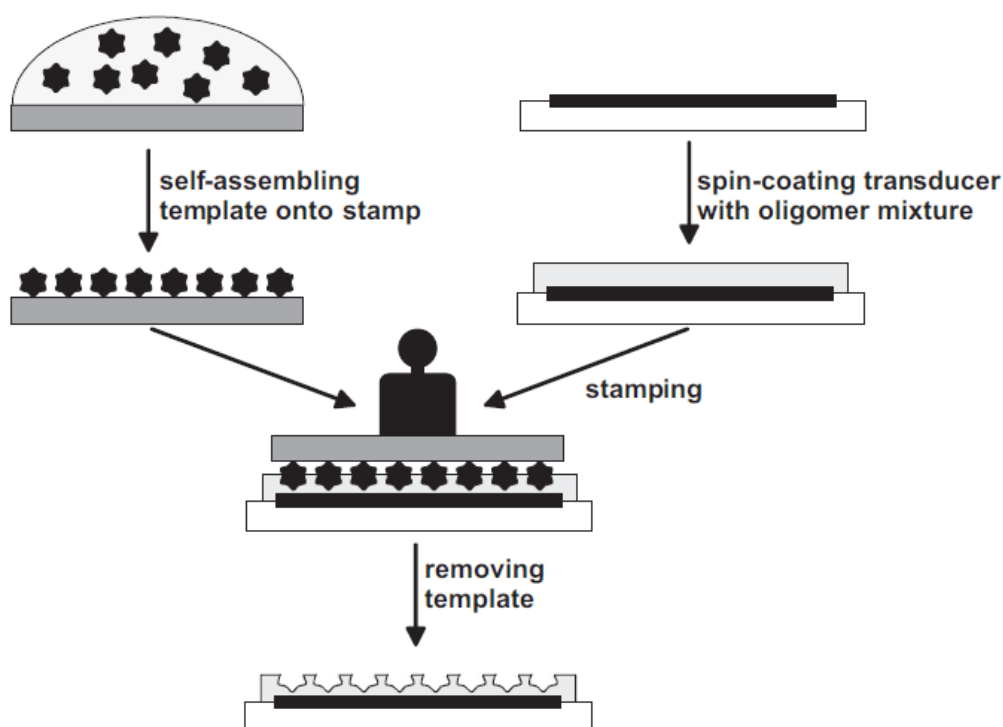


**Figure 1.9 | Stamping scheme for virus imprinting.** The template is self-assembled on a glass slide stamp and then used as a mold on the monomer mixture in order to form the polymer. [Reproduced with permission from ref. 24. Copyright 2006, WILEY-VCH Verlag GmbH & Co. KGaA.]

Using such a format, the binding performance of the imprinted polymers was readily assayed. Two different pre-polymerization mixtures were applied on QCM sensors: polyurethane- and polyacrylate-based polymers for tobacco mosaic virus (TMV),<sup>102</sup> and polyurethane for human rhinovirus (HRV)<sup>24</sup> and parapox ovis virus (PPOV).<sup>103</sup> Both polyurethane and polyacrylate-based polymers were produced from a non-aqueous pre-polymerization mixture. In all cases, after applying the pre-polymerization mixture on QCM sensors, a virus mold was applied in the presence of blockers (*i.e.* glucose, 4-aminophenol, or 4-aminobenzoic acid), which avoids covalent linking of the virus to the pre-polymerized mixture. Owing to the enveloped morphology of PPOV, which make this virus sensitive to mechanical stress, it was first adsorbed on polydimethylsiloxane as a stamp support before the stamping procedure. The final imprinting polymerization was achieved at room temperature overnight under a nitrogen atmosphere for polyurethane, and in saturated humidity under UV-light overnight for polyacrylates. Finally, viruses were removed by washing with a sodium dodecyl sulfate (SDS) aqueous solution. The QCM binding assay results showed that the imprinted polymers bound preferentially to their template virus. Despite using a sensitive detection device, as represented by QCM, the authors had to apply a high virus concentration (1 mg/ml) to observe a sensor response. The high virus concentration used in the rebinding assay suggests that, owing to the imprinting methodology, the imprinting efficiency was strongly affected. It has to be added that the monomer composition used and the stamping procedure applied increased the possibility of virus disassembling. Indeed, as stated by the authors, a series of blocker agents was used in order to avoid covalent linking of the virus with the polymerization mixture. In addition, the overnight UV irradiation of the sample, in the polyacrylate based polymer, may partially damage the viruses, resulting in the unfolding and disassembling of the viral morphology, and thus resulting in the imprint of the virus in a non-native structure. As a consequence, a variable fraction of the imprints may not

be available for specific interaction, but rather for unspecific ones. Finally, as is quite often seen in a number of MIP reports,<sup>7,8</sup> a mixture of poor monomer composition was applied, thus reducing the possibility of producing a chemical imprint of the template virus. All together, the described protocols appear to be tedious and non-versatile. As a consequence it is reasonable to conclude that this procedure may not be applicable for a large variety of viruses.

By using hydrogels, Bolisay *et al.* prepared a TMV imprinted polymer.<sup>104</sup> They used a poly(allylamine hydrochloride)-based hydrogel in the presence of sodium hydroxide. Upon addition of epichlorohydrin, the hydrogel was allowed to cure for five days. A long and tedious procedure for template removal was applied. It included: (i) cutting the formed hydrogel and resuspension in 70% ethanol; (ii) 24 h shaking; (iii) 1 mM sodium chloride treatment at 100 °C for 1 h; (iv) 1 h boiling treatment in 1 M sodium chloride followed; (v) then the polymer was washed for three days in water and (vi) finally it was dried at 55 °C (Fig. 1.10a).

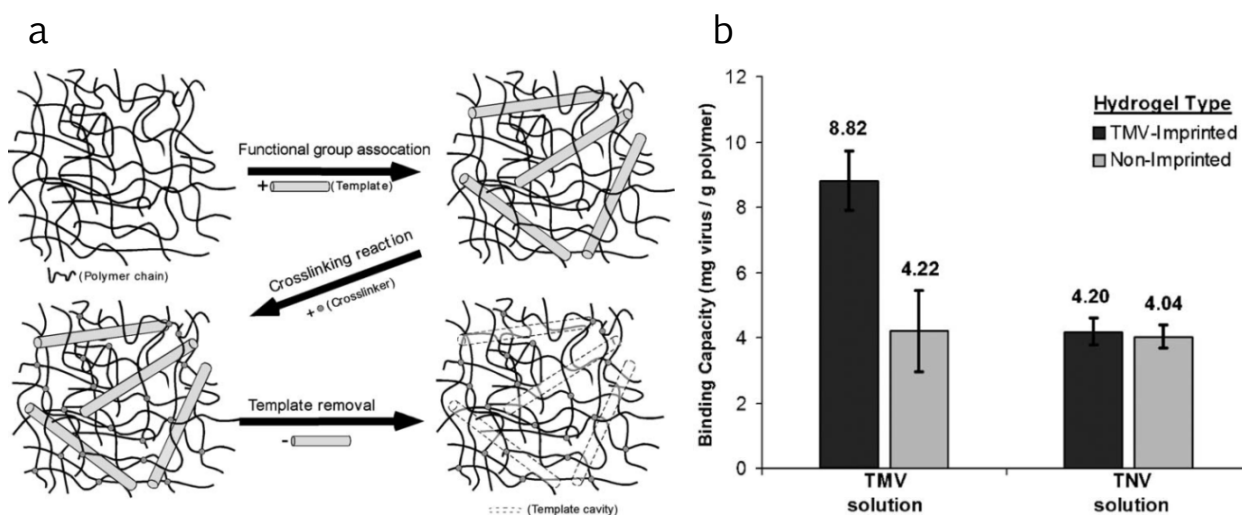


**Figure 1.10 | Scheme for TMV imprinting using a hydrogel and a binding assay.** (a) Principle of bulk polymerization for a TMV imprinted hydrogel. (b) Binding assay of TMV-imprinted polymers compared to non-imprinted polymers. The TMV-imprinted polymer preferentially binds the template, rod-shape TMV virus over the non-template icosahedral TNV virus (tobacco necrosis virus). [Reproduced with permission from ref. 104. Copyright 2006, Elsevier.]



The final polymer was shown to preferentially bind 50% more template TMV virus than the non-imprinted polymer. It must be added that the control virus (TNV, tobacco necrosis virus), with an icosahedral morphology, was bound to the same extent to both imprinted and non-imprinted polymer (Fig. 1.10b). The choice of a control virus possessing an icosahedral morphology contrasted with the shape of the template virus, which had rod-shape morphology. Indeed, a relevant virus to serve as a control would have possessed a rod-shaped morphology similar to that of the template virus. In addition, this is a clear example where the drawbacks of bulk polymerization can be appreciated. Indeed, a very long and tedious procedure was applied in order to remove the template virus from the polymer, which, *per se* already limits the versatility of the approach. Moreover, the long procedure could partially damage the newly created imprints, resulting in reduced efficiency of the overall imprinting process.

More recently, a mini-emulsion approach to produce virus imprinted polymers has been proposed.<sup>105</sup> Virus imprinted nanoparticles were obtained by the addition of the template virus (bacteriophage  $\phi$ r) to a mini-emulsion containing the monomer phase (methacrylate and acrylic acid as monomers and ethylene glycol dimethacrylate as cross-linker).

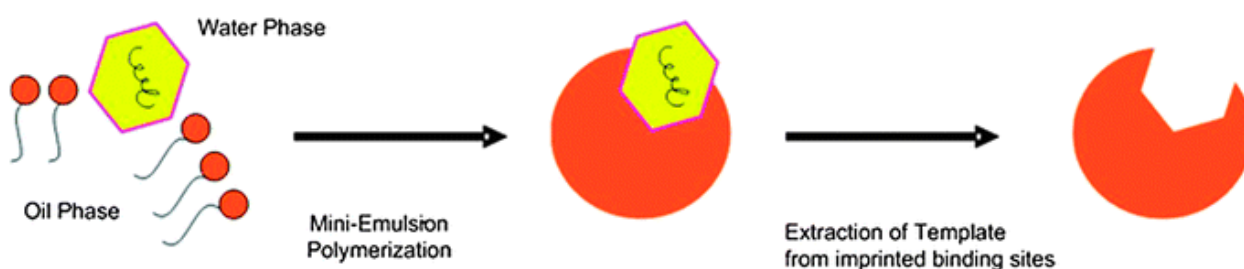


**Figure 1.11 | Mini-emulsion polymerization strategy.** One-stage mini-emulsion polymerization allows the formation of imprinted polymers via the (i) adsorption of the template virus to the micelle followed by (ii) the polymerization in the oil phase, and (iii) template removal. [Reproduced with permission from ref. 105. Copyright 2013, The Royal Society of Chemistry.]

Owing to its binding performance, the imprinted polymer was demonstrated to slow down phage growth and thus reduce *E. coli* infection. Indeed, by using a standard plaque counting assay to quantify the phages, the authors showed that, after incubation of the bacteria with the phage in the presence of the phage-imprinted particles, the viral titer in the supernatant was 1.46 units lower (logarithmic reduction) than in the presence of the corresponding non-imprinted particles.

In order to overcome the difficulties of large target imprinting, a new approach, called epitope imprinting, was developed.<sup>106</sup> As for antigen – antibody interaction, the imprinted polymer is produced using a small portion of the whole, large target molecule as a template. The final polymer is thus able to recognize the original, large target molecule. The first example was proposed by Minoura.<sup>106</sup> As proof of concept, as a template the authors used the tetrapeptide Tyr-Pro-Leu-Gly-NH<sub>2</sub>, which is the N-terminus of oxytocin, for the production of an imprinted polymer. The final MIP was able to bind oxytocin and oxytocin-related peptides. This approach was extended to dengue virus capsid protein,<sup>107</sup> to glycoprotein 41 of human immunodeficiency virus,<sup>108</sup> and to human papillomavirus-derived E7 protein.<sup>109</sup> The produced polymers were used as recognition elements of QCM sensors,<sup>107,108</sup> or of electrochemical impedance spectroscopy sensors.<sup>109</sup> Nevertheless, even though this approach seems to be promising, the target finally recognized by the imprinted polymer is not the entire virus, but rather the viral capsid protein.

The examples reported in this literature overview cover the principal strategies for virus imprinting, including their application (*e.g.* sensing, removal, attenuation). The polymers produced were shown to possess variable degrees of specific and unspecific binding. The use of solvents, the limited variability of the monomers that are used to interact with the template chemical functionality, long template extraction procedures, reduced control of binding sites size and structured

imprinting strategies make these approaches weak in terms of applicability to a variety of relevant viruses and to their large scale production for industrial uses.

### **Author's critical view of MIP technology**

Despite a history extending almost 50 years, the molecularly imprinted polymers approach struggles to present itself as a mature and established science. Together with an elegant, stimulating and convincing theory, the MIP technique carries a series of limitations that inevitably constrain its development in the academic world and exploitation in industry. One main limiting factor is template availability. Indeed, for every molecule that will be newly bound on the imprinted polymer, one molecule was used and sacrificed to create that binding site. Alternatively, the possibility of recycling the template is a limited option, since the vast majority of template removal procedures tend to destroy/denature the template. Thus, large-scale production of MIPs targeting templates that are expensive, hazardous or difficult to produce at large-scale would be challenging. This limitation, originating at the theoretical level, may explain why the vast majority of reports on protein imprinting describe the use of non-relevant template proteins available in large quantities (*i.e.* bovine serum albumin, lysozyme and bovine hemoglobin).<sup>17</sup>

A second limitation is deduced from the experimental evidence. Indeed, non-imprinted polymers used as reference often exhibit high template binding capacity. Therefore, with the aim of creating a high template binding polymer, it seems logical to avoid the use of the template during the polymer synthesis. Instead, using a monomer/cross linker combinatorial approach would lead to the synthesis of random polymers possessing selective binding capabilities.<sup>110</sup>

Finally, the experience that has matured in macromolecular imprinting leads me to a simple consideration that may contribute to the additional clarification of the high unspecific binding that is often observed in an imprinted polymer that

targets large biological templates. Indeed, a consistent difference between MIPs and natural antibodies lies in the size of the portion recognized in the template. While antibodies recognize a small epitope (linear or conformational, of 5 – 15 amino acids), MIPs recognize the entire template, or at least half of it. Therefore, MIPs possess larger binding sites than antibodies for the same template. Thus, a larger imprinted surface, enriched with functional monomers, is available for nonspecific interaction.

Having considered such aspects of MIP technology, I remain optimistic for the future development of the technique. A tighter exchange between chemists and biologists would be favorable in order to push MIP technology toward a mature state of this field of research. Among others, efforts from the scientific community should invest in: (i) a procedure to allow the large scale production and purification of relevant templates; (ii) a more realistic, rational design of appropriate monomers for protein imprinting (amino acid-like monomers); (iii) fostering the epitope imprinting approach in order to favor the creation of imprinting strategies leading to the formation of artificial antibodies mimicking the natural ones.

## Silica nanoparticles - SNPs

The carrier material used to develop the virus imprinted particles method was silica nanoparticles (SNPs). These particles, produced using the classic Stöber method,<sup>111</sup> possess a high surface area to mass ratio and are extensively used. In this last part of this chapter, a brief overview of biogenic silica and of the biocompatibility of SNPs is given.

### Biosilica and biocompatibility

Silicon (Si) is one of the most abundant elements on Earth.<sup>112</sup> With its oxide forms (silicate-SiO<sub>4</sub> and silica-SiO<sub>2</sub>), the principal element of sand and quartz, it constitutes 90% of Earth's crust. Biosilica, or biogenic silica, is amorphous and is produced by marine and terrestrial organisms to build their exoskeletons, with a turnover of 6.7 gigatonnes of silicon every year.<sup>113</sup> Major silicon processing organisms include diatoms, sponges, choanoflagellates, radiolarians and plants.<sup>114</sup> Diatoms and sponges, as biosilicifying organisms, are able to form a stunning variety of biogenic silica possessing hierarchical structure (Fig. 3.3).<sup>115</sup>

Biosilica formation in sponges is an enzymatically catalyzed active process of silicon deposition. The main enzyme involved in this process was initially described by Morse and is named silicatein.<sup>116</sup> The natural substrate of this class of enzymes is not yet known.<sup>117</sup> Nevertheless, the formation of silica *in vitro* is catalyzed by silicatein using TEOS (tetraethylorthosilicate, the most commonly used silicatein substrate) as a monomeric precursor.<sup>118</sup> TEOS is also the most common synthetic precursor for SNP synthesis, *e.g.* with the Stöber process.<sup>111</sup> In contrast to sponges, the mechanism of biosilica formation in diatoms is induced by polycationic peptides, with a molecular weight ranging from 4 to 17 kDa, named silaffins.<sup>119</sup> Such short peptides were found to carry a great number of positively (arginine residues) and negatively (post-transcriptionally phosphorylated serine and lysine residues) charged groups.<sup>117</sup>

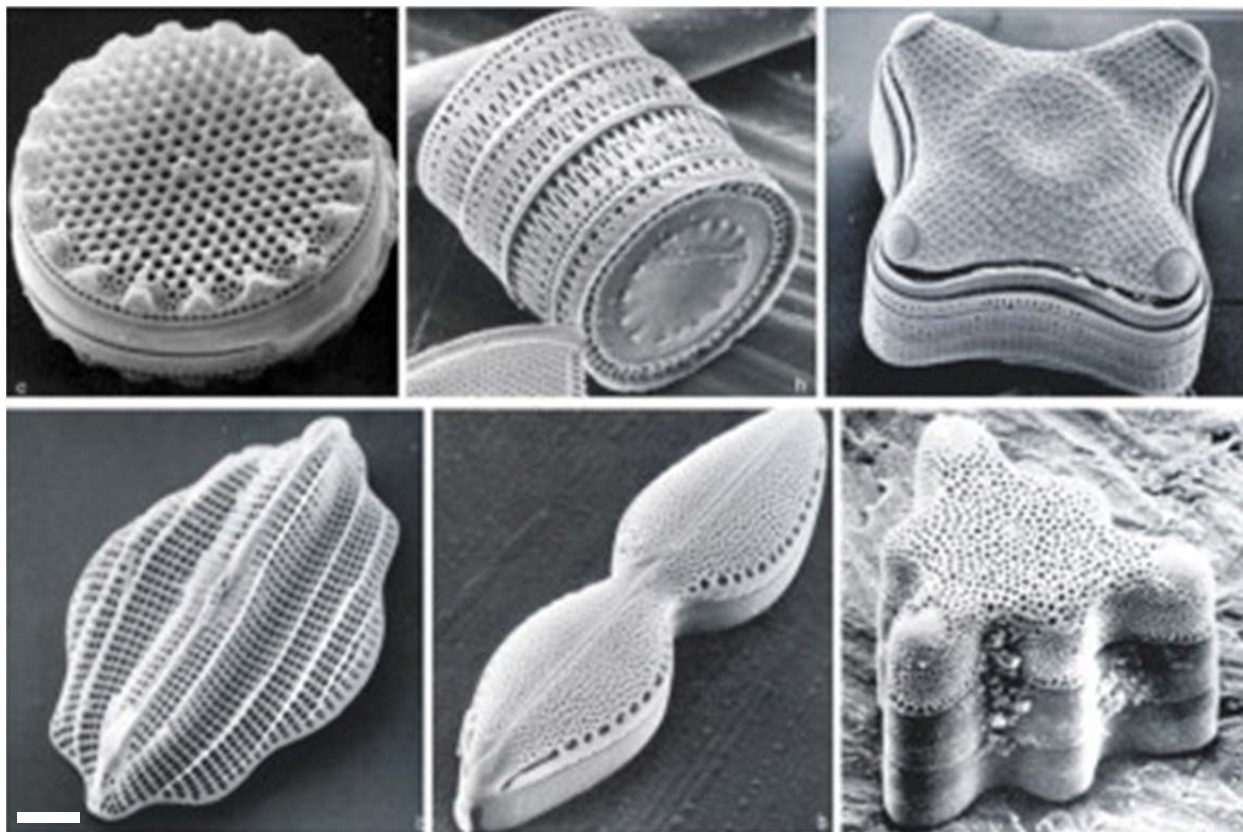


**Figure 3.3 | Biogenic structures of diatom cell walls.** Scanning electron microscopy images of different single silica cell walls. Scale bar represents 1  $\mu\text{m}$ . [Reproduced with permission from ref. 115. Copyright 2007, Elsevier.]

Owing to its polycationic and polyanionic character, silaffins are capable of facilitating the precipitation of silicic acid in solution, thus forming silica nanoparticles.<sup>119,120</sup> Both silicatein and silaffins were recently applied to promote the hydrolysis of silica precursors, namely TEOS, in order to encapsulate an enzyme in a protective silica shell, stabilizing its conformation and thus its activity.<sup>76,121</sup>

Silica finds application in various industrial sectors that span construction,<sup>122</sup> electronics,<sup>123</sup> the food industry,<sup>124</sup> and biomedical engineering/medicine.<sup>125</sup> In the latter, thanks to the large surface area of SNPs (and mesoporous SNPs: MSNPs) and to the possibility of easily tuning surface properties by chemical means,<sup>126</sup> the use of silica as a supportive material for drug and gene delivery, biocatalysis, cancer treatment, bioimaging and biosensing is being intensively

fostered.<sup>127-129</sup> The possibility of tuning both size and surface chemical properties of SNPs converts this known element into a new material. Therefore, concerns for human health in the use of nanoparticulate materials have risen in particular in biological applications and for human exposure in general.<sup>130-132</sup> Results obtained from *in vivo* experiments have shown toxicity to varying degrees. One generally accepted toxicity-causing effect of SNPs is linked to the interaction of negatively charged SiO<sup>-</sup> groups with cell membranes, resulting in cell surface distortion, thus leading to membranolysis.<sup>133</sup> A second stress factor lies in oxidative stress. Indeed, nanoparticles are considered to increase the generation of reactive oxygen species leading to necrosis or apoptosis.<sup>130,133</sup> In addition, they may induce the release of endosomal substances, cytokines and chemokines and thus induce inflammatory responses.

However, owing to the variability of nanoparticulate systems including sizes, shapes, pore structures, and surface chemistry, and to the even larger variability of cell types, a full understanding of the biocompatibility range of SNPs in different biological systems remains elusive and no general conclusions can be drawn.<sup>126,133-135</sup> This is mainly due to the different kind of cell types used in the toxicity studies (*e. g.* macrophages, HeLa cells, granulocytes or endothelial cells), which, in turn, react differently to particle uptake.<sup>132</sup> Additionally, the attempt to classify the effects of nanoparticulate systems on biological organisms is affected by the fact that the nanomaterials used possess a distribution of physicochemical properties. It is indeed expected that the same test sample may possess a distribution of surface modifications, sizes and morphologies. Nanoparticle uptake by cells is, in addition, strongly influenced by dosage and contact time. Nevertheless, it is generally recognized that exposure to smaller particles (<100 nm) leads to more significant toxic effects than are evident with larger particles.<sup>124</sup> In addition, *in vivo* experiments performed on model animals with unmodified SNPs showed that there was evidence of elimination through physiological excretion mechanisms (*e.g.* renal) and there was no

bioaccumulation, mainly because of their hydrophilic nature.<sup>136</sup> Finally, environmental toxicology results show that, owing to their non-volatile and hydrophilic nature, SNPs are inert materials and bioaccumulation is not expected to occur.<sup>136</sup> In addition no acute toxicity was found for fish or daphnia, even at high concentration exposure.<sup>136</sup>



## References

- 1 Katz, A. & Davis, M. E. Molecular imprinting of bulk, microporous silica. *Nature* **403**, 286-289 (2000).
- 2 Pauling, L. A Theory of the Structure and Process of Formation of Antibodies\*. *J. Am. Chem. Soc.* **62**, 2643-2657 (1940).
- 3 Ye, L. & Mosbach, K. Molecular Imprinting: Synthetic Materials As Substitutes for Biological Antibodies and Receptors. *Chem. Mater.* **20**, 859-868 (2008).
- 4 Wulff, G. in *Molecularly Imprinted Materials: Science and Technology* (eds Mingdi Yan & Olof Ramstrom) 59-92 (Marcel Dekker, 2005).
- 5 Sellergren, B. in *Molecularly Imprinted Polymers: Man-Made Mimics of Antibodies and Their Applications in Analytical Chemistry* (ed Börje Sellergren) 113-184 (Elsevier, 2001).
- 6 Kirsch, N. & Whitcombe, M. J. in *Molecularly Imprinted Materials: Science and Technology* (eds Mingdi Yan & Olof Ramstrom) 93-122 (Marcel Dekker, 2005).
- 7 Alexander, C. *et al.* Molecular imprinting science and technology: a survey of the literature for the years up to and including 2003. *J. Mol. Recognit.* **19**, 106-180 (2006).
- 8 Karim, K. *et al.* How to find effective functional monomers for effective molecularly imprinted polymers? *Adv. Drug Deliv. Rev.* **57**, 1795-1808 (2005).
- 9 Ramström, O. in *Molecularly Imprinted Materials: Science and Technology* (eds Mingdi Yan & Olof Ramstrom) 181-224 (Marcel Dekker, 2005).
- 10 Vlatakis, G., Andersson, L. I., Muller, R. & Mosbach, K. Drug assay using antibody mimics made by molecular imprinting. *Nature* **361**, 645-647 (1993).
- 11 Spivak, D. A. & Shea, K. J. Investigation into the scope and limitations of molecular imprinting with DNA molecules. *Anal. Chim. Acta* **435**, 65-74 (2001).
- 12 Kempe, M. Antibody-Mimicking Polymers as Chiral Stationary Phases in HPLC. *Anal. Chem.* **68**, 1948-1953 (1996).
- 13 Siemann, M., Andersson, L. I. & Mosbach, K. Selective Recognition of the Herbicide Atrazine by Noncovalent Molecularly Imprinted Polymers. *J. Agric. Food Chem.* **44**, 141-145 (1996).
- 14 Cheong, S. H. *et al.* Testosterone Receptor Binding Mimic Constructed Using Molecular Imprinting. *Macromolecules* **30**, 1317-1322 (1997).
- 15 Wulff, G. & Schauhoff, S. Enzyme-analog-built polymers. 27. Racemic resolution of free sugars with macroporous polymers prepared by molecular imprinting. Selectivity dependence on the arrangement of functional groups versus spatial requirements. *J. Org. Chem.* **56**, 395-400 (1991).
- 16 Turner, N. W. *et al.* From 3D to 2D: A Review of the Molecular Imprinting of Proteins. *Biotechnol. Prog.* **22**, 1474-1489 (2006).
- 17 Kryscio, D. R. & Peppas, N. A. Critical review and perspective of macromolecularly imprinted polymers. *Acta Biomater.* **8**, 461-473 (2012).
- 18 Ge, Y. & Turner, A. P. F. Too large to fit? Recent developments in macromolecular imprinting. *Trends Biotechnol.* **26**, 218-224 (2008).
- 19 Guo, T. Y., Xia, Y. Q., Hao, G. J., Song, M. D. & Zhang, B. H. Adsorptive separation of hemoglobin by molecularly imprinted chitosan beads. *Biomaterials* **25**, 5905-5912 (2004).
- 20 Shiomi, T., Matsui, M., Mizukami, F. & Sakaguchi, K. A method for the molecular imprinting of hemoglobin on silica surfaces using silanes. *Biomaterials* **26**, 5564-5571 (2005).
- 21 Ou, S. H., Wu, M. C., Chou, T. C. & Liu, C. C. Polyacrylamide gels with electrostatic functional groups for the molecular imprinting of lysozyme. *Anal. Chim. Acta* **504**, 163-166 (2004).
- 22 Jenik, M. *et al.* Sensing Picornaviruses Using Molecular Imprinting Techniques on a Quartz Crystal Microbalance. *Anal. Chem.* **81**, 5320-5326 (2009).
- 23 Bolisay, L. D., Culver, J. N. & Kofinas, P. Optimization of Virus Imprinting Methods To Improve Selectivity and Reduce Nonspecific Binding. *Biomacromolecules* **8**, 3893-3899 (2007).
- 24 Hayden, O., Lieberzeit, P. A., Blaas, D. & Dickert, F. L. Artificial Antibodies for Bioanalyte Detection—Sensing Viruses and Proteins. *Adv. Funct. Mater.* **16**, 1269-1278 (2006).

- 25 Polyakov, M. V. Adsorption properties and structure of silica gel. *Zhur. Fiz. Khim.* **2**, 799–804 (1931).
- 26 Dickey, F. H. The Preparation of Specific Adsorbents. *Proc. Natl. Acad. Sci. U. S. A.* **35**, 227-229 (1949).
- 27 Wulff, G. & Sarhan, A. Use of polymers with enzyme-analogous structures for the resolution of racemates. *Angew. Chem., Int. Ed. Engl.* **11**, 341 (1972).
- 28 Takagishi, T. & Klotz, I. M. Macromolecule-small molecule interactions; introduction of additional binding sites in polyethyleneimine by disulfide cross-linkages. *Biopolymers* **11**, 483-491 (1972).
- 29 Arshady, R. & Mosbach, K. Synthesis of substrate-selective polymers by host-guest polymerization. *Makromol. Chem.* **182**, 687-692 (1981).
- 30 Norrlöw, O., Glad, M. & Mosbach, K. Acrylic polymer preparations containing recognition sites obtained by imprinting with substrates. *J. Chromatogr. A* **299**, 29-41 (1984).
- 31 Glad, M., Norrlöw, O., Sellergren, B., Siegbahn, N. & Mosbach, K. Use of silane monomers for molecular imprinting and enzyme entrapment in polysiloxane-coated porous silica. *J. Chromatogr. A* **347**, 11-23 (1985).
- 32 Bowen Jenna, L., Manesiotis, P. & Allender Chris, J. Twenty years since 'antibody mimics' by molecular imprinting were first proposed: A critical perspective. *Molecular Imprinting* **1**, 35 (2013).
- 33 Goldsby, R. A., Kindt, T. J. & Osborne, B. A. *Kuby Immunology, 4th Edition*. (W. H. Freeman, 2000).
- 34 Hansel, T. T., Kropshofer, H., Singer, T., Mitchell, J. A. & George, A. J. T. The safety and side effects of monoclonal antibodies. *Nat. Rev. Drug Discovery* **9**, 325-338 (2010).
- 35 Ehrlich, P. in *The Collected Papers of Paul Ehrlich Vol. II Immunology and Cancer Research* (ed E. Himmelweit) 178-195 (Pergamon, 1957).
- 36 Fischer, E. Einfluss der Configuration auf die Wirkung der Enzyme. *Ber. Dtsch. Chem. Ges.* **27**, 2985-2993 (1894).
- 37 Kaufmann, S. H. E. Immunology's foundation: the 100-year anniversary of the Nobel Prize to Paul Ehrlich and Elie Metchnikoff. *Nat. Immunol.* **9**, 705-712 (2008).
- 38 Kaufmann, S. H. E. Elie Metchnikoff's and Paul Ehrlich's impact on infection biology. *Microbes Infect.* **10**, 1417-1419 (2008).
- 39 Landsteiner, E. & van der Scheer, J. Serological studies on azoproteins: antigens containing azocomponents with aliphatic side chains. *J. Exp. Med.* **59**, 751-768 (1934).
- 40 Landsteiner, K. & Jacobs, J. Studies on the sensitization of animals with simple chemical compounds. *J. Exp. Med.* **61**, 643-656 (1935).
- 41 Landsteiner, K. & van der Scheer, J. On Cross Reactions of Immune Sera to Azoproteins. *J. Exp. Med.* **63**, 325-339 (1936).
- 42 Goldsby, R. A., Kindt, T. J. & Osborne, B. A. in *Kuby Immunology, 4th Edition* 269-300 (W. H. Freeman, 2000).
- 43 Burnet, F. M. A modification of Jerne's theory of antibody production using the concept of clonal selection. *Aust. J. Sci.* **20**, 67-69 (1957).
- 44 Jerne, N. K. The Natural-Selection Theory of Antibody Formation. *Proc. Natl. Acad. Sci. U. S. A.* **41**, 849-857 (1955).
- 45 Nossal, G. J. V. & Lederberg, J. Antibody Production by Single Cells. *Nature* **181**, 1419-1420 (1958).
- 46 Tonegawa, S. Somatic generation of antibody diversity. *Nature* **302**, 575-581 (1983).
- 47 Goldsby, R. A., Kindt, T. J. & Osborne, B. A. in *Kuby Immunology, 4th Edition* 115-147 (W. H. Freeman, 2000).
- 48 Ramström, O. & Mosbach, K. Synthesis and catalysis by molecularly imprinted materials. *Curr. Opin. Chem. Biol.* **3**, 759-764 (1999).
- 49 Wulff, G. in *Molecularly Imprinted Materials: Science and Technology* (eds Mingdi Yan & Olof Ramstrom) 59-92 (Marcel Dekker, 2005).
- 50 Wulff, G., Vesper, W., Grobe-Einsler, R. & Sarhan, A. Enzyme-analogue built polymers, 4. On the synthesis of polymers containing chiral cavities and their use for the resolution of racemates. *Makromol. Chem.* **178**, 2799-2816 (1977).

- 51 Shea, K. J. & Dougherty, T. K. Molecular recognition on synthetic amorphous surfaces. The influence of functional group positioning on the effectiveness of molecular recognition. *J. Am. Chem. Soc.* **108**, 1091-1093 (1986).
- 52 Wulff, G., Best, W. & Akelah, A. Enzyme-analogue built polymers, 17 Investigations on the racemic resolution of amino acids. *React. Polym., Ion Exch., Sorbents* **2**, 167-174 (1984).
- 53 Mayes, A. G. & Whitcombe, M. J. Synthetic strategies for the generation of molecularly imprinted organic polymers. *Adv. Drug Deliv. Rev.* **57**, 1742-1778 (2005).
- 54 Yilmaz, E., Schmidt, R. H. & Mosbach, K. in *Molecularly Imprinted Materials: Science and Technology* (eds Mingdi Yan & Olof Ramstrom) 25-58 (Marcel Dekker, 2005).
- 55 Kirsch, N. & Whitcombe, M. J. in *Molecularly Imprinted Materials: Science and Technology* (eds Mingdi Yan & Olof Ramstrom) 93-122 (Marcel Dekker, 2005).
- 56 Sellergren, B. & Andersson, L. Molecular recognition in macroporous polymers prepared by a substrate analog imprinting strategy. *J. Org. Chem.* **55**, 3381-3383 (1990).
- 57 Caro, E. *et al.* Non-covalent and semi-covalent molecularly imprinted polymers for selective on-line solid-phase extraction of 4-nitrophenol from water samples. *J. Chromatogr. A* **963**, 169-178 (2002).
- 58 Ikegami, T., Mukawa, T., Nariai, H. & Takeuchi, T. Bisphenol A-recognition polymers prepared by covalent molecular imprinting. *Anal. Chim. Acta* **504**, 131-135 (2004).
- 59 Whitcombe, M. J., Rodriguez, M. E., Villar, P. & Vulfson, E. N. A New Method for the Introduction of Recognition Site Functionality into Polymers Prepared by Molecular Imprinting: Synthesis and Characterization of Polymeric Receptors for Cholesterol. *J. Am. Chem. Soc.* **117**, 7105-7111 (1995).
- 60 Yan, M. & Ramstrom, O., Eds., *Molecularly Imprinted Materials: Science and Technology*, (Marcel Dekker, New York, 2005), pp. 734.
- 61 Hilt, J. Z. & Byrne, M. E. Configurational biomimesis in drug delivery: molecular imprinting of biologically significant molecules. *Adv. Drug Deliv. Rev.* **56**, 1599-1620 (2004).
- 62 Puoci, F. *et al.* Molecularly imprinted polymers in drug delivery: state of art and future perspectives. *Expert Opin. Drug Deliv.* **8**, 1379-1393 (2011).
- 63 Dickert, F. *et al.* Chemical Sensors – from Molecules, Complex Mixtures to Cells – Supramolecular Imprinting Strategies. *Sensors* **3**, 381-392 (2003).
- 64 Severin, K. in *Molecularly Imprinted Materials: Science and Technology* (eds Mingdi Yan & Olof Ramstrom) 619-640 (Marcel Dekker, 2005).
- 65 Ruigrok, V. J. B., Levisson, M., Eppink, M. H. M., Smidt, H. & van der Oost, J. Alternative affinity tools: more attractive than antibodies? *Biochem. J.* **436**, 1-13 (2011).
- 66 Zhang, H., Ye, L. & Mosbach, K. Non-covalent molecular imprinting with emphasis on its application in separation and drug development. *J. Mol. Recognit.* **19**, 248-259 (2006).
- 67 Nicholls, I. A. & Rosengren, J. P. Molecular imprinting of surfaces. *Bioseparation* **10**, 301-305 (2001).
- 68 Verheyen, E. *et al.* Challenges for the effective molecular imprinting of proteins. *Biomaterials* **32**, 3008-3020 (2011).
- 69 Takeuchi, T. & Hishiya, T. Molecular imprinting of proteins emerging as a tool for protein recognition. *Org. Biomol. Chem.* **6**, 2459-2467 (2008).
- 70 Matsunaga, T., Hishiya, T. & Takeuchi, T. Surface plasmon resonance sensor for lysozyme based on molecularly imprinted thin films. *Anal. Chim. Acta* **591**, 63-67 (2007).
- 71 Kimhi, O. & Bianco-Peled, H. Study of the Interactions between Protein-Imprinted Hydrogels and Their Templates. *Langmuir* **23**, 6329-6335 (2007).
- 72 Hawkins, D. M., Stevenson, D. & Reddy, S. M. Investigation of protein imprinting in hydrogel-based molecularly imprinted polymers (HydroMIPs). *Anal. Chim. Acta* **542**, 61-65 (2005).
- 73 Janiak, D. S., Ayyub, O. B. & Kofinas, P. Effects of Charge Density on the Recognition Properties of Molecularly Imprinted Polymeric Hydrogels. *Macromolecules* **42**, 1703-1709 (2009).
- 74 Wulff, G. Molecular Imprinting in Cross-Linked Materials with the Aid of Molecular Templates—A Way towards Artificial Antibodies. *Angew. Chem., Int. Ed. Engl.* **34**, 1812-1832 (1995).

- 75 Gill, I. & Ballesteros, A. Bioencapsulation within synthetic polymers (Part 1): sol-gel encapsulated biologicals. *Trends Biotechnol.* **18**, 282-296 (2000).
- 76 Betancor, L. & Luckarift, H. R. Bioinspired enzyme encapsulation for biocatalysis. *Trends Biotechnol.* **26**, 566-572 (2008).
- 77 Sanchez, C., Arribart, H. & Giraud Guille, M. M. Biomimetism and bioinspiration as tools for the design of innovative materials and systems. *Nat. Mater.* **4**, 277-288 (2005).
- 78 Tatemichi, M., Sakamoto, M.-a., Mizuhata, M., Deki, S. & Takeuchi, T. Protein-Templated Organic/Inorganic Hybrid Materials Prepared by Liquid-Phase Deposition. *J. Am. Chem. Soc.* **129**, 10906-10910 (2007).
- 79 Deki, S. *et al.* Growth of metal oxide thin films from aqueous solution by liquid phase deposition method. *Solid State Ionics* **151**, 1-9 (2002).
- 80 Lin, H.-Y. *et al.* The microcontact imprinting of proteins: The effect of cross-linking monomers for lysozyme, ribonuclease A and myoglobin. *Biosens. Bioelectron.* **22**, 534-543 (2006).
- 81 Shi, H., Tsai, W.-B., Garrison, M. D., Ferrari, S. & Ratner, B. D. Template-imprinted nanostructured surfaces for protein recognition. *Nature* **398**, 593-597 (1999).
- 82 Shi, H. & Ratner, B. D. Template recognition of protein-imprinted polymer surfaces. *J. Biomed. Mater. Res.* **49**, 1-11 (2000).
- 83 Copeland, R. A., Harpel, M. R. & Tummino, P. J. Targeting enzyme inhibitors in drug discovery. *Expert Opin. Ther. Targets* **11**, 967-978 (2007).
- 84 Copeland, R. A., Ed., *Evaluation of Enzyme Inhibitors in Drug Discovery: A Guide to Medicinal Chemists and Pharmacologists*, (John Wiley & Sons, Chichester, 2005), pp. 296.
- 85 Cutivet, A., Schembri, C., Kovensky, J. & Haupt, K. Molecularly Imprinted Microgels as Enzyme Inhibitors. *J. Am. Chem. Soc.* **131**, 14699-14702 (2009).
- 86 Flint, S. J., Enquist, L. W., Racaniello, V. R. & Skalka, A. M. *Principles of Virology, 3rd Edition: Volume I; Molecular Biology*. (ASM Press, 2009).
- 87 Flint, S. J., Enquist, L. W., Racaniello, V. R., Skalka, A. M. & Editors. in *Principles of Virology, 3rd Edition: Volume I; Molecular Biology* 2-23 (ASM Press, 2009).
- 88 Flint, S. J., Enquist, L. W., Racaniello, V. R. & Skalka, A. M. in *Principles of Virology, 3rd Edition: Volume I; Molecular Biology* 82-125 (ASM Press, 2009).
- 89 Baltimore, D. Expression of animal virus genomes. *Bacteriol. Rev.* **35**, 235-241 (1971).
- 90 Miller, E. S. *et al.* Bacteriophage T4 Genome. *Microbiol. Mol. Biol. Rev.* **67**, 86-156 (2003).
- 91 Fraenkel-Conrat, H. & Williams, R. C. Reconstitution of Active Tobacco Mosaic Virus from Its Inactive Protein and Nucleic Acid Components. *Proc. Natl. Acad. Sci. U. S. A.* **41**, 690-698 (1955).
- 92 Miller, J. L. *et al.* Three-dimensional reconstruction of Heterocapsa circularisquama RNA virus by electron cryo-microscopy. *J. Gen. Virol.* **92**, 1960-1970 (2011).
- 93 Zhang, W. *et al.* Placement of the Structural Proteins in Sindbis Virus. *J. Virol.* **76**, 11645-11658 (2002).
- 94 Flint, S. J., Enquist, L. W., Racaniello, V. R., Skalka, A. M. & Editors. in *Principles of Virology, 3rd Edition: Volume I; Molecular Biology* 24-48 (ASM Press, 2009).
- 95 Mouquet, H. & Nussenzweig, M. C. HIV: Roadmaps to a vaccine. *Nature* **496**, 441-442 (2013).
- 96 Inchauspé, G., Bach, G., Martin, P. & Bonnefoy, J. Y. Vaccination Against Hepatitis B and C: Towards Therapeutic Application. *Int. Rev. Immunol.* **28**, 7-19 (2009).
- 97 Schiller, J. T. & Lowy, D. R. Understanding and learning from the success of prophylactic human papillomavirus vaccines. *Nat. Rev. Microbiol.* **10**, 681-692 (2012).
- 98 Thibaut, H. J., De Palma, A. M. & Neyts, J. Combating enterovirus replication: State-of-the-art on antiviral research. *Biochem. Pharmacol.* **83**, 185-192 (2012).
- 99 Herrero, L. J. *et al.* Dengue virus therapeutic intervention strategies based on viral, vector and host factors involved in disease pathogenesis. *Pharmacol. Ther.* **137**, 266-282 (2013).
- 100 Kawaoka, Y. & Neumann, G. in *Influenza Virus: Methods and Protocols* *Methods in Molecular Biology* (eds Yoshihiro Kawaoka & Gabriele Neumann) 1-9 (Springer, 2012).
- 101 Morens, D. M., Folkers, G. K. & Fauci, A. S. Emerging infections: a perpetual challenge. *Lancet Infect. Dis.* **8**, 710-719 (2008).

- 102 Dickert, F. *et al.* Bioimprinted QCM sensors for virus detection—screening of plant sap. *Anal. Bioanal. Chem.* **378**, 1929-1934 (2004).
- 103 Lieberzeit, P. A. *et al.* Imprinting as a versatile platform for sensitive materials – nanopatterning of the polymer bulk and surfaces. *Sens. Actuators B* **111–112**, 259-263 (2005).
- 104 Bolisay, L. D., Culver, J. N. & Kofinas, P. Molecularly imprinted polymers for tobacco mosaic virus recognition. *Biomaterials* **27**, 4165-4168 (2006).
- 105 Sankarakumar, N. & Tong, Y. W. Preventing viral infections with polymeric virus catchers: a novel nanotechnological approach to anti-viral therapy. *J. Mater. Chem. B* **1**, 2031-2037 (2013).
- 106 Rachkov, A. & Minoura, N. Recognition of oxytocin and oxytocin-related peptides in aqueous media using a molecularly imprinted polymer synthesized by the epitope approach. *J. Chromatogr. A* **889**, 111-118 (2000).
- 107 Tai, D.-F., Lin, C.-Y., Wu, T.-Z. & Chen, L.-K. Recognition of Dengue Virus Protein Using Epitope-Mediated Molecularly Imprinted Film. *Anal. Chem.* **77**, 5140-5143 (2005).
- 108 Lu, C.-H. *et al.* Sensing HIV related protein using epitope imprinted hydrophilic polymer coated quartz crystal microbalance. *Biosens. Bioelectron.* **31**, 439-444 (2012).
- 109 Cai, D. *et al.* A molecular-imprint nanosensor for ultrasensitive detection of proteins. *Nat. Nanotechnol.* **5**, 597-601 (2010).
- 110 Xiao, P., Corvini, P., Dudal, Y. & Shahgaldian, P. Design of Cyclodextrin-Based Photopolymers with Enhanced Molecular Recognition Properties: A Template-Free High-Throughput Approach. *Macromolecules* **45**, 5692-5697 (2012).
- 111 Stöber, W., Fink, A. & Bohn, E. Controlled growth of monodisperse silica spheres in the micron size range. *J. Colloid Interface Sci.* **26**, 62-69 (1968).
- 112 Carey, J. C. & Fulweiler, R. W. The Terrestrial Silica Pump. *PLoS One* **7**, e52932 (2012).
- 113 Tréguer, P. *et al.* The Silica Balance in the World Ocean: A Reestimate. *Science* **268**, 375-379 (1995).
- 114 Perry, C. C. Silicification: The Processes by Which Organisms Capture and Mineralize Silica. *Rev. Mineral. Geochem.* **54**, 291-327 (2003).
- 115 Kröger, N. Prescribing diatom morphology: toward genetic engineering of biological nanomaterials. *Curr. Opin. Chem. Biol.* **11**, 662-669 (2007).
- 116 Shimizu, K., Cha, J., Stucky, G. D. & Morse, D. E. Silicatein  $\alpha$ : Cathepsin L-like protein in sponge biosilica. *Proc. Natl. Acad. Sci. U. S. A.* **95**, 6234-6238 (1998).
- 117 Schroder, H. C., Wang, X., Tremel, W., Ushijima, H. & Muller, W. E. G. Biofabrication of biosilica-glass by living organisms. *Nat. Prod. Rep.* **25**, 455-474 (2008).
- 118 Cha, J. N. *et al.* Silicatein filaments and subunits from a marine sponge direct the polymerization of silica and silicones in vitro. *Proc. Natl. Acad. Sci. U. S. A.* **96**, 361-365 (1999).
- 119 Kröger, N., Deutzmann, R. & Sumper, M. Polycationic Peptides from Diatom Biosilica That Direct Silica Nanosphere Formation. *Science* **286**, 1129-1132 (1999).
- 120 Kröger, N., Deutzmann, R. & Sumper, M. Silica-precipitating Peptides from Diatoms. The chemical structure of silaffin-A from *Cylindrotheca fusiformis*. *J. Biol. Chem.* **276**, 26066-26070 (2001).
- 121 Luckarift, H. R., Spain, J. C., Naik, R. R. & Stone, M. O. Enzyme immobilization in a biomimetic silica support. *Nat. Biotechnol.* **22**, 211-213 (2004).
- 122 Morse, D. E. Silicon biotechnology: harnessing biological silica production to construct new materials. *Trends Biotechnol.* **17**, 230-232 (1999).
- 123 Kenneth, K. O. *et al.* On-chip antennas in silicon ICs and their application. *IEEE Trans. Electron Devices* **52**, 1312-1323 (2005).
- 124 Jaganathan, H. & Godin, B. Biocompatibility assessment of Si-based nano- and micro-particles. *Adv. Drug Deliv. Rev.* **64**, 1800-1819 (2012).
- 125 Lewinski, N., Colvin, V. & Drezek, R. Cytotoxicity of Nanoparticles. *Small* **4**, 26-49 (2008).
- 126 Asefa, T. & Tao, Z. Biocompatibility of Mesoporous Silica Nanoparticles. *Chem. Res. Toxicol.* **25**, 2265-2284 (2012).
- 127 Wu, S.-H., Hung, Y. & Mou, C.-Y. Mesoporous silica nanoparticles as nanocarriers. *Chem. Commun.* **47**, 9972-9985 (2011).

- 128 Schroeder, A. *et al.* Treating metastatic cancer with nanotechnology. *Nat. Rev. Cancer* **12**, 39-50 (2012).
- 129 Davis, M. E., Chen, Z. & Shin, D. M. Nanoparticle therapeutics: an emerging treatment modality for cancer. *Nat. Rev. Drug Discovery* **7**, 771-782 (2008).
- 130 Sun, L. *et al.* Cytotoxicity and mitochondrial damage caused by silica nanoparticles. *Toxicol. in Vitro* **25**, 1619-1629 (2011).
- 131 Kunzmann, A. *et al.* Toxicology of engineered nanomaterials: Focus on biocompatibility, biodistribution and biodegradation. *Biochim. Biophys. Acta, Gen. Subj.* **1810**, 361-373 (2011).
- 132 Mahmoudi, M., Azadmanesh, K., Shokrgozar, M. A., Journeay, W. S. & Laurent, S. Effect of Nanoparticles on the Cell Life Cycle. *Chem. Rev.* **111**, 3407-3432 (2011).
- 133 Tarn, D. *et al.* Mesoporous Silica Nanoparticle Nanocarriers: Biofunctionality and Biocompatibility. *Acc. Chem. Res.* **46**, 792-801 (2013).
- 134 Li, Z., Barnes, J. C., Bosoy, A., Stoddart, J. F. & Zink, J. I. Mesoporous silica nanoparticles in biomedical applications. *Chem. Soc. Rev.* **41**, 2590-2605 (2012).
- 135 Tang, F., Li, L. & Chen, D. Mesoporous Silica Nanoparticles: Synthesis, Biocompatibility and Drug Delivery. *Adv. Mater.* **24**, 1504-1534 (2012).
- 136 Fruijtier-Pöllöth, C. The toxicological mode of action and the safety of synthetic amorphous silica—A nanostructured material. *Toxicology* **294**, 61-79 (2012).

# 2

Objective of the research

The possibility of producing man-made mimics of natural antibodies has been inspiring researchers since the seminal works of Wulff (1972)<sup>1</sup> and Mosbach (1981).<sup>2</sup> In 1972, Wulff reported the possibility of discriminating between enantiomers of glyceric acid using an organic, imprinted polymer produced according to the so-called "covalent approach". In contrast to Wulff, in his 1981 study Mosbach proposed the "non-covalent approach". The simplicity of the method introduced by Mosbach triggered an explosion in MIP reports, as recorded since the 90s.<sup>3</sup> The molecular imprinting approaches that developed allowed the production of a large range of polymers targeting a large variety of templates spanning small molecules to more challenging proteins and viruses. Nevertheless, imprinting approaches using viruses as templates remain unsatisfactory (cf. Virus imprinting, page 27).

The main topic of this thesis is the development of a versatile, synthetic strategy leading to the molecular imprinting of viruses possessing a non-enveloped icosahedral morphology. Two major challenges are associated with imprinting large, self-assembled biological structures: the size, which limits the viral mass transfer within the produced imprinted material; the fragility of the self-assembled nature, which requires the use of bio-friendly polymerization conditions. To address these issues, it was developed a novel surface imprinting approach based on the surface-initiated growth of a hybrid organic-inorganic polymeric layer (polysilsesquioxane, named the recognition layer) in the presence of the immobilized template virus. The developed material is named virus imprinted particles, or VIPs.

A series of questions of fundamental relevance was posed at the start of the project and addressed during its development:



**Is a surface imprinting strategy consistent with the conditions required to maintain the integrity of the viral morphology, a self-assembled structure of 180 protein subunits?**

- Imprinting of the virus in the native conformation is crucial for the formation of specific binding sites. To this end, the imprinting conditions must prevent the unfolding of the virus self-assembly.
- In addition, surface-initiated organosilane polycondensation must occur in water in the presence of immobilized virus. Organosilane hydrolysis is the predominant reaction occurring in acidic solution, while the hydrolytic condensation occurs rapidly in an alkaline condition.<sup>4</sup> Thus, in order to favor condensation reactions and recognition layer growth, alkaline conditions are required. Nevertheless, in alkaline solution the model viral particles used in this project disassemble.

**Are organosilane hydrolysis and condensation (*i.e.* polysilsesquioxane deposition) the predominant reactions around the viruses, leading to the formation of the viral replica?**

- It could be theorized that the use of organosilanes, available to establish non-covalent interactions with the viral chemical functionalities, would favor the formation of a chemical imprint of the virus rather than a simple shape imprint. If so, a similar process that mimics the silicatein protein mode of action (catalyst for silica biomineralization)<sup>5</sup> could be obtained.
- The combination of both shape and chemical imprints of the virus is expected to have a beneficial impact on VIP binding performance.

**Does a surface imprinting strategy allow the tuning of the binding performance of a recognition material?**

- It is probable that varying the composition of the organosilanes used to build the recognition layer would have an effect on the binding capacity of the VIPs.
- Secondly, it could be hypothesized that the affinity of the material can be tuned by varying the recognition layer thickness. Indeed, with a thicker recognition layer the number of contact points between virus and imprint is greater than with a thinner recognition layer. This could have an effect on the affinity of the particles for the template virus.

# 3

VIP synthesis and characterization

## Virus imprinted particles – Concept

The synthetic strategy leading to the creation of virus recognition sites at the surface of silica nanoparticles (SNPs) includes: (i) immobilization of the target virus on the SNP surface, (ii) surface-initiated growth of a polysilsesquioxane layer, named the recognition layer, and (iii) removal of the template virus, thus freeing the imprints (Fig. 3.1).<sup>6</sup> The final particles are named virus imprinted particles, or VIPs.

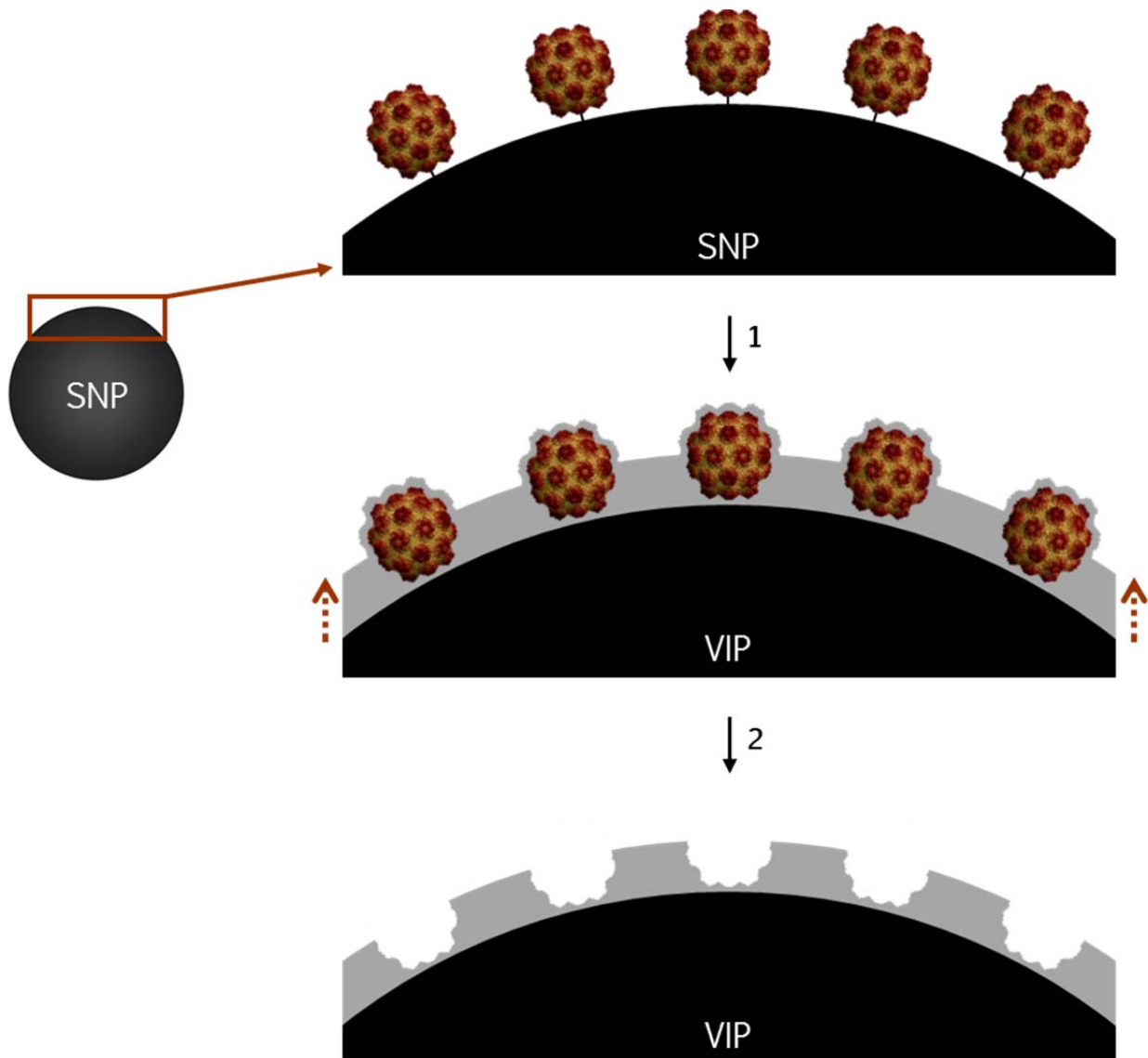


**Figure 3.1 | VIP synthetic strategy.** The template virus was immobilized on amino modified SNPs using glutaraldehyde as cross-linker. (1) An organosilane mixture was then added and the recognition layer was grown. (2) Viruses are removed in order to free the imprints. SNPs: silica nanoparticles; VIPs: virus imprinted particles.

## Stöber silica nanoparticles

Highly monodisperse SNPs ( $\text{SiO}_2$ ) were used as carrier material to design VIPs. They were produced following the method developed by Stöber.<sup>7</sup> The final protocol used to produce the SNPs is described elsewhere.<sup>8</sup> A relatively small target diameter of approximately 400 nm was chosen in order to have a relatively high surface-area-to-volume ratio ( $1.5 \times 10^7 \text{ m}^{-1}$ , with a surface-area-to-mass ratio of  $7.7 \text{ m}^2/\text{g}$ ), yet compatible with an appropriate, single particle surface capable of accommodating a relevant number of virions (30 nm in diameter). Finally, a constant temperature of  $20^\circ\text{C}$  throughout the polycondensation reaction yielded highly monodisperse SNPs (Fig. 3.2).

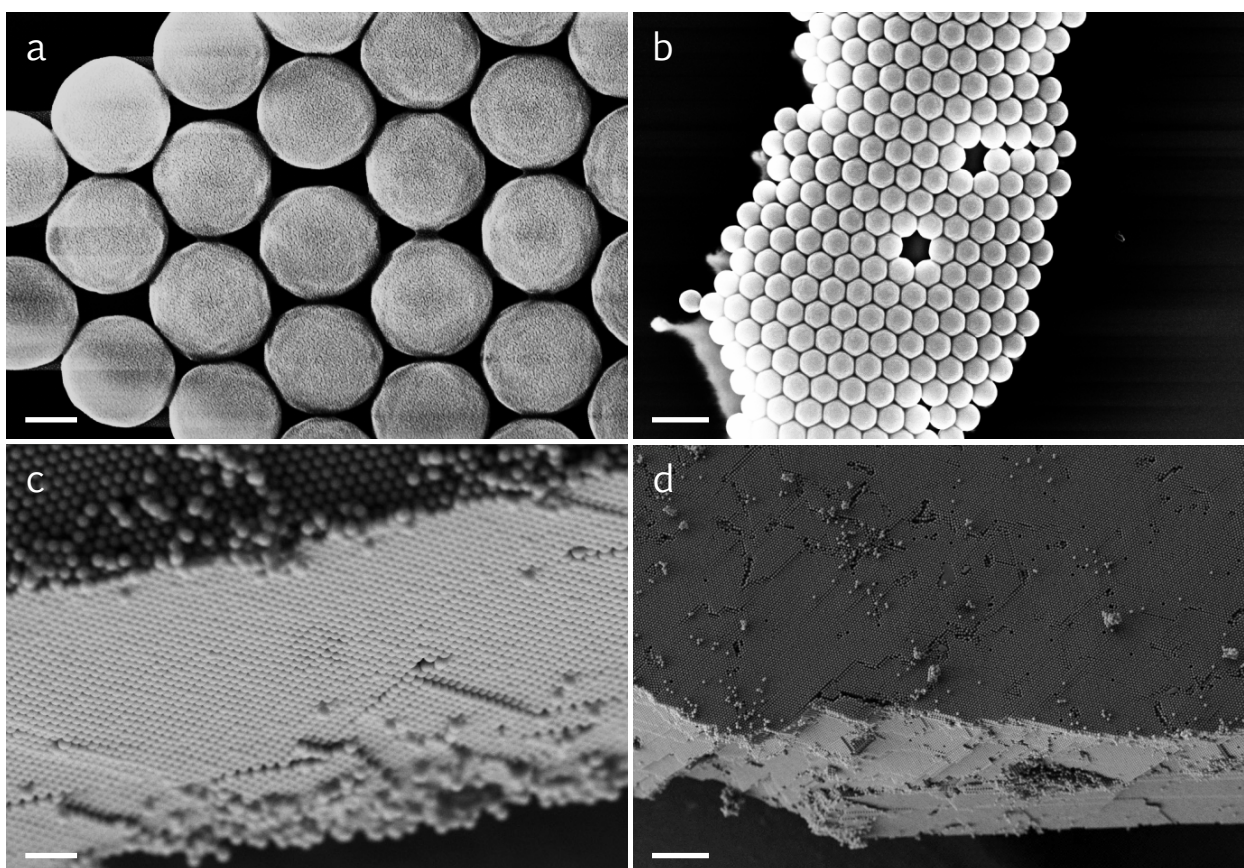


**Figure 3.2** | Representative FESEM micrographs of the produced SNPs. Colloidal, self-assembled two- and three-dimensional arrays formed by the starting SNPs at different magnifications. Scale bar represents: (a) 200 nm; (b) 1  $\mu\text{m}$ ; (c) 2  $\mu\text{m}$ ; (d) 10  $\mu\text{m}$ ;

The statistical analysis of micrographs acquired using high-resolution field emission scanning electron microscopy (FESEM) and size analysis software

revealed a mean diameter of 410 nm. The high propensity of these nanoparticles to self-assemble into three-dimensional colloidal arrays represents additional evidence of their high monodispersity. This is beneficial asset, allowing more accurate statistical particle size analyses and thus recognition layer thickness measurement.

## Model viruses

The model viruses used to develop the imprinting strategy possess a non-enveloped icosahedral morphology. They are small, single-stranded RNA plant viruses: tomato bushy stunt virus (TBSV) and turnip yellow mosaic virus (TYMV) (Table 3.1; Fig. 3.3). Both viruses belong to group IV of the Baltimore classification.<sup>9</sup> Indeed, they possess a positive, single stranded RNA readily available for protein synthesis once inside the vegetal cell ((+)ssRNA).

	TYMV	TBSV
<i>Genome</i>		
Composition	Monopartite (+)ssRNA	Monopartite (+)ssRNA
MW (KDa)	$1.9 \times 10^3$	$1.67 \times 10^3$
Kb	6.32	4.78
<i>Capsid protein</i>		
MW (KDa)	20.088	40.54
Number of aa	180	387
Copies	180	180
<i>Viral particle</i>		
MW (KDa)	$5.5 \times 10^3$	$9 \times 10^3$
Diameter (nm)	28	33
pI	3.8	4.1

**Table 3.1 | Structural properties of the model viruses used as the template to produce the VIPs.** MW: molecular weight; aa: amino acid; pI: isoelectric point.

TBSV, belonging to the tombusviridae family, is composed of a unique capsid protein of a molecular weight of 40 kDa that self-assembles to form the viral

capsid.<sup>9</sup> The encapsulated ribonucleic acid has a length of 4.78 kb and a molecular weight of  $1.67 \times 10^3$  kDa. The entire viral particle has a diameter of 33 nm, a molecular weight of  $9.0 \times 10^3$  kDa and an isoelectric point (pI) of 4.1 (Table 3.1).<sup>9</sup> TYMV belongs to the tymoviridae family and its viral capsid is a self-assembly of a unique capsid protein of 20 kDa molecular weight.<sup>9</sup> The encapsulated ribonucleic acid has a length of 6.32 kb and a molecular weight of  $1.9 \times 10^3$  kDa. The entire viral particle has a diameter of 28 nm, a molecular weight of  $5.5 \times 10^3$  kDa and a pI of 3.8 (Table 3.1).<sup>9</sup>

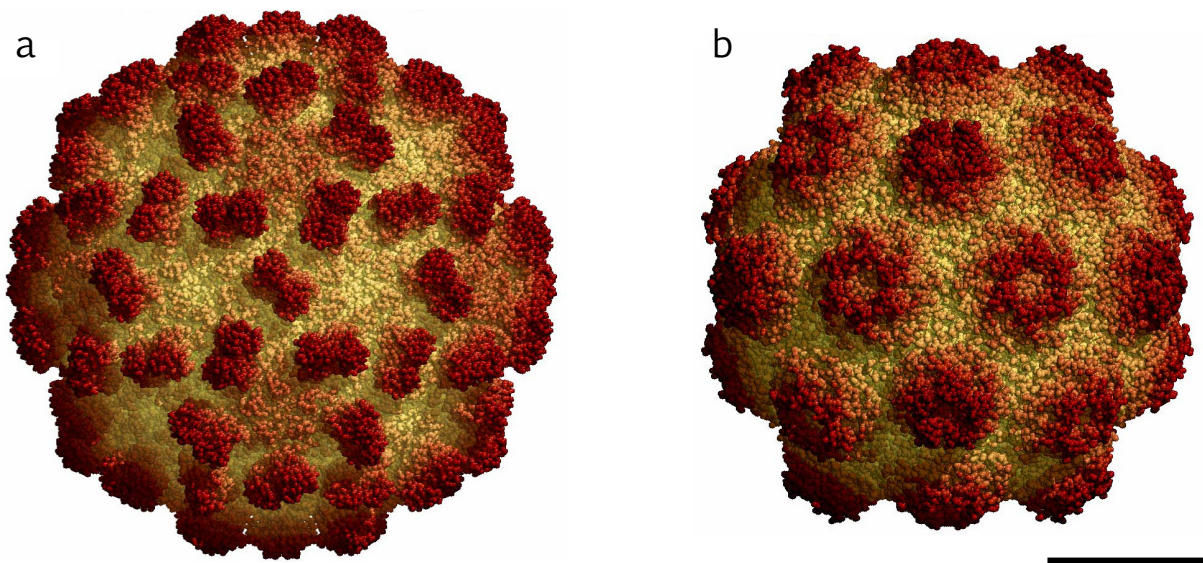


**Figure 3.3 | Surface rendering images of the model viruses used as a template to produce the VIPs.** Images of the surface of the virions of (a) TBSV and (b) TYMV were computed using VIPER particle ExploreR<sup>2</sup> (10), based on high resolution X-ray crystallographic data.<sup>11,12</sup> Scale bar represents 10 nm.

The capsid proteins of these viruses assemble into morphological units, named capsomers, of five (pentamers) and six (hexamers) proteins. In 1962, Casper and Klug described the so-called triangular number (T-number) concept, in order to describe the relationship between pentamer and hexamer symmetry in the capsid shell.<sup>13</sup> Both TBSV and TYMV viruses possess a  $T = 3$  icosahedral surface lattice morphology. Therefore, their morphology could overlay a truncated icosahedron, an Archimedean solid with 12 regular pentagonal faces and 20 regular hexagonal faces.

These viruses were chosen as models for two main reasons: primarily, because the viral icosahedral morphology is one of the most diffuse in nature, due to free energy minimization of the capsid protein assembly.<sup>14,15</sup> Indeed, a series of relevant, pathogenic, non-enveloped viruses possess this morphology, including adenoviruses, papillomaviruses, enteroviruses, polioviruses and hepatitis viruses, to name but a few. Secondly, icosahedral symmetry reduces the number of possible orientations assumed by the viruses once immobilized on the silica nanoparticle surface. As a consequence, the complexity of the system required to establish proof of concept was reduced.

## VIP synthesis

As previously stated, grafting the viral particles to the surface of SNPs was the initial VIP synthesis step. In order to provide anchoring amine moieties at the surface of the SNPs for this cross-linking, they were partially modified with aminopropyltriethoxysilane (APTES). A low density of amine groups at the SNP surface was essential for further synthetic steps, for three main reasons. Indeed, it could be hypothesized that increasing the amino group surface density would increase the anchoring points between each virus and the SNP surface. The excess of anchoring points could, in turn, increase the possibility of viral particle disassembly, owing to a flattening effect of the icosahedral viral particles on the particle surface. Secondly, a low density of amino groups was necessary in order to leave enough silanol groups available for the surface-initiated organosilane polycondensation reaction, thus securing the recognition layer to the particle surface. Finally, controlling the amine group density at this step of the synthesis was expected to provide the opportunity to control the imprint density at the SNP surface. In order to find the appropriate level of amino modification, a series of conditions was assayed (0.13, 0.4, 0.8 and 1.47  $\mu\text{mol}$  of APTES per mg of SNPs for 30 minutes). The final control of amino group surface density was achieved by applying fairly low concentrations of APTES and



short reaction times in water (1.47  $\mu\text{mol}$  APTES per mg of SNPs, 30 minutes). Results are reported and discussed on page 77. Further coupling of the virions, through lysine residues, was carried out in water using glutaraldehyde as a homo-bifunctional crosslinker. The choice of a “weak” coupling strategy was guided by the need to release, at the end of the procedure, the template virus to free the binding sites. Aldehydes and primary amines react to form an imine bond (carbon nitrogen double bond).<sup>16</sup> The reaction mechanism presupposes the nucleophilic attack of the nitrogen electron lone pair on the carbon of aldehyde group to yield a Schiff base (imine).<sup>16</sup> Imine bond stability is affected by pH. It is indeed well known that a Schiff base undergoes rapid hydrolysis in acidic condition upon nitrogen protonation.<sup>17</sup>

After the coupling of the virus to the surface of the SNPs, the next step consists of growth of an additional polysilsesquioxane layer using organosilanes as building blocks. The layer grows from the surface of the nanoparticles, owing to the presence of silanol groups, thus partially embedding the immobilized virions. As this layer was expected to be the recognition part of the VIPs, its building blocks were selected so as to possess the ability to establish non-covalent bonds with the virus surface.

## Organosilanes

Protein – protein interactions are known to be influenced by a number of factors not yet fully understood. Nevertheless, a set of principles was established and a series of amino acids was defined as “hot-spots”, since they contribute significantly to the stability of protein – protein interactions.<sup>18</sup> Examples of these amino acids include isoleucine and valine (aliphatic), tryptophan (aromatic), serine and threonine (neutral polar), and arginine (cationic).<sup>18,19</sup>

To produce the recognition layer following a protein mimetic approach, a class of molecules, named organosilanes (or ORMOSIL, organically modified silanes) was used. They are derivatives of alkyl esters of orthosilicic acid, possessing a silicon-carbon bond. The experimental findings reported here were achieved exclusively using ethyl ester organosilane derivatives of orthosilicic acid (tetraethyl orthosilicate, TEOS) (Fig. 3.4).

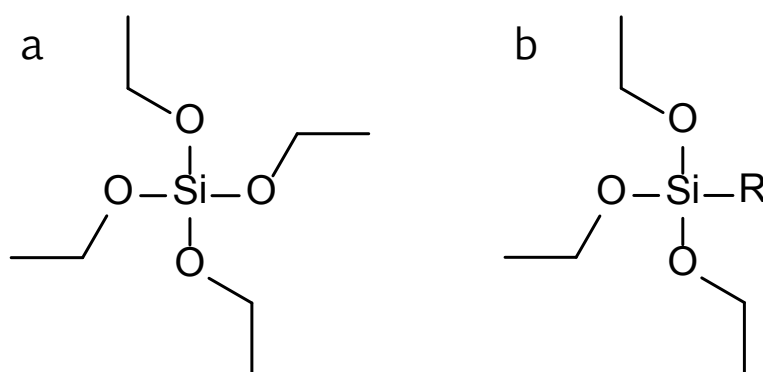


**Figure 3.4** | TEOS and general structure of the organosilanes used to produce the VIPs. (a) tetraethyl orthosilicate, TEOS; (b) general organosilane structure.

The ability of organosilanes to hydrolyze and thus condensate in water at ambient conditions (room temperature, slightly acidic or basic pH), was consistent with the conditions needed to maintain the structural stability of biological macromolecules. Additionally, the variety of commercially available organosilane variants makes these molecules excellent candidates as building blocks for the recognition layer. The final matrix resulting from the polycondensation of the organosilanes, named polysilsesquioxane, is a hybrid material combining the structural stability of the siloxane bond and the features of the organic R groups. From the molecular imprinting standpoint, the moieties carried by the organosilanes provide the opportunity to establish non-covalent interactions with the chemical functionalities of the template molecule. A series of organosilanes that mimic amino acid lateral chains was selected. It comprises

aliphatic (propyl), aromatic (benzyl), neutral polar (alcohol), cationic (amine) and anionic (surface silanol) chemical functions (Fig. 3.5).

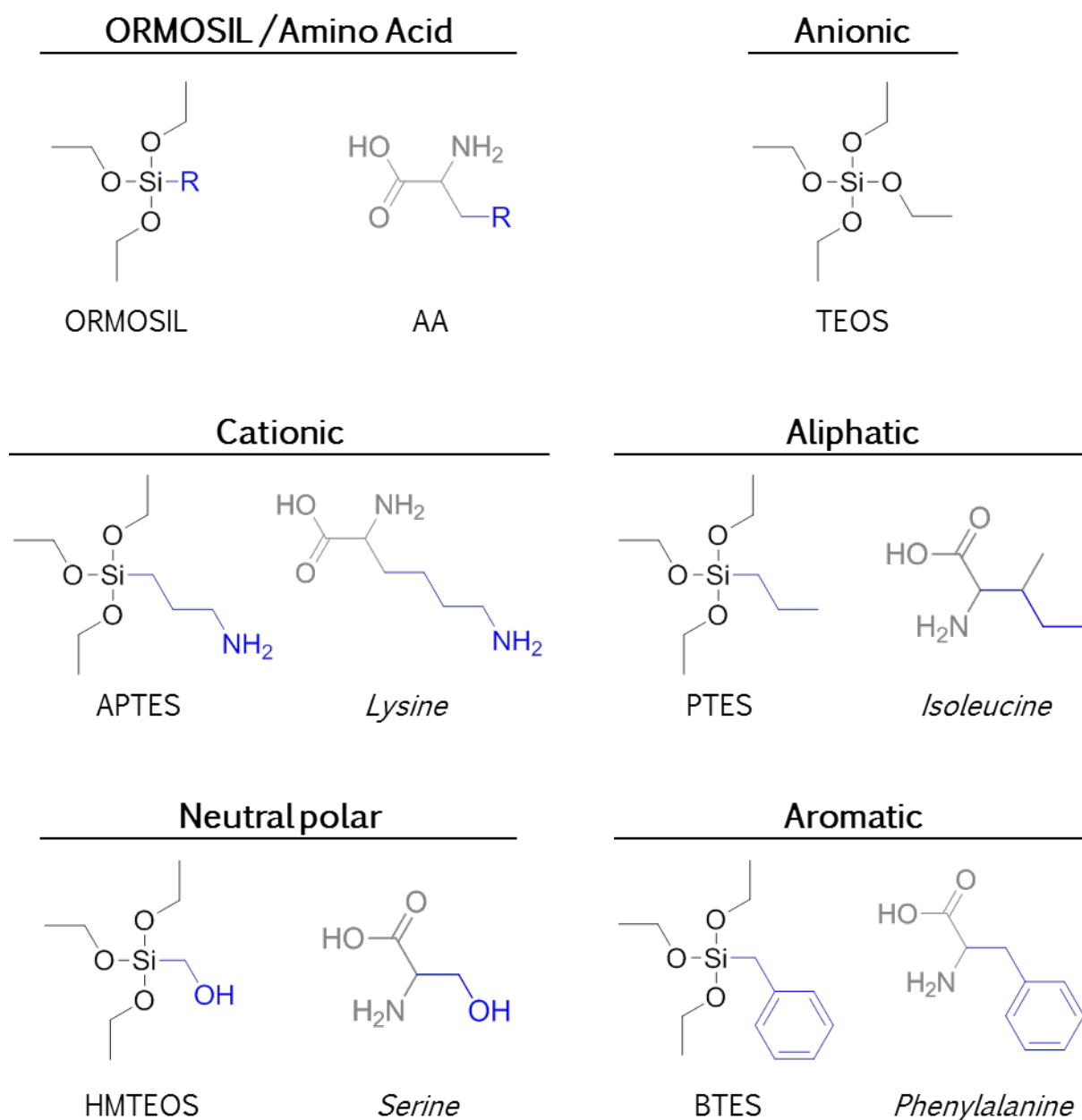


**Figure 3.5 | Organosilanes used for VIP synthesis.** Organosilanes sharing chemical similarities with lateral chains of amino acids were selected using a protein mimetic approach. ORMOSIL: organically modified silanes; AA: amino acid; TEOS: tetraethyl orthosilicate; APTES: aminopropyltriethoxysilane; PTES: propyltriethoxysilane; HMTEOS: hydroxymethyltriethoxysilane; BTES: benzyltriethoxysilane.

It was hypothesized that these building blocks self-assemble at the surface of the virus prior to their covalent incorporation within the recognition layer. This was expected to improve the recognition properties of the VIPs by creating not only a shape, but also a chemical imprint.<sup>20</sup>

The initial virus immobilization step was performed at a constant temperature of 20 °C. Consequently, without performing any particle washing step, TEOS was added. After two hours, the temperature was reduced to 10 °C and the final organosilane mixture was added to the reaction suspension. The addition of TEOS at 20 °C was performed in order to initiate its hydrolysis, thus becoming water-soluble. Thanks to its four hydrolysable ester bonds and thus the possibility of forming four siloxane bonds, TEOS provides structural stability to the growing recognition layer once the organosilanes are added.

Three different organosilane mixtures were assayed for the polycondensation leading to recognition layer growth. A first, simple mixture of APTES and TEOS was used (AT). The corresponding VIPs that are produced using TYMV as a template are called  $VIPs_{AT (TYMV)}$ . Control, non-imprinted particles produced with the same mixture in the absence of template are named  $NIPs_{AT}$ . The second organosilane mixture (OM) includes propyltriethoxysilane (PTES), aminopropyltriethoxysilane (APTES), hydroxymethyltriethoxysilane (HMTEOS) and benzyltriethoxysilane (BTES) (Fig. 3.5). The corresponding VIPs are named  $VIPs_{OM (TYMV)}$ , with the template virus used in brackets, and control, non-imprinted particles are named  $NIPs_{OM}$ . A third, complex organosilane mixture (COM) includes the OM silanes and: isobutyltriethoxysilane (IBTES), n-octyltriethoxysilane (OTES), ureidopropyltriethoxysilane (UPTES), bis(2-hydroxyethyl)-3-aminopropyltriethoxysilane (BHEAPTES) (Fig. 3.10). The corresponding VIPs are called  $VIPs_{COM (TYMV)}$ , with the template virus used in brackets, and the control non-imprinted particles are called  $NIPs_{COM}$ .

## FESEM characterization

Produced particles were characterized by means of field emission scanning electron microscope (FESEM). The ability to acquire high-magnification micrographs (magnification factor of 150,000) allowed the morphological characterization of the produced VIPs and their statistical size analysis, using a particles size measurement software.

### Characterization of the VIPs<sub>AT</sub>

The VIPs produced using APTES and TEOS to grow the recognition layer revealed the presence of open cavities at their surfaces. For a layer thickness of ~8 nm, open cavities showed a diameter of ~18 nm (Fig 3.6).

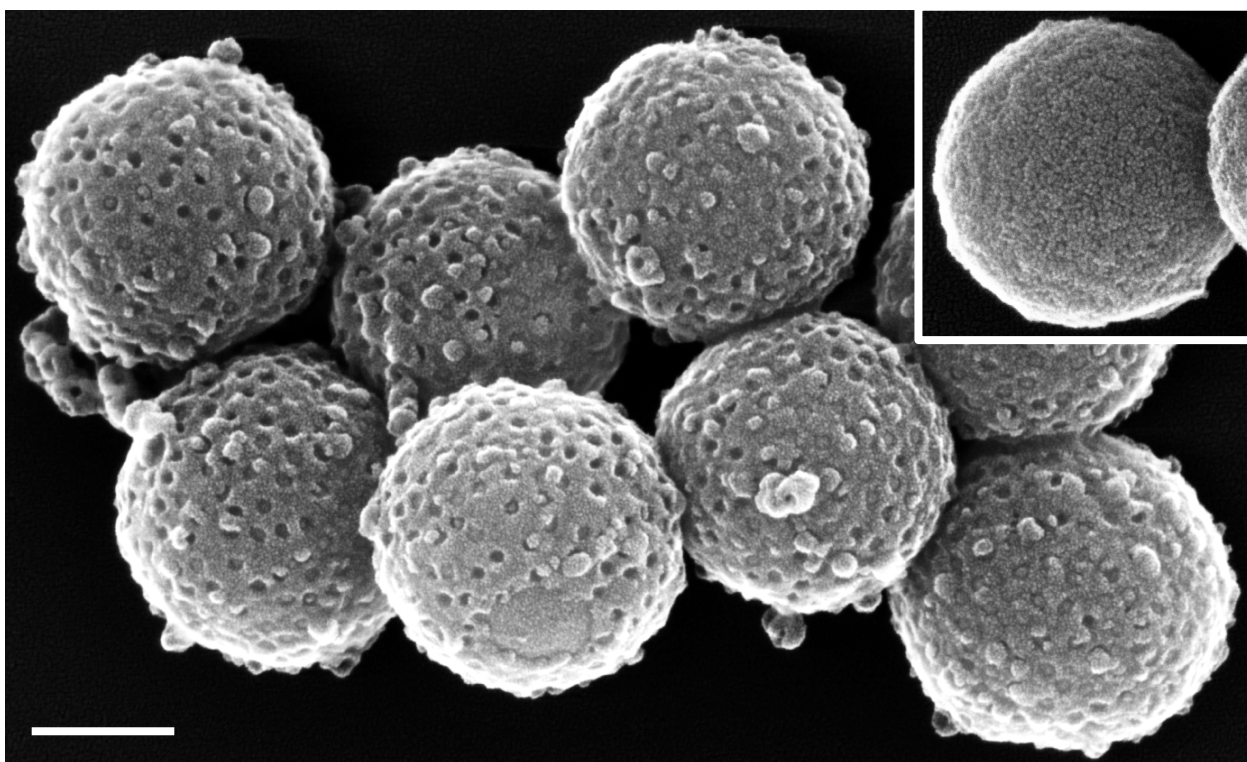


**Figure 3.6** | Scanning electron micrographs of the VIPs<sub>AT</sub>. Representative virus imprinted particle micrographs after recognition layer growth were provided using APTES and TEOS. A sample collected at four hours of polycondensation possesses a recognition layer of 8 nm. The inset on the top, right-hand side shows a single NIP<sub>AT</sub>. Scale bar represents 200 nm.

The diameter of the observed cavities at a layer thickness of 8 nm was compatible with the size of the template virus, at a diameter of 28 nm. Therefore, FESEM visual analysis of the produced particles, also comparing VIP morphology with that of NIPs, clearly suggested that the visualized cavities represented the virus imprints. This crater-like imprint morphology suggests that layer growth was mainly initiated from the surface of the SNPs and was hindered by the virions, resulting in the formation of open imprints. Particles underwent the physical treatment associated with the sample preparation for the FESEM imaging, including desiccation, vacuum, gold-platinum alloy sputter-coating, and impact with high voltage electrons. Such treatment may result in partially damaging the virions before and/or during FESEM imaging. Thus, virions may partially lose their structural integrity.

### Kinetics of VIPs<sub>AT (TYMV)</sub> recognition layer growth

The influence of the monomers that build the recognition layer on the binding performance of the VIPs relative to the template virus was one of the key parameters taken into consideration in this study. In order to characterize the VIPs<sub>AT (TYMV)</sub>, their recognition layer growth kinetics was characterized before performing any binding assay (Fig. 3.7).

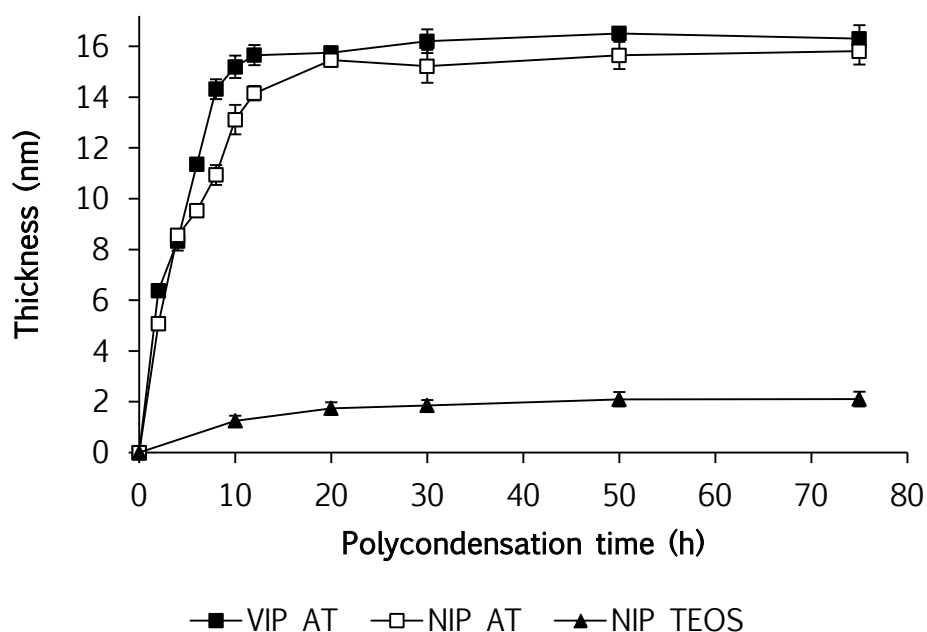


**Figure 3.7** | Kinetics of the recognition layer growth for NIPs<sub>AT</sub> and VIPs<sub>AT (TYMV)</sub>. The thickness of the recognition layer is reported as a function of the polycondensation time for VIPs (solid squares) and NIPs (open squares). Results for NIPs synthesized using only TEOS (solid triangles) are also reported. Each value represents the average value of 100 measurements  $\pm$  the s. e. m.

The recognition layer for these particles reached a thickness of 15 nm in 10 hours of polycondensation. The layer growth kinetics study shows that, when the reaction is carried out with only TEOS, the particles presented a relevant but limited increase in size (Fig. 3.7). Indeed, the thickness of the external layer was 2 nm at the longest incubation time (75 h). The kinetics of VIPs<sub>AT (TYMV)</sub> layer growth was boosted in the presence of APTES. Indeed, it is known that, thanks to its primary amine function, APTES has a catalytic effect on the hydrolysis of

organosilanes, as previously demonstrated for the formation of an organosilica shell on silsesquioxane nanoparticles.<sup>21</sup>

The statistical analysis of the particle size measurement ( $\geq 100$ ) for the VIPs revealed a standard deviation of  $< 15$  nm for particles with a diameter of 445 nm (longest incubation time). The statistical analysis performed on the starting SNPs (more than 100 measurements) revealed a standard deviation of  $< 10$  nm. Therefore, although the polydispersity index was not experimentally measured, the tiny standard deviation increase between the starting SNPs and VIPs suggested that the final VIPs still possessed a high degree of monodispersity. This suggested that the polycondensation was homogeneous for all particles, resulting in homogeneous layer thickness and size of the binding sites.



## Characterization of the VIPs<sub>OM</sub>

Particles produced using the organosilane mixture showed the presence of protuberances at their surfaces (approximately 32 nm in diameter) representing a thin organosilica shell around every virion. The representative FESEM micrograph is shown in Figure 3.8.

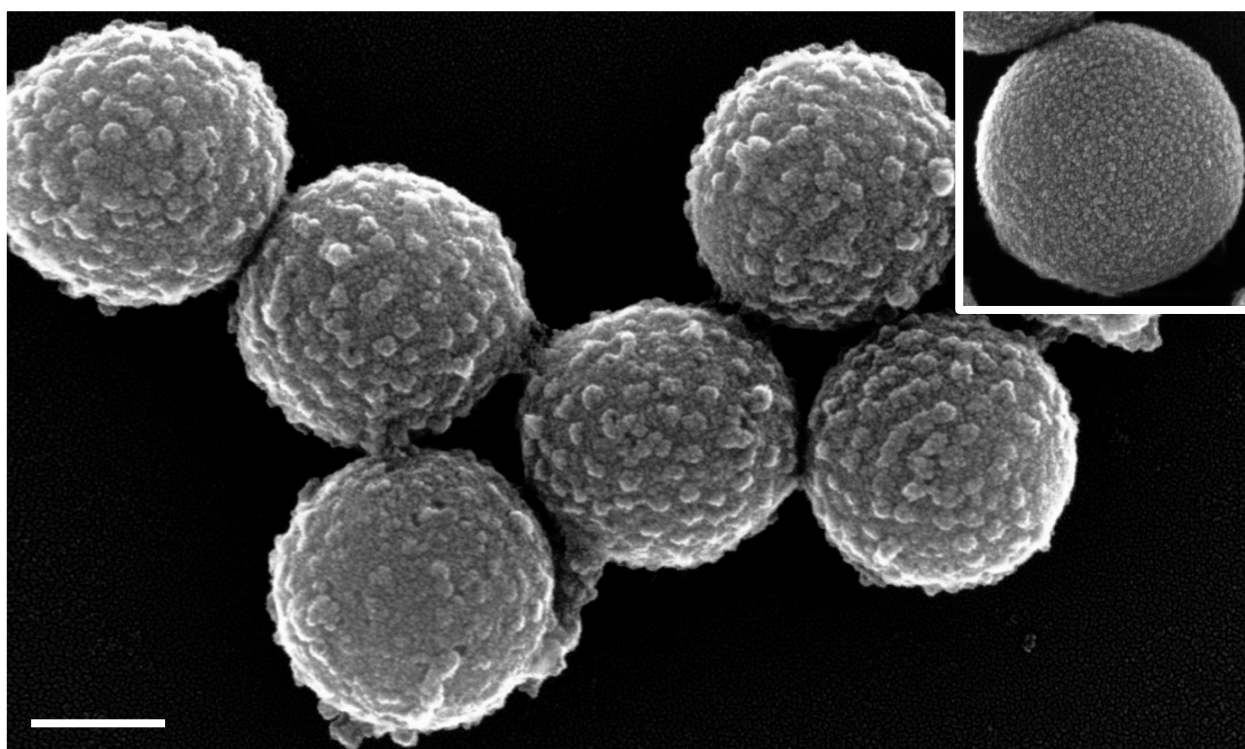


**Figure 3.8** | Scanning electron micrographs of the VIPs<sub>OM</sub>. Representative micrograph of virus imprinted particles after recognition layer growth performed using an organosilane mixture. Sample collected after 25 hours of polycondensation, with an 8 nm recognition layer. The inset on the top right shows an NIP<sub>OM</sub>. Scale bar represents 200 nm.

The presence of protuberances at VIP surfaces suggested that polycondensation started not only at the surface of the SNPs but also at the surface of the virions that act as a template for this reaction. Thus, the selected pool of organosilanes interacted with the viral surface via non-covalent interaction before being incorporated in the recognition layer, resulting in the formation of a thin, organosilane layer ( $\leq 5$  nm) surrounding each virion.

## Kinetics of the VIPs<sub>OM</sub> (TYMV) recognition layer growth

The surface-initiated growth of the recognition layer prepared using the organosilanes mixture (OM) at 10 °C in water showed different kinetics compared with the VIPs<sub>AT</sub> (TYMV). Samples were collected at increasing reaction times and analysed by FESEM and the Olympus particle size measurement software (Fig. 3.9).

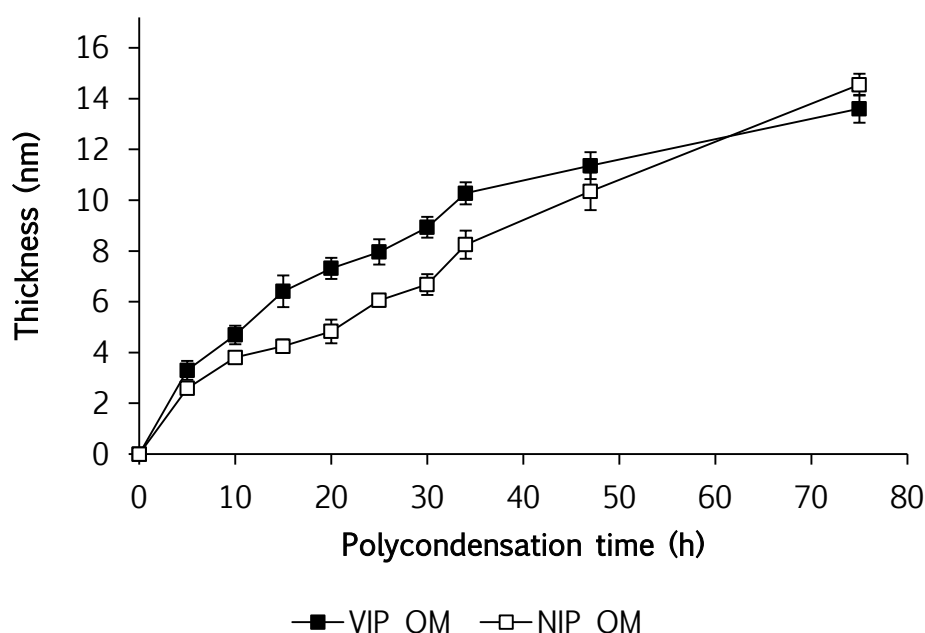


**Figure 3.9** | Kinetics of recognition layer growth for NIPs<sub>OM</sub> and VIPs<sub>OM</sub> (TYMV). The thickness of the recognition layer is reported over polycondensation time for VIPs (solid squares) and NIPs (open squares). Each value represents the average value of 100 measurements  $\pm$  s. e. m.

In the case of the particles prepared with the mixture of organosilanes, the size measurement study reveals a sigmoidal increase reaching an external layer thickness of 14 nm after 75 hours of polycondensation. The slower kinetics as compared with that of the VIPs<sub>AT</sub> may be explained by the lower amount of APTES present in a constant total amount of organosilanes. Indeed, for all the organosilane mixtures assessed, a fixed amount of organosilanes (54  $\mu$ l, 0.233

$\mu\text{mol}$ ) was applied to the SNPs (18 ml, 3.2 mg/ml). In the specific case of APTES, 18- and 9  $\mu\text{l}$  were applied for the AT and OM mixtures, respectively.

### FESEM characterization of the VIPs<sub>COM</sub>

In order to provide additional functionalities to create non-covalent interactions with the viral surface, an even more complex organosilane mixture was assayed. The organosilanes used, in addition to the one depicted in Figure 3.5 (TEOS, APTES, PTES, HMTEOS and BTES), includes: isobutyltriethoxysilane (IBTES), n-octyltriethoxysilane (OTES), ureidopropyltriethoxysilane (UPTES) and bis(2-hydroxyethyl)-3-aminopropyltriethoxysilane (BHEAPTES) (Fig. 3.10).

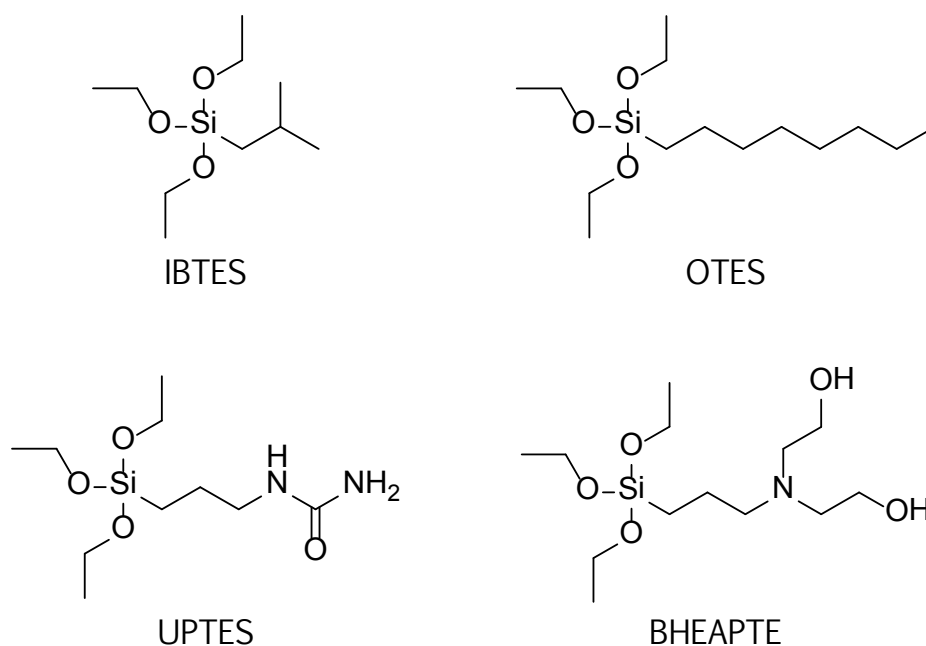


**Figure 3.10 | Additional organosilanes used for the VIPs<sub>COM</sub> synthesis.** Chemical structures of the organosilanes used to increase the complexity of the mixture used to build the VIPs<sub>COM</sub> recognition layer. IBTES: isobutyltriethoxysilane; OTES: n-octyltriethoxysilane; UPTES: ureidopropyltriethoxysilane; BHEAPTES: bis(2-hydroxyethyl)-3-aminopropyltriethoxysilane.

Besides IBTES, which partially mimics the apolar side chain of leucine, other organosilanes were not selected to follow a protein mimetic approach. They

were rather chosen because of their strong H-bond donor/acceptor capabilities (UPTES and BHEAPTES) or for their hydrophobic properties (OTES), finally providing organosilanes that strongly interact with the corresponding chemical functionalities on the virus surface.

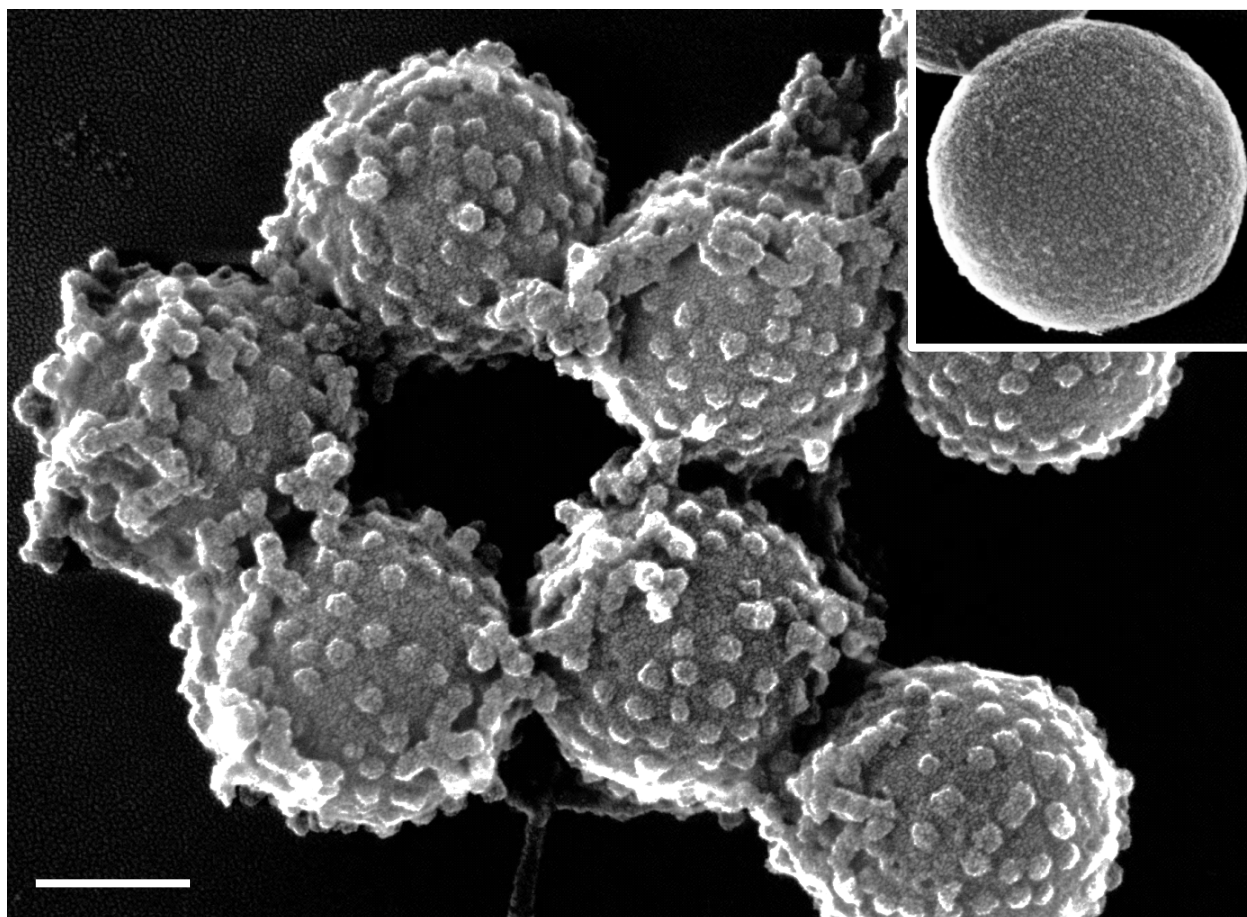


**Figure 3.11** | Scanning electron micrographs of the complex organosilane mixture VIPs. Representative virus imprinted particle micrographs after recognition layer growth performed using a complex organosilane mixture. Sample collected at eight hours of polycondensation with a 9 nm recognition layer. The inset at the top right shows a non-imprinted particle (NIP). Scale bar represents 200 nm.

VIPs<sub>COM (TYMV)</sub> particles possess, as with VIPs<sub>OM</sub>, pronounced protuberances at their surfaces (36 nm). This once again confirmed the robustness of the original hypothesis. Indeed, owing to their H-bond donor/acceptor and hydrophobic character, the supplementary organosilanes (IBTES, OTES, UPTES and BHEAPTES)

added to the mixture provided additional, non-covalent interaction points at the virus surface. Therefore, during the polycondensation, a shell forms around each virion. Furthermore, despite possessing similar recognition layer thickness (9 nm), the sizes of the protuberances were bigger for VIPs<sub>COM</sub> than for VIPs<sub>OM</sub>. This difference may be attributable to the sum of the known APTES catalytic effect and that of the UPTES and the BHEAPTES. Indeed, by extending the APTES catalytic effect concept to the new organosilanes, it could be hypothesized that, owing to the presences of primary, secondary and tertiary amines carried by the additional organosilanes (primary and secondary for UPTES; tertiary for BHEAPTES), the final organosilane mixture may feature increased basic properties. Therefore, an enhanced hydrolysis/condensation effect of the final COM organosilane mixture may be suggested. Additionally, as could be seen from Figures 3.6, 3.8 and 3.11, the number of imprints was reduced in the VIPs<sub>COM</sub> compared to VIPs<sub>AT</sub> and VIPs<sub>OM</sub> (~80 for VIPs<sub>COM</sub> < ~120 for VIPs<sub>AT</sub> and VIPs<sub>OM</sub>). Finally, the FESEM micrographs showed the presence of considerable isolated debris, most probably single virus coated with an organosilane shell, as seen in Figure 3.11. This evidence suggests that the combination of the high affinity organosilanes with basic properties may cause a partial detachment of the viruses from the particle surface during the polycondensation reaction. Indeed, it could be hypothesized that a base-catalyzed hydrolysis of the imine bond anchoring the viruses to the SNPs occurred, thus reducing the number of imprints per particle.

## Kinetics of VIPs<sub>COM (TYMV)</sub> recognition layer growth

The kinetics study of the VIPs<sub>COM (TYMV)</sub> particles was performed by collecting samples at increasing reaction times. Particles size measurement performed on FESEM micrographs are reported in Figure 3.12.

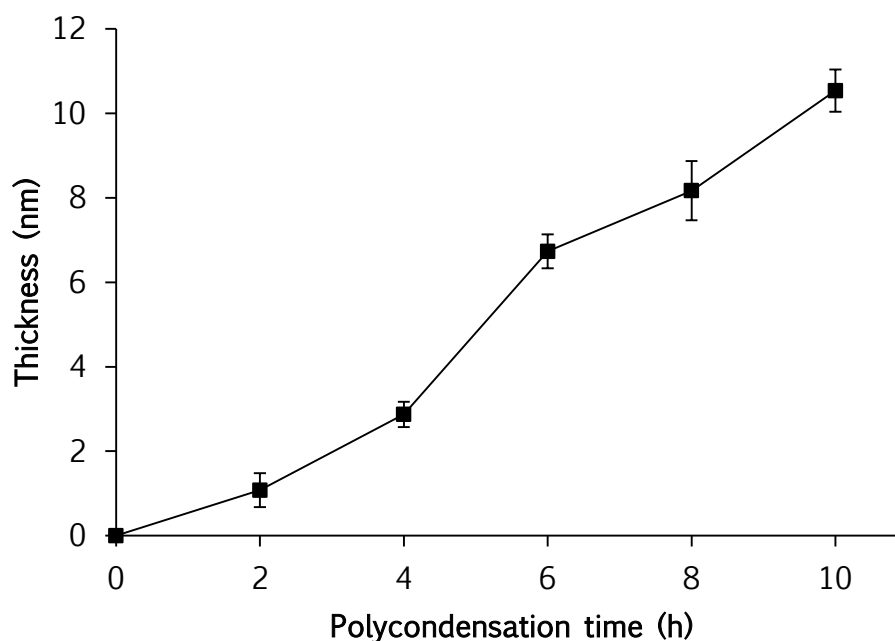


**Figure 3.12** | Kinetics of recognition layer growth for VIPs<sub>COM (TYMV)</sub>. The thickness of the recognition layer is reported as a function of polycondensation time for VIPs (solid squares) and NIPs (open squares). Each value represents the average value of 100 measurements  $\pm$  the standard error.

Size measurement analysis of VIPs<sub>COM (TYMV)</sub> showed a linear increase of the thickness over time, reaching a layer thickness of 11 nm at 10 hours of polycondensation. As already mentioned, the suggested catalytic effect of the UPTES and BHEPTES, together with their strong H-bond donor/acceptor character and the hydrophobic character of IBTES and OTES, strongly favor the growth of a polysilsesquioxane layer around each virion, thus reducing the portion of organosilanes available for recognition layer formation. In addition, as shown in Figure 3.11, a reduced number of viruses were observed at the particle surfaces. Therefore a similar total amount of organosilanes was applied

to a larger, non-imprinted surface, compared to VIPs<sub>AT</sub> and VIPs<sub>OM</sub>. As a consequence of these two phenomena, layer growth kinetics of the VIPs<sub>COM</sub> particles is faster than for the VIPs<sub>OM</sub> particles, but slightly slower than for VIPs<sub>AT</sub> particles.

The VIP method results as reported in this part of the manuscript demonstrate that silica deposition on viruses can be obtained by using a mixture of organosilanes that self-assemble around the native template. In nature, a similar biomineralization effect is governed by a class of enzymes and peptides named silicatein and silaffins, respectively. Silicatein and silaffins are proteins that naturally occur in sponges and diatoms, respectively, and they are responsible for catalyzing/templating the formation of biosilica.<sup>22</sup> Artificially mimicking their activity, in order to encapsulate/protect enzymes in silica, has been reported in a number of research manuscripts.<sup>23,24</sup> The approaches described are mainly based on genetic or chemical modification of the target enzyme in order to introduce the catalytic/template sequences.<sup>23-25</sup> The findings achieved during the VIP method development provide an alternative solution to enzyme protection. Indeed, selecting the organosilanes according to a protein mimetic approach provides a powerful tool that forces the polycondensation to occur principally at the surface of the biological entity, rather than in the aqueous solution, owing to the non-covalent nature of the interactions between the biological entity and organosilane organic functionalities before polycondensation takes place. Moreover, it could be speculated that a balanced organosilane selection based on the amino acid residues of the protein exposed to the solvent would yield a contiguous layer, providing protection against a broad spectrum of chemical, mechanical and biological stresses.

## Virus removal

In order to remove the template viruses from the VIPs, and thus free the newly created imprints, particles were subjected to ultrasonication treatment under acidic conditions in the presence of a minimum amount of surfactant. Ultrasonication was the method of choice in order to break the polysilsesquioxane layer surrounding each virion and to unfold the viral self-assembly. The acidic condition (1 M HCl) was chosen in order to favor the acid-catalyzed hydrolysis of the imine bond anchoring the viruses to the SNPs. Finally, the surfactant (0.1% triton X-100) was included in the removal medium in order to favor viral disassembly. Different, increasing ultrasonication times were tested, ranging from 5 to 60 minutes. Efficient removal of the viruses from the particles, without damaging the non-imprinted surface of the recognition layer, was found to be at 30 minutes. Results are reported in Figure 3.13.

As shown in Figure 3.13, the ultrasonic treatment under acidic conditions allowed virus removal by breaking off the thin shell surrounding each virion without altering the recognition layer. Thus, the final, cleaned particles reveal unoccupied cavities at their surfaces. Indeed, it is evident that the protuberances observed previously were eliminated. Higher magnification of the imprints revealed their hexagonal shape (with an edge length of 11 nm), which originated from that of the template virus (Fig. 3.13d). This finding indicates that the three-dimensional icosahedral architecture of the template virions was preserved under the mild conditions used throughout the full chemical synthesis.



This effect was true for VIPs<sub>AT</sub> and VIPs<sub>OM</sub>, as shown by the FESEM micrographs in Figure 3.13 a – b. The particles produced using the complex organosilane mixture (VIPs<sub>COM</sub>) turned out to be refractory to the removal treatment (Fig. 3.13c). Indeed, even after longer sonication times (up to five hours), the particles still exhibit protuberances at their surfaces.

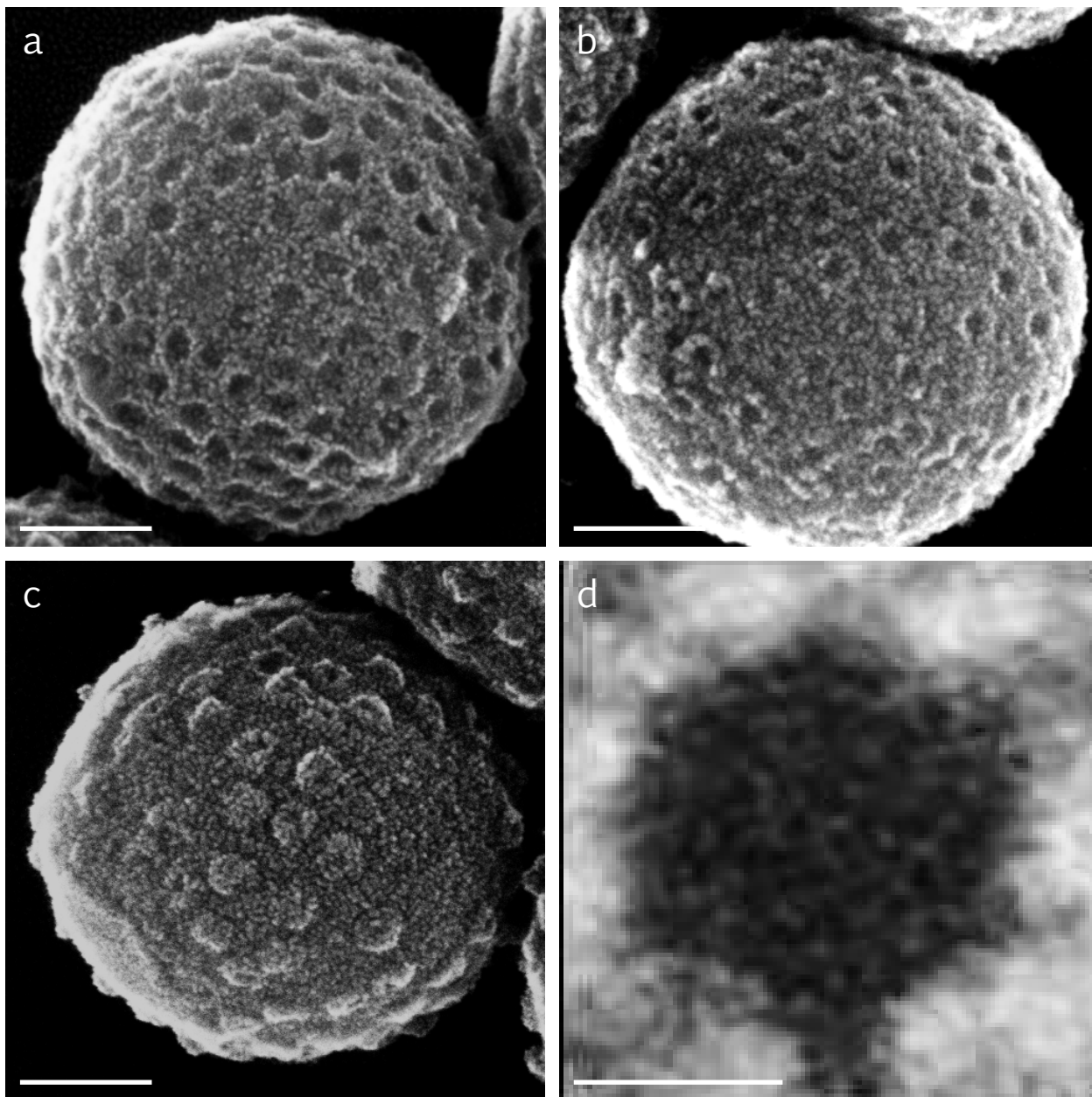


**Figure 3.13** | Scanning electron micrographs of the VIPs after virus removal treatment. (a) VIPs<sub>AT</sub>; (b) VIPs<sub>OM</sub>; (c) VIPs<sub>COM</sub>; (d) High magnification of VIPs<sub>OM</sub> imprint. Scale bar represents: a – c, 100 nm; d, 10 nm.

It could be hypothesized that, owing to the presence of high affinity monomers producing a thick shell around the virions, the stability of the entire organosilane layer (recognition layer and shell around the virions) was increased as compared with the other organosilane mixtures tested (VIPs<sub>AT</sub> and VIPs<sub>OM</sub>). Aside from tuning the sonication time and ultrasonication frequency (high frequency ultrasonication tip rather than ultrasonication bath), no additional tests were performed on these particles. Therefore, the complex organosilane composition was rejected in further binding assay studies.

In relation to the original objectives set at the beginning of the project (Ch. 2), the reported results allow us to answer certain questions:

**Is a surface imprinting strategy consistent with the conditions required to maintain the integrity of the viral morphology, a self-assembled structure of 180 protein subunits?**

**Are organosilane hydrolysis and condensation (*i.e.* polysilsesquioxane deposition) the predominant reactions around the viruses, leading to the formation of the viral replica?**

The first set of findings, reported in this part of the manuscript, clearly showed that the original, surface-initiated organosilane polycondensation hypothesis was confirmed. It was demonstrated that the surface initiated growth of a polysilsesquioxane layer on silica nanoparticles, in water and in the presence of immobilized virus, yielded the intended viral replica at the particle surface. Moreover, high magnification micrographs of the imprints strongly suggest that the developed method was bio-friendly. Indeed, the imprints showed a hexagonal profile, originating from the icosahedral viral morphology. It could thus be assumed that the virions retain their morphology throughout the entire synthesis. Also clearly demonstrated and explained was how the organosilane composition affected the kinetics of recognition layer formation. Despite the slightly acidic

conditions of the reaction mixture (pH 5.8), which favor organosilane hydrolysis, the presence of APTES and/or UPTES and BHEAPTES in the organosilane mixture produced different results: (i) when TEOS only was applied, no relevant polycondensation occurred and no layer growth was observed; (ii) the AT mixture favored growth of the silsesquioxane layer mainly from particle surfaces at the fastest measured kinetics (15 nm in 10 hours); (iii) the OM mixture, in which, together with APTES, other hydrophobic organosilanes were present, favored both layer growth from the SNPs and the viral surface, with slower kinetics compared with the AT mixture (14 nm in 75 hours); (iv) the COM mixture, owing to the extreme variety of organosilanes used, favored the growth of the layer on viral surfaces. The resulting layer growth kinetics was measured to be intermediate between the AT and OM mixture (11 nm in 10 hours).

A series of advantages was noticed to be associated with the developed VIP method over other, existing virus imprinting approaches reported in the literature. Kofinas described a hydrogel-based virus imprinting strategy that requires 9 – 10 days in order to obtain the final, imprinted polymer (cf. virus imprinting, Fig. 1.10, page 33).<sup>26-28</sup> The VIP method noticeably allows a faster synthesis of 2 – 3 days for the imprinted particles, including the template virus removal procedure. In addition, the ability to control the kinetics of layer growth (by tuning the organosilane composition and the polycondensation reaction time) and thus the thickness of the recognition layer allows the fine-tuning of imprint size and shape. Such a feature, which is expected to affect the binding performance of the VIPs, has never been reported in the literature. Indeed, neither Kofinas, with a TMV imprinted hydrogel, nor Dickert, with a soft lithography stamping approach on QCM sensor chips (cf. virus imprinting Fig. 1.9, page 31),<sup>29</sup> reported the possibility of tuning imprint size and shape for a virus imprinted polymer.

## SNPs amino modification and number of imprints

At this stage, together with the organosilane composition, the effect of the initial amino modification of the SNPs with APTES was also investigated. Indeed, the degree of amino modification of the SNPs was expected to affect the number of imprints per particle. In order to provide amine functions on particle surfaces, bare SNPs were treated in water with increasing amounts of APTES (0.13, 0.4, 0.8 and 1.47  $\mu\text{mol}$  of APTES per mg of SNPs) for a constant time (30 minutes). Since the surface amino moieties were the anchoring points used for the virus immobilization (glutaraldehyde cross linking chemistry with amino modified particles and viral lysine residues), the effect of APTES modification was evaluated only on the final VIPs by counting the number of virion imprints per particle. Results are reported in Figure 3.15.

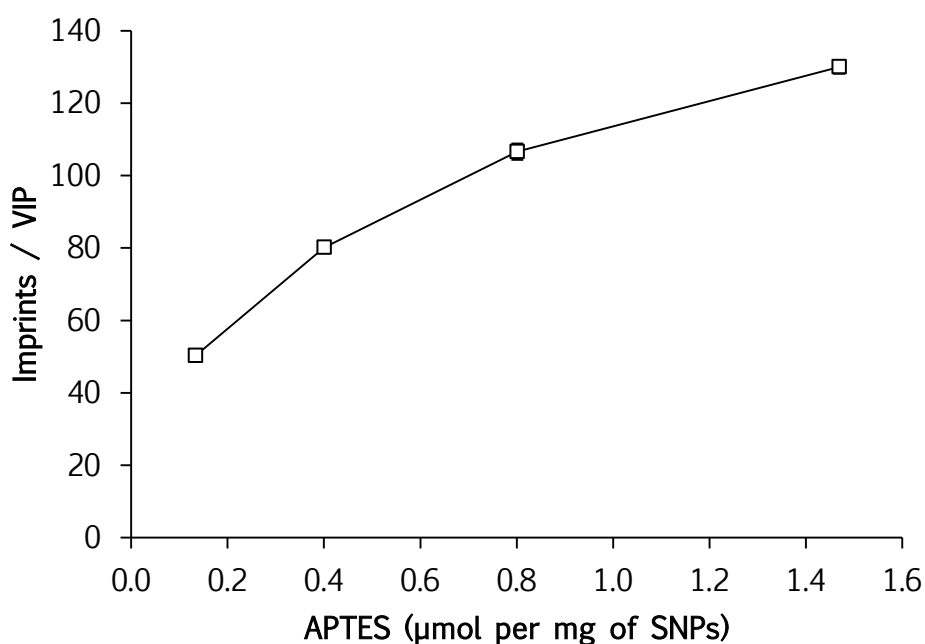


**Figure 3.15** | Number of imprints per VIP as a function of the amount of APTES applied. The density of amino groups at particle surfaces reflects the imprint density per VIP. Four different amounts of APTES were assayed.

From Figure 3.15, it can be seen that there is a clear relationship between the amount of APTES applied and the number of imprints per VIP, ranging from 50 imprints per particle at 0.13  $\mu\text{mol}$  of APTES per mg of SNPs to 130 imprints per particle at 1.47  $\mu\text{mol}$  of APTES per mg of SNPs. Therefore, a low density of amino groups per particle resulted in a low density of imprints per particles after layer growth. The remaining, non-imprinted surface on the VIPs, available for unspecific binding, was thus high at the low APTES concentration used. Opposite effects were observed at higher APTES concentration (*i.e.* lower non-imprinted surface). The density of surface amino groups thus reflected the imprint density per VIP. The best condition used in the already described experiments was the condition that provided the highest number of imprints per particle (1.47  $\mu\text{mol}$  of APTES per mg of SNPs).

## VIPs<sub>OM (TBSV)</sub> characterization and virus removal

In addition to TYMV, the same organosilane mixture (OM) was applied in order to produce VIPs having TBSV as the template virus. Also in this case a thin shell surrounding each virion was observed at the FESEM (Fig. 3.14).

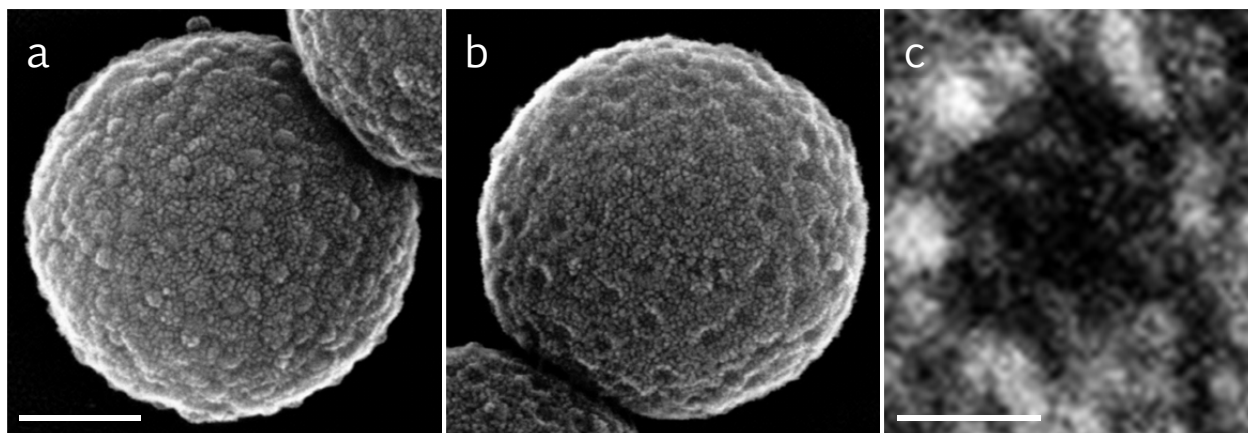


**Figure 3.14** | Scanning electron micrographs of the VIPs<sub>OM (TBSV)</sub>. (a) Particles after layer growth; (b) Particles after virus removal; (c) Imprint high magnification. Scale bar represents: a – b, 100 nm; d, 10 nm.

Compared to the VIPs<sub>OM (TYMV)</sub>, the protuberances observed at particle surfaces are less pronounced, but thick enough to withstand the FESEM sample preparation procedure.

These results confirmed the robustness of the developed method. Indeed, the formulated hypothesis on the non-covalent interaction between organosilane organic moieties and viral surface chemical functionalities was confirmed also using a different template virus, namely the TBSV. As a consequence, imprints of this template virus were also created. Moreover, as shown in Figure 3.14c, the hexagonal profile of the imprint strongly suggests that also the TBSV viral morphology was preserved during recognition layer formation.

## Conclusion

This set of results confirms the possibility of growing, in aqueous conditions, an organosilane layer at the surface of nanoparticles. It confirms that neither the APTES (and glutaraldehyde) crosslinking chemistry modification of the SNPs nor the presence of the virus at the surface of the SNPs hampers this growth. The direct result of the polysilsesquioxane formation, in the presence of the immobilized virus, was the formation of the viral imprints. The use of different organosilane mixtures, which self-assembled at the surface of the virions before their covalent incorporation within the recognition layer, provides different degrees of polycondensation around the virions. Therefore, in the case of a simple mixture (AT), the SNP surface initiated growth was predominant. Increasing the complexity of the organosilane mixtures (OM) yielded a balanced organosilane polycondensation between SNPs and viral surfaces, visualized by FESEM as protuberances on VIP surfaces. The results observed using the complex organosilane mixture (COM), including organosilanes possessing strong H-bond donor/acceptor and hydrophobic character, suggest that the virus surface organosilane polycondensation was predominant. The observed effect was so strong that regular virus removal treatment was not sufficient to break the polysilsesquioxane layer surrounding each virion.

Imprinting of the viruses in the native conformation was a key asset of the developed method. It was demonstrated that tuning the composition of the organosilane mixtures used to grow the recognition layer resulted in the formation of a more or less contiguous polysilsesquioxane layer surrounding each virion. The virus removal procedure and the FESEM image acquisition finally revealed that the viral imprints possessed a hexagonal profile, originating from the icosahedral morphology of the virus. This evidence suggested that not only virus shape imprinting was successfully achieved, but also that the mild synthesis conditions applied preserved the viral particle morphology and

prevented unfolding or denaturation. This evidence was demonstrated to be true for both TYMV and TBSV template viruses.



## References

- 1 Wulff, G. & Sarhan, A. Use of polymers with enzyme-analogous structures for the resolution of racemates. *Angew. Chem., Int. Ed. Engl.* **11**, 341 (1972).
- 2 Arshady, R. & Mosbach, K. Synthesis of substrate-selective polymers by host-guest polymerization. *Makromol. Chem.* **182**, 687-692 (1981).
- 3 Alexander, C. *et al.* Molecular imprinting science and technology: a survey of the literature for the years up to and including 2003. *J. Mol. Recognit.* **19**, 106-180 (2006).
- 4 Cheng, X., Chen, D. & Liu, Y. Mechanisms of Silicon Alkoxide Hydrolysis–Oligomerization Reactions: A DFT Investigation. *ChemPhysChem* **13**, 2392-2404 (2012).
- 5 Cha, J. N. *et al.* Silicatein filaments and subunits from a marine sponge direct the polymerization of silica and silicones in vitro. *Proc. Natl. Acad. Sci. U. S. A.* **96**, 361-365 (1999).
- 6 Cumbo, A., Lorber, B., Corvini, P. F. X., Meier, W. & Shahgaldian, P. A synthetic nanomaterial for virus recognition produced by surface imprinting. *Nat. Commun.* **4**, 1503 (2013).
- 7 Stöber, W., Fink, A. & Bohn, E. Controlled growth of monodisperse silica spheres in the micron size range. *J. Colloid Interface Sci.* **26**, 62-69 (1968).
- 8 Imhof, A. *et al.* Spectroscopy of Fluorescein (FITC) Dyed Colloidal Silica Spheres. *J. Phys. Chem. B* **103**, 1408-1415 (1999).
- 9 Lorber, B., Adrian, M., Witz, J., Erhardt, M. & Harris, J. R. Formation of two-dimensional crystals of icosahedral RNA viruses. *Micron* **39**, 431-446 (2008).
- 10 Carrillo-Tripp, M. *et al.* VIPERdb2: an enhanced and web API enabled relational database for structural virology. *Nucleic Acids Res.* **37**, D436-D442 (2009).
- 11 van Roon, A.-M. M. *et al.* Crystal Structure of an Empty Capsid of Turnip Yellow Mosaic Virus. *J. Mol. Biol.* **341**, 1205-1214 (2004).
- 12 Olson, A. J., Bricogne, G. & Harrison, S. C. Structure of tomato bushy stunt virus IV: The virus particle at 2.9 Å resolution. *J. Mol. Biol.* **171**, 61-93 (1983).
- 13 Caspar, D. L. D. & Klug, A. Physical Principles in the Construction of Regular Viruses. *Cold Spring Harb. Symp. Quant. Biol.* **27**, 1-24 (1962).
- 14 Aznar, M., Luque, A. & Reguera, D. Relevance of capsid structure in the buckling and maturation of spherical viruses. *Phys. Biol.* **9**, 036003/036001-036003/036012 (2012).
- 15 Zandi, R., Reguera, D., Bruinsma, R. F., Gelbart, W. M. & Rudnick, J. Origin of icosahedral symmetry in viruses. *Proc. Natl. Acad. Sci. U. S. A.* **101**, 15556-15560 (2004).
- 16 Wine, Y., Cohen-Hadar, N., Freeman, A. & Frolow, F. Elucidation of the mechanism and end products of glutaraldehyde crosslinking reaction by X-ray structure analysis. *Biotechnol. Bioeng.* **98**, 711-718 (2007).
- 17 del Vado, M. A. G., Echevarría, G. R., Blanco, J. S. & Blanco, F. G. Determination of the rates of formation and hydrolysis of the Schiff bases formed by 5'-deoxyripyridoxal and poly-L-lysine. *J. Mol. Catal. A: Chem.* **118**, 21-26 (1997).
- 18 Keskin, O., Gursoy, A., Ma, B. & Nussinov, R. Principles of Protein–Protein Interactions: What are the Preferred Ways For Proteins To Interact? *Chem. Rev.* **108**, 1225-1244 (2008).
- 19 Clackson, T. & Wells, J. A hot spot of binding energy in a hormone-receptor interface. *Science* **267**, 383-386 (1995).
- 20 Marx, S. & Liron, Z. Molecular Imprinting in Thin Films of Organic–Inorganic Hybrid Sol–Gel and Acrylic Polymers. *Chem. Mater.* **13**, 3624-3630 (2001).
- 21 Kind, L. *et al.* Silsesquioxane/Polyamine Nanoparticle-Templated Formation of Star- Or Raspberry-Like Silica Nanoparticles. *Langmuir* **25**, 7109-7115 (2009).
- 22 Schroder, H. C., Wang, X., Tremel, W., Ushijima, H. & Muller, W. E. G. Biofabrication of biosilica-glass by living organisms. *Nat. Prod. Rep.* **25**, 455-474 (2008).
- 23 Betancor, L. & Luckarift, H. R. Bioinspired enzyme encapsulation for biocatalysis. *Trends Biotechnol.* **26**, 566-572 (2008).

- 24 Luckarift, H. R., Spain, J. C., Naik, R. R. & Stone, M. O. Enzyme immobilization in a biomimetic silica support. *Nat. Biotechnol.* **22**, 211-213 (2004).
- 25 Sanchez, C., Arribart, H. & Giraud Guille, M. M. Biomimetism and bioinspiration as tools for the design of innovative materials and systems. *Nat. Mater.* **4**, 277-288 (2005).
- 26 Bolisay, L. D., Culver, J. N. & Kofinas, P. Molecularly imprinted polymers for tobacco mosaic virus recognition. *Biomaterials* **27**, 4165-4168 (2006).
- 27 Janiak, D. S., Ayyub, O. B. & Kofinas, P. Effects of Charge Density on the Recognition Properties of Molecularly Imprinted Polymeric Hydrogels. *Macromolecules* **42**, 1703-1709 (2009).
- 28 Bolisay, L. D., Culver, J. N. & Kofinas, P. Optimization of Virus Imprinting Methods To Improve Selectivity and Reduce Nonspecific Binding. *Biomacromolecules* **8**, 3893-3899 (2007).
- 29 Hayden, O., Lieberzeit, P. A., Blaas, D. & Dickert, F. L. Artificial Antibodies for Bioanalyte Detection—Sensing Viruses and Proteins. *Adv. Funct. Mater.* **16**, 1269-1278 (2006).

# 4

VIP binding performance

The binding performance of the produced particles was evaluated in an aqueous batch rebinding assay. Fundamentally, the VIPs and control particles – NIPs – were incubated with template and/or non-template virus in well-defined conditions (*i.e.* contact time, buffer, pH, and ionic strength) and, after centrifugation, the unbound portion of virus present in the supernatant was quantified.

## Quantification techniques

Binding assays were performed in the presence of bovine serum albumin (BSA). As with most of the common bioanalytical techniques, BSA was used as the unspecific binding prevention agent.<sup>1,2</sup> Therefore, owing to the presence of BSA, simple and general protein quantification methods (such as UV spectroscopic absorbance, Lowry or Bradford assays)<sup>3</sup> could not be applied to quantify the viruses. Over the entire course of the project, three main techniques that allow the specific quantification of the model viruses were explored:

- (i) Sodium dodecyl sulfate polyacrylamide gel electrophoresis (SDS-PAGE),
- (ii) Quantitative reverse transcription polymerase chain reaction (qRT-PCR),
- (iii) Enzyme-linked immunosorbent assay (ELISA).

### **Sodium dodecyl sulfate polyacrylamide gel electrophoresis (SDS-PAGE)**

SDS-PAGE allows for protein separation based on mass under an electrical field.<sup>4</sup> Indeed, upon binding with the anionic surfactant SDS, proteins are unfolded, forming negatively charged complexes. The amount of SDS bound, and thus the net negative charge of a complex, is directly linked to the length of the polypeptide chain. In an electrical field the negatively charged, unfolded-protein therefore migrates within the polyacrylamide gel matrix toward the anode. Proteins possessing different molecular masses will thereby migrate differently,

thus being separated.<sup>5</sup> After staining, it is possible to visualize and quantify (based on a standard) the migrated proteins. Coomassie G-250 staining is one of the most common staining procedures used to visualize proteins in a gel.<sup>6</sup> The model viruses used to develop the VIP method possess a unique capsid protein (CP), which is self-assembled to form the icosahedral viral capsid (180 copies). The CP of TYMV and TBSV have molecular masses of 20 and 40 kDa, respectively. Thus, it was possible to apply the SDS-PAGE to separate and quantify the viruses (Fig. 4.1).

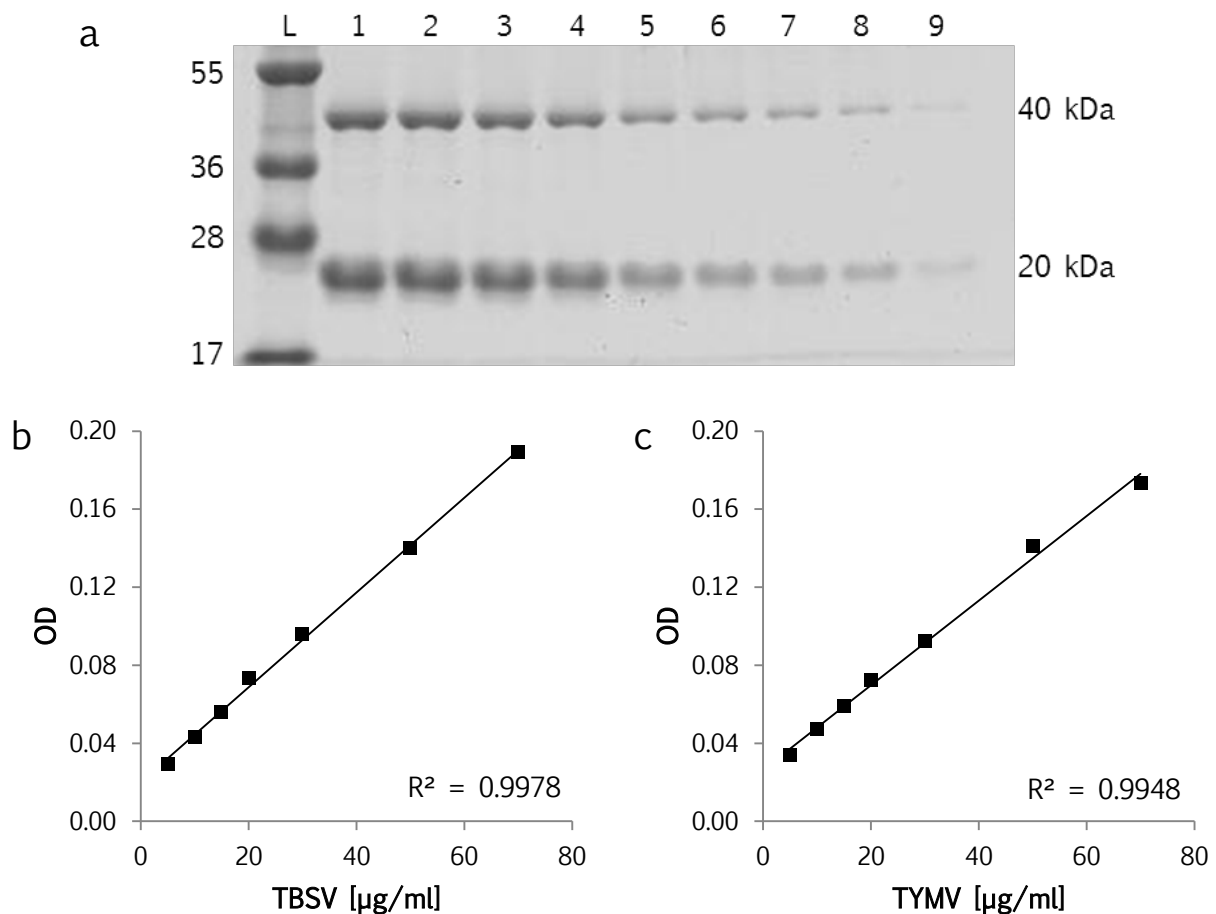


**Figure 4.1 | TBSV and TYMV standard curve determined with SDS-PAGE.** (a) Polyacrylamide gel stained with Coomassie blue. L: ladder, with molecular mass of the standards on the left (in kDa); Virus standard concentrations, from line 1 to 9 (in µg/ml): 100, 90, 70, 50, 30, 20, 15, 10, 5; Capsid protein (CP) molecular mass of TBSV: 40 kDa, TYMV: 20 kDa. (b, c) Charts of the band intensities (optical density, OD) as a function of virus concentration (5 – 70 µg/ml), for TBSV and TYMV, respectively.

By scanning and quantifying the band intensities using a gel densitometer (and the associated software), it was possible to create the standard curves for both viruses. Despite the good fit of the linear interpolation ( $R^2 \geq 0.99$ ), several factors caused us to change the viral quantification method. Indeed, the limit of detection (LOD) of this approach for the model viruses used was found to be 5  $\mu\text{g}/\text{ml}$ . Such high LOD required the use of large amounts of virus in relation to the amount of particles. Owing to the long and tedious SDS-PAGE protocol, in addition to the variability in staining and quantification of the bands, the method turned out not to be suited to high-throughput screening of multiple VIP/virus interaction assay conditions.

### **Quantitative reverse transcription polymerase chain reaction (qRT-PCR)**

qRT-PCR is a detection method based on the amplification of DNA.<sup>7</sup> In the specific case of ss(+)RNA model viruses, an additional step of reverse transcription of the viral RNA into DNA is required (named complementary DNA, cDNA). This step is enzymatically catalyzed (by reverse transcriptase) in the presence of a specific DNA primer (short DNA fragment specifically designed to anneal with the model virus RNA). Once the cDNA is synthesized, it is amplified by a DNA polymerase. The polymerase chain reaction is performed as a result of several specific DNA primers and a series of repeated thermal cycles that allows DNA melting and enzymatically catalyzed replication.<sup>7</sup> In the case of qPCR, an additional fragment of DNA is required in order to follow the exponential increase in the number of DNA copies. This short DNA fragment (20 – 25 mer), named the probe, is designed to hybridize onto the central part of the cDNA fragment to be amplified. The probe is conjugated from one side (3'-OH) to a fluorescent dye molecule, while on the other (5'-OH) to a molecule that quenches the fluorescent light emitted by the dye, named the quencher. Basically, thanks to its 5'-3' exonuclease activity, a specific DNA polymerase simultaneously polymerizes the new complementary DNA strand and degrades

the annealed probe. As a result, the dye carried by the probe is no longer quenched, thus emitting a detectable fluorescence signal.<sup>7</sup> Measuring the thermal cycle at which the fluorescent signal goes above the threshold (threshold cycle,  $C_t$ ) allows the calculation of the original number of copies present in the sample.

Specific primers and a probe have been designed for both model viruses in accord with the viral sequence deposited in the NCBI database (National Center for Biotechnology Information, USA). The results of the virion quantification, assessed through qRT-PCR, are reported in Figure 4.2.

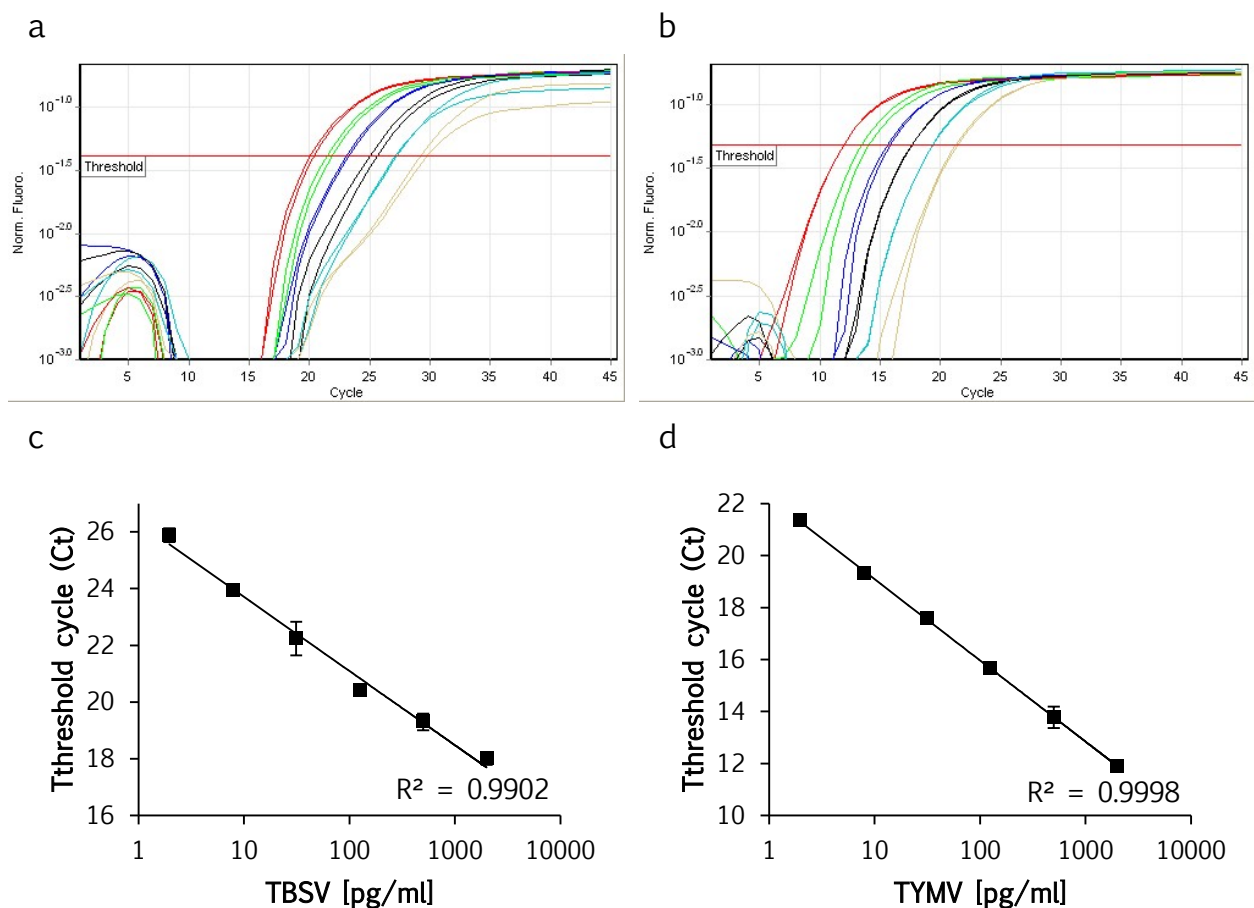


**Figure 4.2 | TBSV and TYMV standard curve determined with qRT-PCR.** Amplification plots showing normalized fluorescence versus the thermal cycles for (a) TBSV and (b) TYMV. Corresponding standard curves showing threshold cycle (CT) versus concentration (pg/ml) for (c) TBSV and (d) TYMV (error bars as s. e. m.).

In order to avoid unpredictable losses of viral RNA due to extraction/purification of the capsid protein encapsulated nucleic acid, the reaction was performed in a single tube, coupling the retro-transcription (cDNA synthesis) with the qPCR. The detection limit of the model viruses was determined by performing cascade dilutions of TBSV and TYMV (See Material and Methods for primers and probe sequences and thermal cycling parameters.). In both cases, a concentration of 2 ng/ml of virus (corresponding to 200 pg/ml of RNA) was subjected to 4-fold serial dilutions. The lowest concentration detectable for TBSV was 7.8 pg/ml, while for TYMV it was 0.4 pg/ml. The differential LOD for the two viruses may be attributed to the different molecular weights of the model viruses ( $9.0 \times 10^3$  kDa for TBSV and  $5.5 \times 10^3$  kDa for TYMV); thus, similar masses of viruses would correspond to more viral RNA copies of TYMV rather than TBSV.

Although standard curves were highly correlated to linear fitting ( $R^2 \geq 0.99$ ), quantification of the viruses after the binding assay was not reproducible. Indeed, when performing the binding assays at such low virus concentrations, phenomena such as adsorption of the virus to the test tubes<sup>8</sup> or dead volumes remaining in the tips while pipetting had a stronger impact on the precision of the measurement. In addition, time-consuming protocols for qRT-PCR prevented us from using this bioanalytical technique as a high-throughput method for virus quantification.



## Enzyme-linked immunosorbent assay (ELISA)

The final bioanalytical technique of choice for viral quantification was ELISA. Based on natural antibody recognition properties and on enzymatically catalyzed amplification of the signal,<sup>9</sup> ELISA allows the quantification of the viral content in a high-throughput fashion and in a reasonable period of time (one day per 96-well plate, including the time needed to perform the binding assays). Among different formats, double antibody sandwich (DAS) ELISA was chosen. Briefly, classical DAS-ELISA includes the adsorption of the primary antibody on the well surface of a 96-well plate, the addition of the analyte-containing samples, and finally the addition of an enzyme-conjugated secondary antibody. Upon addition of substrate, the antibody conjugated enzyme catalyzes the conversion of substrate into a detectable molecule, thus allowing signal measurement.<sup>10</sup> By using a commercial kit, model virus quantification was assessed. Results are reported in Figure 4.3.

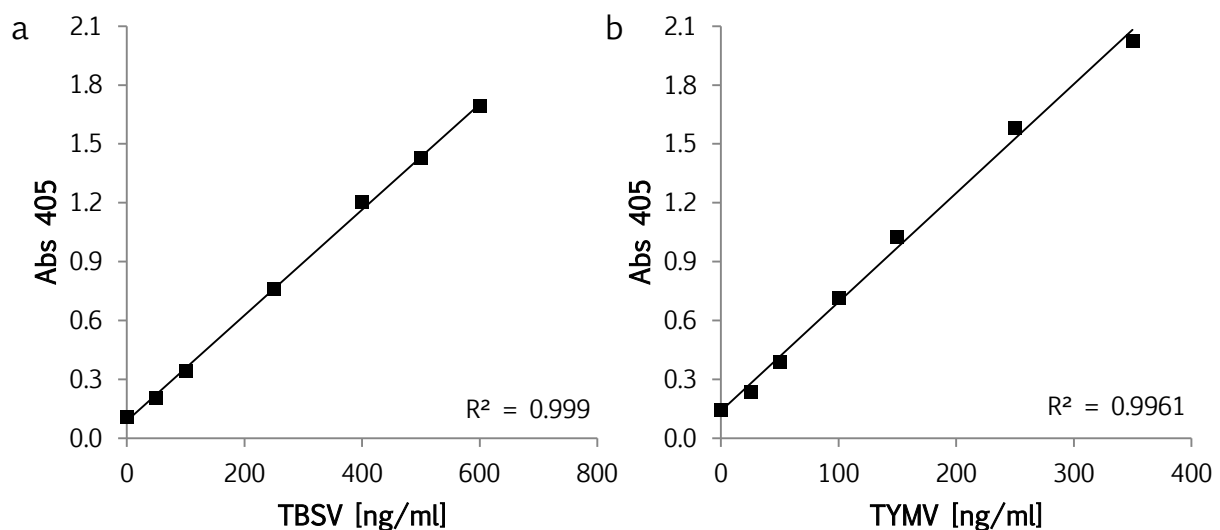


**Figure 4.3** | TBSV and TYMV standard curve determined with ELISA. Linear correlation between the absorbance at 405 nm and different virus concentrations for (a) TBSV and (b) TYMV.

LOD was 50 ng/ml for TBSV and 25 ng/ml for TYMV. The LOD for the model viruses, determined using ELISA, positioned the bioanalytical assay between the

LOD of SDS-PAGE (5 µg/ml) and the qRT-PCR (7.8 pg/ml for TBSV and 0.4 pg/ml for TYMV). Indeed, ELISA was 100 times more sensitive than SDS-PAGE and approximately 5000 times less sensitive than qRT-PCR. In addition, the reproducibility, the straightforward protocol, and the ability to perform the quantification in a high-throughput fashion (96-well plate) made ELISA the method of choice for the quantification of the model viruses used for the development of the VIP surface imprinting approach.

## Batch rebinding assays

The binding performance of the produced particles was studied by carrying out aqueous batch rebinding assays and by quantifying the unbound virus, present in the supernatant, using ELISA. The binding event was influenced by a variety of factors, including the VIP – virus contact time, the thickness, and the composition of the VIP recognition layer, the amount of particles, and the composition of the binding medium. In addition to these parameters, all of the binding assays were performed using the non-template virus and the non-imprinted particles (NIPs) as controls.

## Time course binding assays for VIPs<sub>AT (TYMV)</sub> and VIPs<sub>OM (TYMV)</sub>

The results of the binding experiments performed over time for the particles produced using the AT mixture are reported in Figure 4.4. Viral quantification reveals that VIPs<sub>AT (TYMV)</sub> (100 µg per 120 µl), with an 8 nm thick recognition layer, bound 80% of the TYMV virions in 30 min (starting virus concentration of 65 pM), while binding of TBSV virions was <5%. NIPs<sub>AT</sub> with the same recognition layer thickness bound significantly more TYMV virions (*i.e.* 40% in 30 min) than TBSV virions (5% in 30 min), showing that their binding performance was lower than that of the VIPs<sub>AT (TYMV)</sub> (Fig. 4.4). The difference in TYMV binding between VIPs<sub>AT</sub> and NIPs<sub>AT</sub> evidently originates with the imprinting effect.

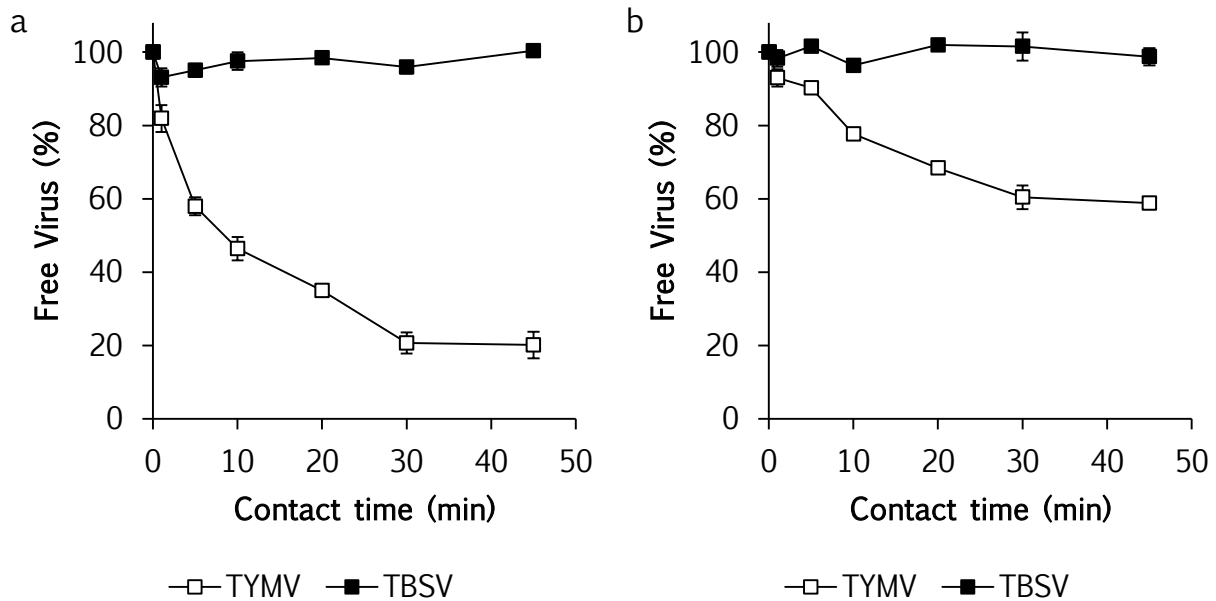


**Figure 4.4 | Time course binding assay of VIP<sub>AT</sub> (TYMV) and NIP<sub>AT</sub> with the template (TYMV) and the non-template (TBSV) virus.** Both (a) VIPs<sub>AT</sub> (TYMV) and (b) NIPs<sub>AT</sub> particles possess a recognition layer 8 nm thick. Samples were collected after 1, 5, 10, 20, 30 and 45 minutes contact time. A solution containing a viral concentration of 65 pM, 10 mM phosphate buffer, 50 mM NaCl and 75 µg/ml of bovine serum albumin (pH of 5.8) was mixed with the particles (834 µg/ml) in a final volume of 120 µl. All values are normalized as percentage of free virus remaining in solution (mean ± s. e. m.).

The binding assays performed with the particles produced by using the OM mixture to grow the recognition layer are reported in Figure 4.5. Under the same binding conditions as VIPs<sub>AT</sub> (TYMV), 8 nm thick VIPs<sub>OM</sub> (TYMV) recognition layer bound as much as 95% of TYMV after 30 minutes. Again under the same conditions, these nanoparticles bound no more than 12% of TBSV after 30 minutes contact time. Additionally, VIPs<sub>OM</sub> (TYMV) bound almost 50% of the initial virus concentration after one minute, in contrast to the VIPs<sub>AT</sub> (TYMV) that bound only 20% of the virus in the same period of time. The binding performance of NIPs<sub>OM</sub> showed that there was a reduction of the unspecific binding for both template and non-template virus. Indeed, after 45 minutes contact time, only 21% and 6% of the template TYMV and non-template TBSV were bound to

these control particles, respectively (Fig. 4.5). These results strongly suggest that the organosilane composition of the recognition layer positively affected both specific and unspecific binding of the produced particles.

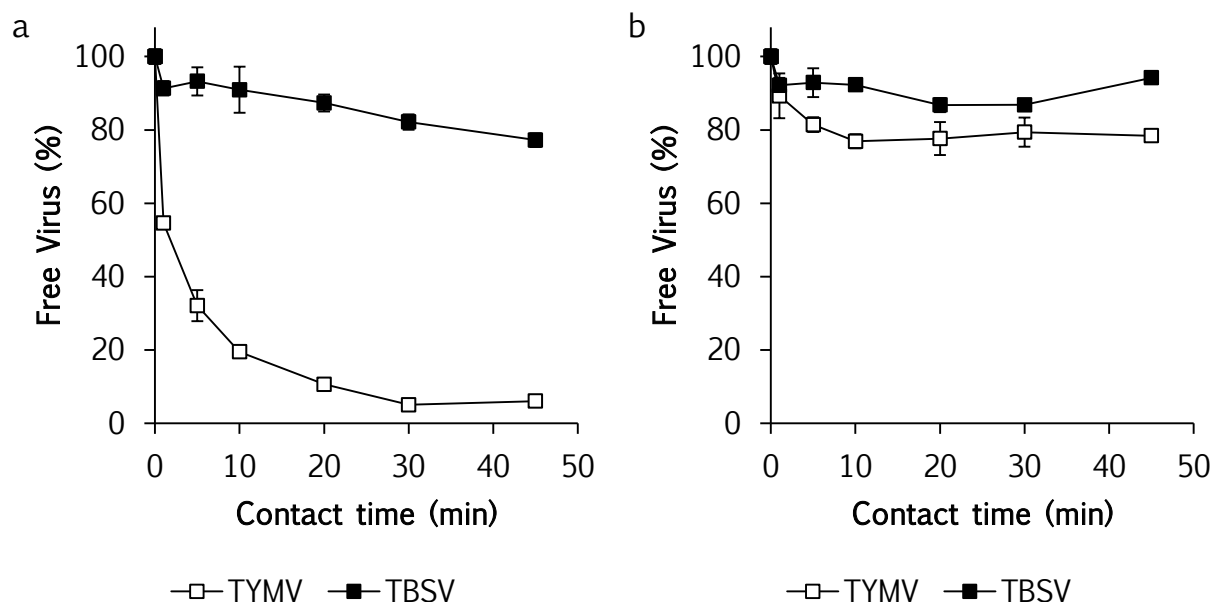


**Figure 4.5 | Time course binding assay for VIPs<sub>OM</sub> (TYMV) and NIPs<sub>OM</sub> with the template (TYMV) and the non-template (TBSV) virus. Both (a) VIPs<sub>OM</sub> (TYMV) and (b) NIPs<sub>OM</sub> particles possess a recognition layer 8 nm thick. Samples were collected after 1, 5, 10, 20, 30 and 45 minutes contact time. A solution containing a viral concentration of 65 pM, 10 mM phosphate buffer, 50 mM NaCl and 75 µg/ml of bovine serum albumin (pH of 5.8) was mixed with the particles (834 µg/ml) in a final volume of 120 µl. All values are normalized in percentage of free virus remaining in solution (mean ± s. e. m.).**

The binding assay results reported in this part of the manuscript allowed us to achieve the initial objectives set at the beginning of the project (Ch. 2):

**Is a surface imprinting strategy consistent with the conditions required to maintain the integrity of the viral morphology, a self-assembled structure of 180 protein subunits?**

Are organosilane hydrolysis and condensation (*i.e.* polysilsesquioxane deposition) around the viruses the predominant reactions leading to the formation of the viral replica?

Does a surface imprinting strategy allow the tuning of the binding performance of a recognition material?

Indeed, these first sets of results clearly suggested that binding and selectivity performance of the produced VIPs were essentially the result of the presence of the virion imprints at the surface of the nanoparticles. Indeed, despite the fact that TYMV adsorbed on NIPs more than did TBSV, the difference between both viruses (pl, shape and size) was too small to explain the strong effect observed with the VIPs. This greater adsorption was true for the particles produced using the AT mixture. Interestingly, the binding assay results for the OM particles revealed the importance of the chemical composition of the recognition layer and supported the original protein mimetic approach hypothesis. The results also suggested that the self-sorting of the organosilanes by immobilized virions was driven by the non-covalent interaction set between the virus amino acid lateral chain functionalities exposed to the solvent and organic groups of organosilanes. As a result, not only was shape imprinting of the virus achieved (shown by the high magnification micrographs of the imprints, Fig. 3.13), but also an organosilane chemical imprinting of the virus. Thus, it was demonstrated that increasing the organosilane composition complexity (OM compared to AT mixture) was beneficial for improving the binding performance of the VIPs, resulting in increased specificity and reduced unspecific binding.

Bolisay *et al.* reported a hydrogel-imprinted polymer based on poly(allylamine hydrochloride) targeting the rod shape tobacco mosaic virus.<sup>11</sup> It was demonstrated that the imprinted polymer bound 50% more virus than the non-imprinted polymer, and that the control virus (icosahedral morphology; tobacco necrosis virus) bound to both imprinted and non-imprinted polymer to the same

extent. Our synthetic strategy allowed the creation of imprinted particles where the difference in binding between VIPs and NIPs was  $\geq 90\%$  (with NIPs binding less than 10% of virus). Moreover, the control virus we used shares important chemical and morphological similarities with the template virus (diameter,  $\rho$ , symmetry), thus increasing the relevance of the selectivity performance of the particles.

### Recognition layer thickness effect on VIP binding performance

In addition to the effect of recognition layer composition and contact time, the effect of the thickness of the polysilsesquioxane layer on the binding performance of the particles was studied. Indeed, it was hypothesized that the highest number of potential, non-covalent interaction points between hosts and guests (virus and artificial binding sites) could be obtained with thick recognition layer (equal to the viral radius). In contrast, imprints of VIPs possessing thin recognition layers ( $<$  viral radius) have a reduced number of host – guest contact points. Consequently, particles possessing different thicknesses of recognition layers may exhibit different binding behaviors. This hypothesis was verified by producing a series of VIPs with layers of increasing thickness and by testing their binding performances.

The results of the batch rebinding assays for VIPs<sub>AT (TYMV)</sub> particles are reported in Figure 4.6. In order to better discriminate the binding differences between particles possessing a recognition layer differing only by 2 - 3 nm, the particle concentration was lowered to 625  $\mu\text{g/ml}$  (compared to a concentration of 834  $\mu\text{g/ml}$  in the time course experiments). As much as 40% of the TYMV virions were bound to particles (75  $\mu\text{g}$  per 120  $\mu\text{l}$ ) with a recognition layer of 6 nm and 70% to the particles with recognition layers of 8, 11, 14 and 16 nm (Fig. 4.6a). The control NIPs<sub>AT</sub> possessing an increasing thickness of the recognition layer bound neither virus (Fig. 4.6b).

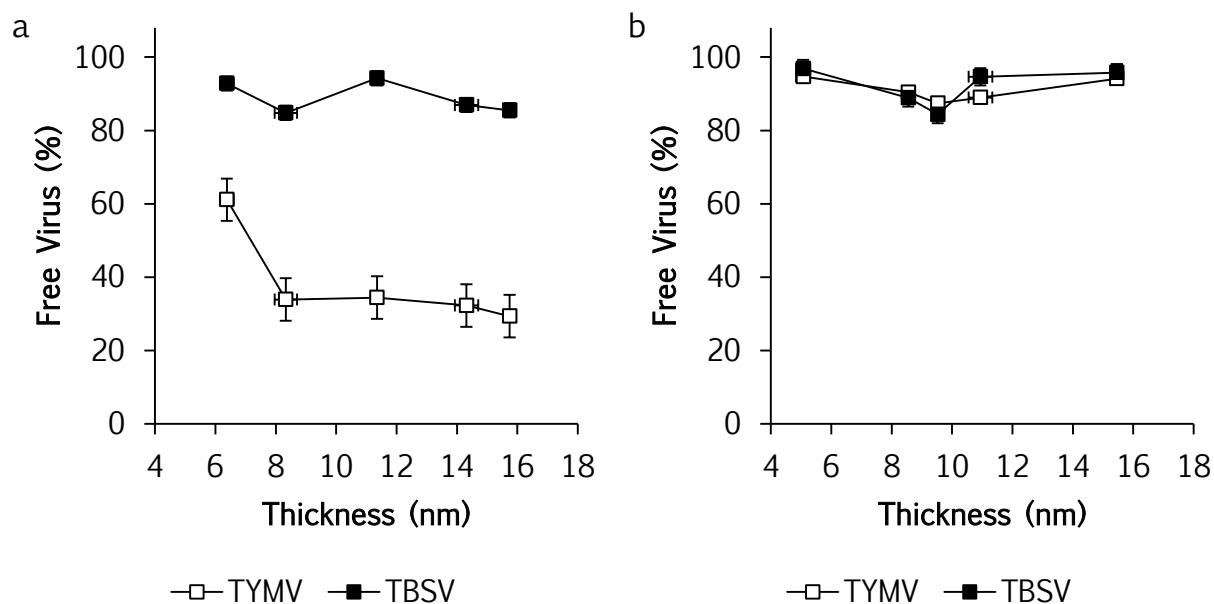


**Figure 4.6** | Recognition layer thickness effect on VIPs<sub>AT (TYMV)</sub> and NIPs<sub>AT</sub> binding performance. Both (a) VIPs<sub>AT (TYMV)</sub> and (b) NIPs<sub>AT</sub> particles exhibit increasing thickness of the recognition layer. Samples were collected after 30 minutes contact time. A solution containing a viral concentration of 65 pM, 10 mM phosphate buffer, 50 mM NaCl and 75 µg/ml of bovine serum albumin (pH of 5.8) was mixed with the particles (625 µg/ml) in a final volume of 120 µl. All values are normalized as percentage of free virus remaining in solution (mean ± s. e. m.).

These results show that VIPs<sub>AT (TYMV)</sub> particles bound specifically to their template, but no major effect of the recognition layer thickness was observed (Fig. 4.6).

When the same kinds of experiments were performed on the particles produced with the organosilane mixture, much more interesting results were observed. The binding assay results for VIPs<sub>OM (TYMV)</sub> (and for NIP<sub>OM</sub>) are reported in Figure 4.7.

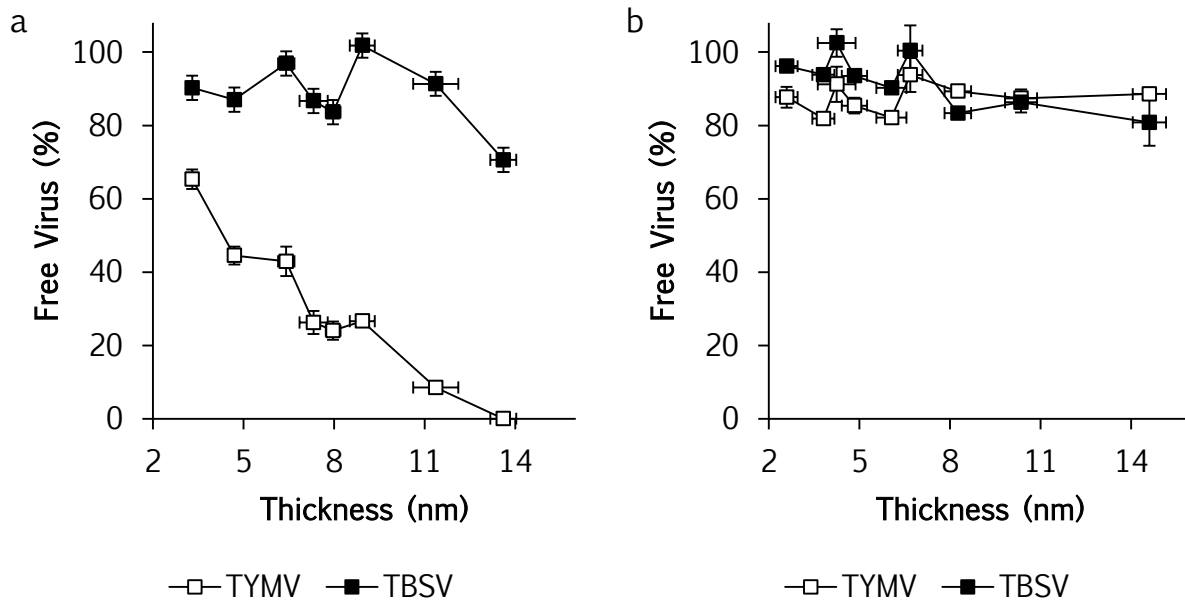


**Figure 4.7 | Recognition layer thickness effect on VIPs<sub>OM</sub> (TYMV) and NIPs<sub>OM</sub> binding performance.** Both (a) VIPs<sub>OM</sub> (TYMV) and (b) NIPs<sub>OM</sub> particles exhibit increasing thickness of the recognition layer. Samples were collected after 30 minutes contact time. A solution containing a viral concentration of 65 pM, 10 mM phosphate buffer, 50 mM NaCl and 75 µg/ml of bovine serum albumin (pH of 5.8) was mixed with the particles (625 µg/ml) in a final volume of 120 µl. All values are normalized as percentage of free virus remaining in solution (mean ± s. e. m.).

The fraction of bound virus was 34% for a layer thickness of 3 nm, 74% for 9 nm and 100% for a layer thickness of 14 nm (Fig. 4.7a). The non-template virus (TBSV) was bound only to a limited extent to particles with thin recognition layers: 10% on 8 nm thick recognition layer particles. Binding of the TBSV on thicker recognition layer particles (14 nm) was 30%. Binding assays performed with NIPs<sub>OM</sub> revealed that, on average, only 10% of each virus was bound to particles possessing increasing thickness of the recognition layer (Fig. 4.7b).

Finally, the influence of the recognition layer thickness on the binding performance of the VIPs allows us to reply to the last question of the initial objectives (Ch. 2):



**Does a surface imprinting strategy allow the tuning of the binding performance of a recognition material?**

Once again, these results not only confirmed that the produced VIPs possess selective recognition properties for the template virus at different thickness of the recognition layer, but that the thickness of the recognition layer has a relevant effect on the affinity of the VIP for its template virus. Indeed, a clear correlation between the amounts of bound template virus and the  $VIP_{S_{OM}} (TYMV)$  recognition layer thickness was shown. These results confirm the possibility of tuning the affinity of the VIP material for its template virus by varying the thickness of the recognition layer.

## Particles concentration effect

The relative ratio of particles to virus in the binding assays was also assessed. Basically, particle concentrations were changed while the virus concentration was kept constant. The virus concentration was indeed chosen according to the sensitivity of the quantification method (ELISA).

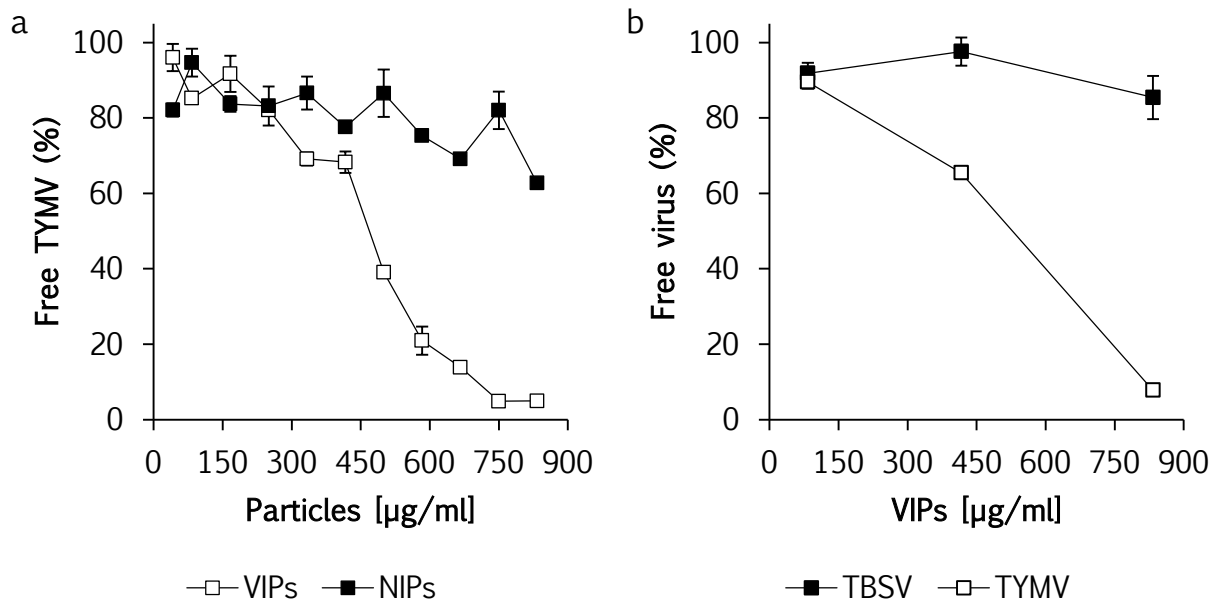


**Figure 4.8 | Particle concentration effect.** Results for  $VIPs_{OM(TYMV)}$  and  $NIPs_{OM}$  with TYMV in (a); Results for  $VIPs_{OM(TYMV)}$  with TYMV and TBSV in (b). The binding assays were performed with particles possessing an 8 nm thick recognition layer in buffer. Samples were collected after 30 minutes contact time. All values are presented normalized as percentage of initial virus concentration (mean  $\pm$  s. e. m.).

Binding assay results are reported in Figure 4.8. The results showed that, in the binding assay conditions, the amount of template virus bound to the  $VIPs_{OM(TYMV)}$  increased with an increase in the particle concentration, reaching saturation at 834  $\mu\text{g/ml}$  (Fig. 4.8a). At this particle concentration, low unspecific binding of TBSV was measured (Fig. 4.8b).

## BSA concentration effect

In immunoassays, an agent preventing unspecific binding is usually applied during antibody – antigen binding. Indeed, without that, no specificity is observed and a high background signal predominates. BSA, non-fat milk, and serum are most often utilized as unspecific binding prevention agents. In contrast to skim milk and serum, which are rather complex matrices, BSA, as pure protein, represents a simple, unspecific binding prevention agent. Thus, BSA was chosen as the unspecific binding prevention agent for the VIP binding assays (Fig. 4.9).

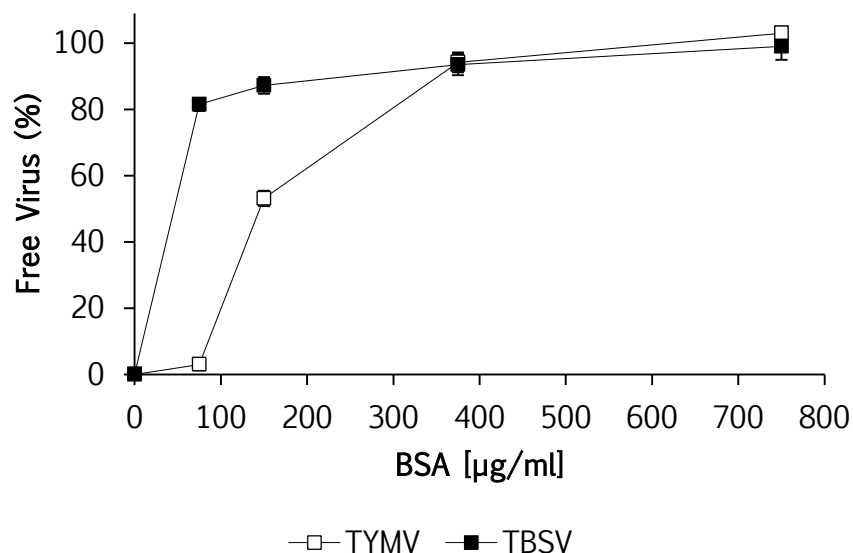


**Figure 4.9 | BSA concentration effect.** Results for VIPs<sub>OM</sub> (TYMV) with TYMV and TBSV at different BSA concentrations. The binding assays were performed with particles possessing an 8 nm thick recognition layer in buffer. Samples were collected after 30 minutes contact time. All values are presented normalized as percentage of initial virus concentration (mean  $\pm$  s. e. m.).

Different BSA concentrations were evaluated in order to study their effects on the specific/unspecific binding performance of the produced particles (Fig. 4.9). The results suggest that, in the absence of BSA, VIPs<sub>OM</sub> (TYMV) were not discriminating between the two viruses, thus binding them equally (100 %). As soon as the BSA concentration was increased, the particles selectively bound the template, still without binding the non-template virus. At higher

concentrations of BSA, no binding was observed for both viruses. Thus, similar to biological systems, VIPs were not able to discriminate between the template and control virus in the absence of a non-specific binding prevention agent (BSA).

### Binding the virus to VIPs: scanning electron microscopy

In order to definitively corroborate the interaction of the template TYMV virions with the  $VIP_{SOM(TYMV)}$  particles, with visual proof of the binding event, a sample was collected after the binding assay and processed for FESEM acquisition (Fig. 4.10).

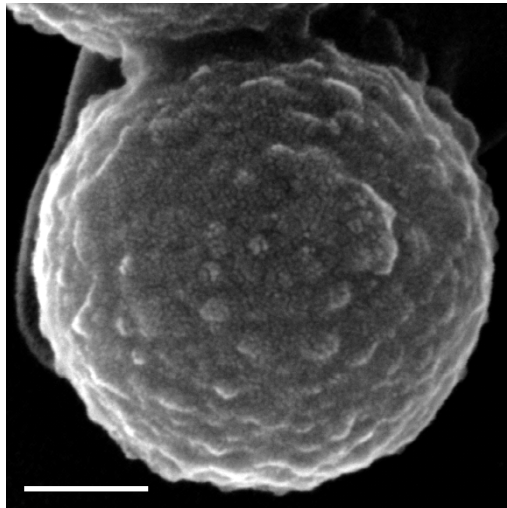


**Figure 4.10** | Scanning electron micrograph of the  $VIP_{SOM(TYMV)}$  after rebinding with the template TYMV virus. The protuberances observed on the VIP surface represent the free viruses rebound to the artificial imprints. The sample was not washed prior the SEM acquisition treatment. Scale bar represents 100 nm.

The micrograph shown in Figure 4.10 suggests that the virions occupy the imprints, as indirectly shown by the binding assay results. Furthermore, the number of protuberances observed on the particle surfaces after the binding assay is consistent with the number of imprints (cf. Fig 3.8).

## Competition assay and matrix effect

The binding performance of the produced particles was challenged by performing competition binding assays in buffer and human serum (HS). HS is the liquid component of blood minus the white and red cells and all of the coagulation factors. It is a complex matrix possessing a high total protein concentration (60 – 85 g/l, predominantly albumin and immunoglobulin), metabolites, hormones, electrolytes and exogenous substances (including drugs, viruses and microorganisms).<sup>12</sup> The results of the competition binding assays are reported in Figure 4.11.

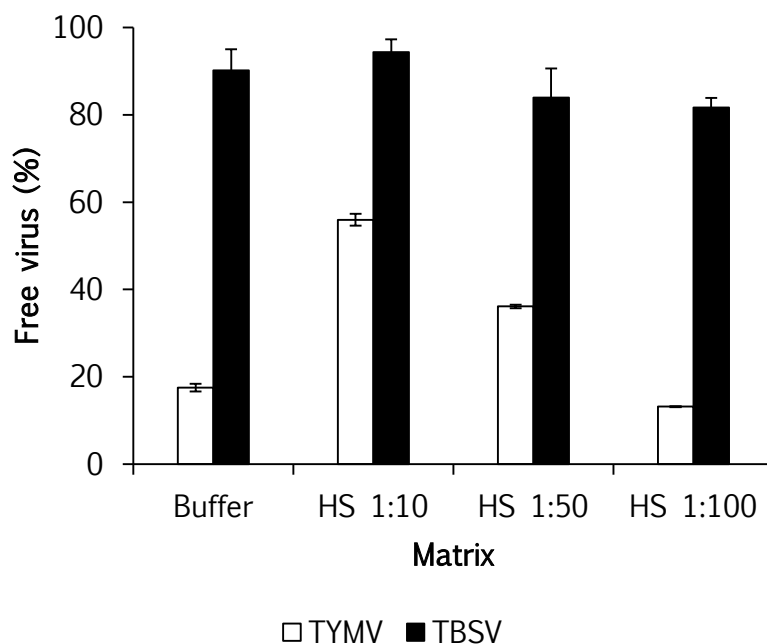


**Figure 4.11 | Competition binding assays in complex matrices.** The competition assays were performed with VIPs<sub>OM</sub> (TYMV) (8 nm thick recognition layer) in buffer containing BSA (75 µg/ml) and in different dilutions of HS (1:10, 1:50 and 1:100). Samples were collected after 30 minutes contact time. All values are presented normalized as percentage of initial virus concentration (mean ± s. e. m.).

The results of the ELISA test showed contradictory responses in the binding assays performed in non-dilute HS. Actually, no signal was produced or detected using the ELISA kit. Most likely, the primary and secondary antibodies did not bind the virus in a non-dilute HS complex matrix, owing to the abundant protein

content. Consequently, VIP binding performance in non-dilute HS was not evaluated.

The binding assays performed in buffer (Fig. 4.11) revealed that 84% of the template TYMV was bound to VIPs<sub>OM (TYMV)</sub>, while only 10% of the non-template TBSV was bound to the particles. The competition assays performed in dilute HS revealed that VIPs<sub>OM (TYMV)</sub> were specifically binding increasing amounts of template at decreasing total concentrations of HS: 45, 64 and 88% of bound template at 1:10, 1:50 and 1:100 HS dilutions, respectively. The binding of the non-template TBSV to the particles was 6, 16, and 18% at 1:10, 1:50 and 1:100 HS dilutions, respectively. These findings corroborated the fact that the produced particles selectively bound the template virus even in the presence of the non-template one. Moreover, it was possible to confirm that the VIPs<sub>OM (TYMV)</sub> preserved their discriminating capabilities between the two viruses in competition assays performed in a complex matrix, such as HS.

## Proof of principle with VIPs<sub>OM (TBSV)</sub>

In order to prove that the template virus self-sorted the organosilanes and drove the formation of its shape and chemical imprint, TBSV was used as a template (with the organosilane mixture, OM) to produce VIPs<sub>OM (TBSV)</sub>. The particles were assessed for their binding performance in buffer (Fig. 4.12).

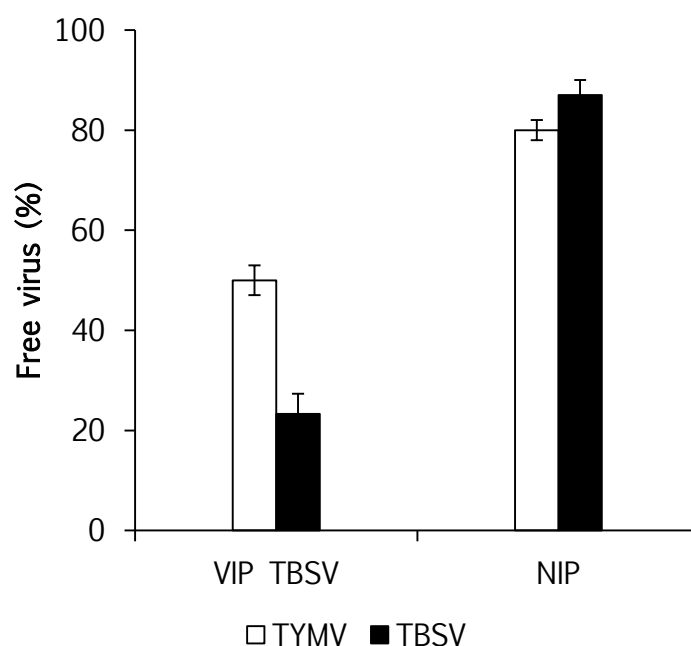


**Figure 4.12 | Binding performance of VIPs<sub>OM (TBSV)</sub>.** The quantity of free virus reported for VIPs<sub>OM (TBSV)</sub> and NIPs<sub>OM</sub> (8 nm thick recognition layer). Samples were collected after 30 minutes contact time. A solution containing a viral concentration of 65 pM, 10 mM phosphate buffer, 50 mM NaCl and 75 µg/ml of BSA (pH of 5.8) was mixed with the particles (834 µg/ml) in a final volume of 120 µl. All values are normalized as percentage of free virus remaining in solution (mean ± s. e. m.).

The results showed that the VIPs<sub>OM (TBSV)</sub> discriminated between the template and non-templates viruses. In the binding condition, VIPs<sub>OM (TBSV)</sub> bound almost 80% of the template virus (TBSV) and 50% of the non-template virus (TYMV). In the same conditions, NIPs<sub>OM</sub> bound 13% of the template virus (TBSV) and 20% of

the non-template virus (TYMV). Despite the high unspecific binding of TYMV, the preferential binding of the TBSV to  $VIP_{s_{OM}} (TBSV)$  proved that the developed method is suitable for different viruses. Nevertheless, a template-dedicated optimization of the organosilane mixture used to grow the recognition layer must be performed in order to provide proper chemical functionalities, as carried by the organosilanes, in order to provide the highest number of non-covalent interactions with the viral amino acid groups exposed to the solvent.

## Conclusion

The findings reported in this chapter of the manuscript clearly show that the produced, imprinted particles selectively recognized the template virus initially used to create the imprints on the VIP surfaces. The binding assays revealed that the recognition layer composition affected the binding performance of the produced particles, thus supporting the hypothesis of organosilane chemical imprinting. Indeed, although the VIPs prepared with the binary mixture of silanes (APTES/TEOS) exhibited a significant selectivity for their template, their binding performance was lower than that of the VIPs prepared with the complex organosilanes mixture (OM).

In our initial hypothesis, we also speculated on the possibility of tuning the affinity of the produced VIPs for its template by tuning the thickness of the recognition layer. This hypothesis was also confirmed by the binding assays, thus introducing an additional parameter in the design of synthetic recognition materials – the tunable affinity. Indeed, the binding assay results of  $VIP_{s_{OM}} (TYMV)$  possessing increasing recognition layer thickness showed a clear correlation with the amount of bound template virus.

Although, the selectivity of the  $VIP_{s_{OM}} (TBSV)$  (using TBSV as template) was not comparable to the  $VIP_{s_{OM}} (TYMV)$ , the binding assay results (together with the FESEM micrographs) showed that the developed method is versatile and suitable



for imprinting a non-enveloped icosahedral virus. Owing to the unique complexity of the chemical functionalities carried by the amino acids exposed to the solvent, a virus-customized organosilane mixture must be considered for every viral template.

The competition binding assays performed in buffer and human serum definitely prove that the produced particles were able to discriminate and bind the template virus in the presence of the non-template virus. Moreover, the binding assay results in HS confirmed the robustness of the VIP binding performance in a complex matrix. However, the results of the binding assay performed at different concentrations of BSA (Fig. 4.9) compared with the one performed in HS (4.11) may appear contradictory. Indeed, at a BSA concentration of 75  $\mu\text{g}/\text{ml}$  more than 95% of the template virus was bound to the particles. Moreover, by increasing the BSA concentration to 375  $\mu\text{g}/\text{ml}$ , less than 10% of the TYMV was bound. The competition binding assays in HS revealed that, at 1:100 HS dilution (600 – 850  $\mu\text{g}/\text{ml}$  total protein concentration), more than 85% of TYMV was bound to the VIPs<sub>OM (TYMV)</sub>. The discrepancy between the amount of virus bound to the particles and the concentration of BSA and HS used in the binding assay may arise from the complex and ill-defined composition of HS. The overall behavior of the various binding assay components in HS is indeed unpredictable. Nevertheless, knowing that human serum albumin (HSA) is one of the major protein components of HS, representing more than 50% of total plasma proteins with a concentration of 35 – 55  $\text{g}/\text{l}$ ,<sup>13</sup> some conclusions can be deduced. Indeed, despite the similar masses of BSA and HSA, with more than an 80% overlap in primary amino acid sequence, it was shown that these two proteins possess slightly different surface sorption behaviors on silica in phosphate buffer. It was indeed shown that BSA sorbs more than HSA on a silica surface, mainly owing to faster HSA desorption.<sup>14,15</sup> Such sorption behavior may justify the differing VIP binding performances in BSA and HS.

## References

- 1 Mahmudi-Azer, S., Lacy, P., Bablitz, B. & Moqbel, R. Inhibition of nonspecific binding of fluorescent-labelled antibodies to human eosinophils. *J. Immunol. Methods* **217**, 113-119 (1998).
- 2 Péterfi, Z. & Kocsis, B. Comparison of Blocking Agents for an Elisa for Lps. *J. Immunoassay* **21**, 341-354 (2000).
- 3 Noble, J. E. & Bailey, M. J. A. in *Methods Enzymol.* Vol. Volume 463 (eds R. Burgess Richard & P. Deutscher Murray) 73-95 (Academic Press, 2009).
- 4 Schägger, H. in *Membrane Protein Purification and Crystallization (Second Edition)* (eds Hunte Carola, Jagow Gebhard Von, Gebhard Von Jagow Hermann SchäggerA2 - Carola Hunte, & Schägger Hermann) 85-103 (Academic Press, 2003).
- 5 Smith, B. J. in *Basic Protein and Peptide Protocols Methods in Molecular Biology™* (ed John M. Walker) 23-34 (Humana Press, 1994).
- 6 Neuhoff, V., Stamm, R. & Eibl, H. Clear background and highly sensitive protein staining with Coomassie Blue dyes in polyacrylamide gels: A systematic analysis. *Electrophoresis* **6**, 427-448 (1985).
- 7 Botes, M., Kwaadsteniet, M. & Cloete, T. Application of quantitative PCR for the detection of microorganisms in water. *Anal. Bioanal. Chem.* **405**, 91-108 (2013).
- 8 Suehiro, N., Matsuda, K., Okuda, S. & Natsuaki, T. A simplified method for obtaining plant viral RNA for RT-PCR. *J. Virol. Methods* **125**, 67-73 (2005).
- 9 Crowther, J. R. & Editor. *The ELISA Guidebook, Second Edition. (Methods in Molecular Biology, Volume 516)*. (Springer GmbH, 2009).
- 10 Hornbeck, P. in *Current Protocols in Immunology* (John Wiley & Sons, Inc., 2001).
- 11 Bolisay, L. D., Culver, J. N. & Kofinas, P. Molecularly imprinted polymers for tobacco mosaic virus recognition. *Biomaterials* **27**, 4165-4168 (2006).
- 12 Psychogios, N. *et al.* The Human Serum Metabolome. *PLoS One* **6**, e16957 (2011).
- 13 Quinlan, G. J., Martin, G. S. & Evans, T. W. Albumin: Biochemical properties and therapeutic potential. *Hepatology* **41**, 1211-1219 (2005).
- 14 Kurrat, R., Prenosil, J. E. & Ramsden, J. J. Kinetics of Human and Bovine Serum Albumin Adsorption at Silica–Titania Surfaces. *J. Colloid Interface Sci.* **185**, 1-8 (1997).
- 15 Svensson, O. & Arnebrant, T. Adsorption of serum albumin on silica – The influence of surface cleaning procedures. *J. Colloid Interface Sci.* **344**, 44-47 (2010).

# 5

## Conclusion and future direction

The research work of this PhD thesis allowed the development of a new, synthetic strategy for the design of a nanoparticulate system capable of selective virus recognition. The core of the method is the controlled, surface-initiated growth of a hybrid organic-inorganic polymeric layer (polysilsesquioxane) on silica nanoparticles in the presence of an immobilized template virus. The model viruses used possess simple, non-enveloped icosahedral morphology, which is one of the most diffuse viral morphologies in Nature.

Combining all of the discussed results, as reported in the manuscript, allowed to completely answer the original questions posed in this doctoral research work:

**Are organosilane hydrolysis and condensation (*i.e.* polysilsesquioxane deposition) the predominant reactions around the viruses, leading to the formation of the viral replica?**

A series of organosilanes, mimicking the lateral chains of amino acids and selected according to a protein mimetic approach, were used in order to create the recognition element for the VIPs (recognition layer). Two parameters were found to be crucial in order to achieve full control of the surface-initiated polycondensation: the composition of the organosilanes used to grow the recognition layer and the polycondensation reaction time. FESEM analysis and the particle size measurements of VIPs, produced by using three different organosilane mixtures, revealed that the level of polycondensation around the virions depends on the composition of this mixture. In the case of the simple APTES and TEOS mixture, SNP surface initiated growth was predominant. The use of an organosilane mixture led to a balanced polycondensation between SNPs and the viral surface. FESEM of the VIPs produced by using the complex organosilane mixture showed that virus surface polycondensation was predominant. Finally, the control of the polycondensation time allowed fine-tuning of the thickness of the recognition layer. In all cases, the growth of the polysilsesquioxane layer resulted in the formation of the viral imprints.

**Is a surface imprinting strategy consistent with the conditions required to maintain the integrity of the viral morphology, a self-assembled structure of 180 protein subunits?**

Structural studies of the VIPs after the virus removal procedure revealed that the viral imprints possessed a hexagonal profile, originating from the icosahedral morphology of the virus. Therefore, the mild synthesis conditions that were applied preserved viral particle morphology, preventing drastic unfolding or denaturation and allowing the formation of virus shape imprinting.

**Does a surface imprinting strategy allow the tuning of the binding performance of a recognition material?**

The effect of the recognition layer composition and thickness on the binding performance of the VIPs was evaluated by performing batch rebinding assays. It was demonstrated that VIPs were capable of selectively binding the template virus in the pM range. The different binding performance assessment of the VIPs produced using different organosilane mixtures revealed the importance of the chemical composition of the recognition layer and supported the original protein mimetic approach hypothesis. Indeed, it was demonstrated that increasing organosilane composition complexity was beneficial for improving the binding performance of the VIPs, resulting in increased specificity and reduced unspecific binding. Thus, not only a shape imprinting of the virus, but also organosilane chemical imprinting of the virus was achieved. The binding assay results for VIPs possessing increasing recognition layer thicknesses also validated our initial hypothesis on the possibility of tuning the affinity of the produced VIPs with respect to its template by tuning the thickness of the recognition layer. Indeed, a clear correlation between recognition layer thickness and amount of bound template virus was demonstrated. Finally, competition binding assays performed in buffer and in HS supported the supposition that the produced particles would selectively bind the template virus, even in the presence of the non-template

counterpart. Moreover, it was possible to confirm that the VIPs preserved their abilities to discriminate between the two viruses in competition assays performed in a complex matrix, such as HS.

The relatively simple cross-linking chemistry used, together with the mild polycondensation conditions required to create the viral imprints, lead us to claim that the VIP method is a versatile approach applicable to a large variety of biological templates, ranging from other, non-enveloped icosahedral viruses to mono- and multimeric proteins. The availability of organosilanes possessing organic moieties that mimic the lateral chains of amino acids is an additional asset of the method. Indeed, it is expected that a rational selection of the organosilane mixtures, based on template surface chemical functionalities, would be beneficial in order to produce highly specific artificial binding sites.

The VIP method was developed using a nonpathogenic plant virus. In order to use the VIP nanoparticulate material to detect viruses in a sample closer to practical application (*i.e.* wastewater), a relevant pathogenic virus has to be used as the template. However, to eliminate the biological risks associated with the handling of large amounts of infectious viruses, the use of virus-like particles, or VLPs, could be envisioned. Indeed, VLPs are non-infectious, self-assembled viral capsid protein structures deprived of nucleic acid, and are produced in host organisms (*e.g.* yeast, insect or mammalian cells). Such artificial viruses, possessing the morphology of the original wild-type virus, are available for a large range of relevant viruses present in the environment, including norovirus, adenovirus and hepatitis virus, to name but a few.

The finding reported in this manuscript goes beyond the MIP technology. Indeed, the possibility of controlling the organosilane deposition around a biological template by tuning the organosilane composition is one of the key achievements of this PhD thesis. As already mentioned, such a phenomenon mimics natural silica deposition as catalyzed by silicatein and silaffins. By extension, it could be

hypothesized that other biological templates, including enzymes, could be targeted for the creation of a protective polysilsesquioxane shell. Thus, the ability to artificially encapsulate an enzyme in a contiguous organosilica layer would provide stabilization and protection of the enzymatic activity. Two approaches are envisioned: the formation of a protection layer after enzyme immobilization on SNPs (similar to the VIPs procedure) and a single, enzyme encapsulation, achieved by applying a mixture of organosilanes to the free enzyme solution. These approaches, original from these PhD findings, are currently under investigation in the laboratory in which this doctoral research work was carried out.





# 6

## Experimental method

## Solvents, chemicals and kits

Glycerol, glycine, sodium dodecyl sulfate, tris-HCl, tris-base ammonium persulfate (APS), ammonium hydroxide (28-30 %) and glutaraldehyde (Grade I, 25% in water) were purchased from Sigma-Aldrich (Switzerland). Ethanol (ACS grade) was purchased from J. T. Baker (Switzerland). Nanopure water was obtained (resistivity  $\geq 18 \text{ M}\Omega\cdot\text{cm}$ ) using a Millipore (Switzerland) Synergy device. Acrylamide (40%), Tetramethylethylenediamine (TEMED) and 2-mercaptoethanol were purchased from BioRad (Switzerland). SuperScript® III One-Step RT-PCR System with Platinum®Taq kit was purchased from Invitrogen (USA). The ELISA KITS for TBSV and TYMV were purchased from AC Diagnostics (USA).

## Organosilanes

Tetraethyl orthosilicate (TEOS,  $\geq 99\%$ ), (3-aminopropyl)-triethoxysilane (APTES,  $\geq 98\%$ ), were purchased from Sigma-Aldrich (Switzerland). Hydroxymethyltriethoxysilane (HMTEOS, 50% in ethanol), n-propyltriethoxysilane (PTES, 97%), benzyltriethoxysilane (BTES, 97%), isobutyltriethoxysilane (IBTES, 97%), n-octyltriethoxysilane (OTES, 97%), bis(2-hydroxyethyl)-3-aminopropyltriethoxysilane (BHEAPTES, 62% in ethanol) and ureidopropyltriethoxysilane (UPTES 50% in methanol) were purchased from ABCR (Germany).

## Viruses

Tomato bushy stunt virus (TBSV) and turnip yellow mosaic virus (TYMV) were provided by Dr. Lorber (University of Strasbourg). Viruses have been propagated and purified as reported elsewhere.<sup>1</sup>

## Silica nanoparticle synthesis

Stöber silica nanoparticles (SNPs) were prepared by adapting the procedures described elsewhere,<sup>2,3</sup> as follows. TEOS, ammonium hydroxide and ethanol were equilibrated at 20 °C for one hour in a water bath prior to use. 40 ml of ammonium hydroxide (28 – 30%) and 345 ml of ethanol were mixed in a 1 l round-bottom flask. TEOS (15 ml) was added and the solution kept under magnetic stirring (600 rpm) for 20 hours, at 20 °C. The produced milky suspension was centrifuged (3220 x g for 10 min) and the resulting SNP pellet was re-suspended in ethanol. Consecutive washing cycles were carried out thrice in water. Finally, the SNPs (4 g) were stored at 4 °C prior to further use.

## Virus imprinted particles – VIPs – synthesis

In a typical synthesis experiment, SNPs (3.2 mg/ml) were reacted with APTES (11 µl, 0.047 mmol) for 30 min in water. The amino modification of the SNPs was performed in 20 ml glass vials, under stirring conditions (400 rpm), in a water bath at 20 °C, in a final volume of 18 ml. After washing twice in nanopure water, the particles were incubated for 30 min in 18 ml of an aqueous solution of glutaraldehyde, to a final concentration of 1%, under stirring conditions (400 rpm). After washing twice in nanopure water, the particles were incubated with the appropriate template virus (0.05 mg/ml) for one hour under magnetic stirring (400 rpm). [NB: the SNPs were not washed after virus immobilization to avoid denaturation or unfolding of the viral particle, owing to the mechanical stress associated with centrifugation and resuspension of the SNP pellet]. Successively, TEOS (18 µl, 0.081 mmol) was added for the production of VIP<sub>OM</sub> and VIP<sub>COM</sub>. While for VIP<sub>AT</sub> and VIP<sub>T</sub>, 36 (0.161 mmol) and 54 (0.242 mmol) µl of TEOS, respectively, were added to the reaction mixture. In both cases, the particles were reacted with TEOS for two hours (20 °C, 400 rpm). The temperature was then lowered to 10 °C. For the particles prepared with TEOS (T): No additional silanes were added at this step. For the particles prepared

with APTES and TEOS (AT): APTES (18  $\mu\text{l}$ , 0.077 mmol) was added. For the particles prepared with the organosilane mixture (OM): BTES (9  $\mu\text{l}$ , 0.035 mmol), PTES (9  $\mu\text{l}$ , 0.039 mmol), HMTEOS (18  $\mu\text{l}$ , 0.04 mmol) and APTES (9  $\mu\text{l}$ , 0.038 mmol) were added sequentially. For the particles prepared with the complex organosilane mixture (COM): BTES (6  $\mu\text{l}$ , 0.023 mmol), PTES (6  $\mu\text{l}$ , 0.032 mmol), HMTEOS (12  $\mu\text{l}$ , 0.026 mmol), APTES (6  $\mu\text{l}$ , 0.026 mmol), IBTES (6  $\mu\text{l}$ , 0.024 mmol), OTES (6  $\mu\text{l}$ , 0.02 mmol), BHEAPTES (12  $\mu\text{l}$ , 0.022 mmol) and UPTES (12  $\mu\text{l}$ , 0.021 mmol) were added sequentially.

For the four different types of particles, samples were collected at increasing reaction times, washed twice with nanopure water and stored at 4 °C. All of the washing steps were performed by centrifugation at 3220 x g for 5 min, the pellets were re-suspended by ultrasonic treatment for 2 min (Elmasonic S30H). NIPs were produced in a similar fashion, omitting the virus addition step.

## **Virus removal**

The virus removal treatment consisted of ultrasonication treatment (Elmasonic S30H ultrasonic bath) in an acid condition. Briefly, VIPs were suspended in a solution containing 1 M HCl and 0.01% Triton-X 100 and submitted to an initial ultrasonic treatment of 10 min. Then, under stirring conditions (600 rpm), the VIP suspension was incubated for 30 min at 40 °C. Afterwards, the so-treated VIPs were submitted to an additional ultrasonic treatment for 30 min, washed thrice in nanopure water (centrifugation at 3220 x g for 5 min), freeze-dried and weighed using an ultra-microbalance (Mettler Toledo XP2U). Freeze-dried VIPs were resuspended in a 0.0025% Triton X-100 solution to a final concentration of 20 mg/ml.

## **Scanning electron microscopy**

A Zeiss SUPRA® 40VP scanning electron microscope (Germany) was used for particle imaging. A 2  $\mu\text{l}$  drop of each sample was placed on freshly cleaved

MICA, dried at ambient conditions and sputter-coated with a gold-platinum alloy for 15 s at 10 mA (SC7620 Sputter coater). SEM micrographs were acquired using the InLens mode, with an accelerating voltage of 20 kV.

### **Particles size measurement**

A series of micrographs (approximately 10 per sample, with approx. 10 particles per micrograph) were acquired at a magnification of 150 kX and used to measure particle diameter (~100 measurements) using the Olympus Analysis® software package (Japan).

### **Batch rebinding assay**

The binding assays were performed by mixing the particles (typically at a concentration of 834 µg/ml) with a solution containing a viral concentration of 65 pM, 10 mM phosphate, 50 mM NaCl and 75 µg/ml of bovine serum albumin (pH adjusted to 5.8), in a final volume of 120 µl, in 0.5 ml test tube. The reaction tube was then incubated at 25 °C under shaking at 650 rpm, in a thermomixer (Eppendorf Thermomixer® Comfort). After reaching the desired contact time, the tube was centrifuged (16,100 x g for 1 min) and a volume of 70 µl of the supernatant was collected for virus quantification by means of ELISA.

For the competition binding assay performed in HS, a solution containing the particles (VIPs at a concentration of 834 µg/ml), 10mM sodium phosphate (pH 5.8), 50 mM NaCl and different dilutions of humans serum (1:10, 1:50 and 1:100) was mixed with a solution containing both template and non-template viruses at a concentration of 65 pM, in a final volume of 120 µl, in 0.5 ml test tube. The reaction tube was then incubated at 25 °C under shaking at 650 rpm for 30 min, in the thermomixer. The resulting suspensions were treated and analysed as per the binding assays performed in buffer. The obtained absorbance values were compared with standard curves prepared with a mixture

containing defined amounts of both viruses (in the corresponding HS dilution as per the interaction assay).

### **Sodium dodecyl sulfate polyacrylamide gel electrophoresis (SDS-PAGE)**

Glycine-SDS-PAGE (as described by Laemmli)<sup>4</sup> was performed using 10% polyacrylamide gel in BioRad vertical gel electrophoresis system (Mini-PROTEAN® Tetra Cell). The glass plates were cleaned with 70% ethanol solution before assembling the glass plate sandwich. The resolving gel (375 mM tris-HCl, 0.01% SDS, 10% acrylamide, 0.01% APS and 3 µl TEMED, pH 8.8) was poured in the glass plates sandwich. After polymerization, the stacking gel solution (126 mM tris-HCl, 0.01% SDS, 5% acrylamide, 0.01% APS and 1.5 µl TEMED, pH 6.8) was poured and the comb was inserted. After polymerization of the stacking gel, the comb was removed and the gel placed into the electrophoresis tank and filled with fresh tris-glycine-SDS buffer (250 mM tris base, 1.92 M glycine, 1% SDS). The virus samples were prepared in reduced forms by mixing the samples with a 4X sample buffer (8% SDS, 40% glycerol, 250 mM tris-HCl, 10% β-mercaptoethanol and traces of bromophenol blue, pH 6.8). The mixture was quickly vortexed and then boiled at 95 °C for five minutes. The samples were loaded on polymerized gel and electrophoresis was performed at a constant voltage of 100 V for 90 minutes.

The gel was then stained using a colloidal Coomassie solution (0.08% Coomassie Brilliant Blue G250, 1.6% ortho-phosphoric acid, 8% ammonium sulphate, 20% methanol) as described by Neuhoff.<sup>5</sup> Gels were placed into the colloidal Coomassie solution directly after the SDS-PAGE overnight and destained with distilled water (three changes). Stained gels were scanned using the BioRad densitometer (GS-800™ Calibrated Densitometer). The acquired gel scan was used for protein band quantification using the BioRad Quantity One® 1-D Analysis Software.

## Quantitative reverse transcription polymerase chain reaction (qRT-PCR)

SuperScript® III One-Step RT-PCR System with Platinum®Taq system (USA) was used to perform the viral RNA retro-transcription (cDNA formation) and the subsequent quantitative amplification according to the manufacturer's instruction. Briefly, 5 µl of native virus sample (at different concentrations) were mixed with a solution containing 0.2 µM of each sense and anti-sense PCR primers, 0.1 µM of probe, 1 µl of SuperScript III reverse transcriptase/platinum taq polymerase, 5.25 µl of nanopure water and 12.5 µl the manufacturer 2X buffer, in a final volume of 25 µl. Tubes were then placed in a fluorometric thermocycler (Rotor-Gene 6000, Corbett Research, Australia) to perform qRT-PCR. The initial viral disassembly (viral RNA release) and retro transcription were performed by incubating the tubes at 55 °C for 30 min. The PCR cycling conditions included an initial denaturation of 94 °C for 2 min followed by 45 cycles of 94 °C for 15 s and 60 °C for 45 s.

The PCR primers and probe used for both TYMV and TBSV were designed in agreement with the viral sequence deposited in the NCBI database (National Center for Biotechnology Information, USA). For TYMV, primers and the probe were designed based on the capsid protein gene sequence: sense primer: 5'-TCCACCTCAAGACCAACGTC-3'; anti-sense primer: 5'-CTGGCGACGACTCACTCA TAG-3'; probe: 5'-CTCCCAGTATGACGTCGGTTCCTGC-3', 5' labeled with the YAK dye (yakima yellow). For TBSV, primers and probe were designed based on the RNA polymerase gene: sense primer sequence: 5'-CCACCGACTTGGGTATGATGG-3'; anti-sense primer: 5'-CGAGGTACAATGTGGA ACTTG-3'; probe: 5'-CAGCGGTGCGAACTCCGTA CTTAC-3', 5' labeled with the FAM dye (fluorescein). Signal quantification and raw data analysis were performed using the Rotor Gene 6000 software version 1.7 (Corbett Research, Australia).

## Enzyme-linked immunosorbent assay (ELISA)

The ELISA KITs (double antibody sandwich) for tomato bushy stunt virus (TBSV) and turnip yellow mosaic virus (TYMV) were purchased from AC Diagnostics (USA). The double antibody sandwich ELISA assays were performed following the manufacturer's protocol with minor modifications. Briefly, wells plate were coated with 100  $\mu$ l of 1:200 diluted primary antibodies (in coating buffer: 15 mM sodium carbonate, 35 mM sodium bicarbonate, 0.02% sodium azide, pH 9.6) and incubated overnight at 4 °C. The plates were subsequently washed six times in washing buffer (8 mM disodium hydrogen phosphate, 1.5 mM potassium dihydrogen phosphate, 137 mM NaCl, 2.7 mM potassium chloride, 0.05% Tween-20, pH 7.3) and 100  $\mu$ l of 1:2 diluted sample in 2X sample buffer (8 mM disodium hydrogen phosphate, 1.5 mM potassium dihydrogen phosphate, 137 mM NaCl, 2.7 mM potassium chloride, 0.2% powdered egg albumin, 1% polyvinylpyrrolidone, 10 mM sodium sulfite, 0.02% sodium azide, 1% Tween-20, pH 7.3), were added to the wells. The samples were incubated for 2.5 hours at room temperature. The plates were washed six times in washing buffer. 100  $\mu$ l of 1:200 diluted alkaline phosphatase-conjugated secondary antibodies (8 mM disodium hydrogen phosphate, 1.5 mM potassium dihydrogen phosphate, 137 mM NaCl, 2.7 mM potassium chloride, 0.2% bovine serum albumin, 1% polyvinylpyrrolidone, 0.02% sodium azide, 0.05% Tween-20, pH 7.3) were added to the wells and incubated for 2.5 hours at room temperature. The plates were washed six times in washing buffer. Then, 100  $\mu$ l of 1 mg/ml alkaline phosphatase substrate (p-nitrophenol phosphate; buffer: 10% diethanolamine, 1 mM magnesium chloride, 0.02 % sodium azide, pH 9.8) were added to each well and incubated for 30 minutes. The enzymatic reaction was stopped by adding 50  $\mu$ l of 3M sodium hydroxide to each well. The colorimetric signal was determined by reading the absorbance of the solution contained in each well on a BioTek plate reader Synergy<sup>TM</sup> H1 (USA) at 405 nm. All washes were performed with a BioTek plate-washer ELx50 (USA).



## References

- 1 Lorber, B., Adrian, M., Witz, J., Erhardt, M. & Harris, J. R. Formation of two-dimensional crystals of icosahedral RNA viruses. *Micron* **39**, 431-446 (2008).
- 2 Stöber, W., Fink, A. & Bohn, E. Controlled growth of monodisperse silica spheres in the micron size range. *J. Colloid Interface Sci.* **26**, 62-69 (1968).
- 3 Imhof, A. *et al.* Spectroscopy of Fluorescein (FITC) Dyed Colloidal Silica Spheres. *J. Phys. Chem. B* **103**, 1408-1415 (1999).
- 4 Laemmli, U. K. Cleavage of Structural Proteins during the Assembly of the Head of Bacteriophage T4. *Nature* **227**, 680-685 (1970).
- 5 Neuhoff, V., Stamm, R. & Eibl, H. Clear background and highly sensitive protein staining with Coomassie Blue dyes in polyacrylamide gels: A systematic analysis. *Electrophoresis* **6**, 427-448 (1985).



# 7

## Resume and list of contributions

# CUMBO Alessandro

University of Applied Sciences and Arts Northwestern Switzerland

Institute of Chemistry and Bioanalytics - ICB

Gründenstrasse 40, 4132 Muttenz, Switzerland



## Social Records

---

Address Davidsbodenstrasse 41, 4056 Basel, Switzerland  
Bate of birth October 12<sup>th</sup> 1981  
Place of birth Caltanissetta, Italy  
Email alessandro.cumbo@fhnw.ch

## Education

---

2009 - 2013 PhD fellow. FHNW, ICB, Muttenz, Switzerland.  
2004 - 2007 M.Sc. in biotechnology. University of Palermo, Italy. With a grade of 110 out of 110 and honors (highest possible grade in the Italian system).  
2001 - 2004 B.Sc. in food biotechnology. University of Studies of Palermo, Italy. With a grade of 110 out of 110.

## Professional experiences

---

2009 - 2013 PhD fellow. FHNW, ICB, Muttenz, Switzerland. *"Virus Imprinted Particles"*.  
2011 Co-founder and CSO of INOFEA GmbH, Basel, Switzerland.  
2007 - 2008 Research fellow. University of Lausanne, Département de biologie cellulaire et de morphologie - DBCM, Lausanne, Switzerland. Study on anxiety mice model.  
2005 - 2006 ERASMUS Student. FHNW, ICB, Muttenz, Switzerland. *"Analysis of PIPPin H1° RNA interaction by surface plasmon resonance (SPR)"*.  
2004 Research assistant. Zooprofilactic Experimental Institute of Sicily, Palermo, Italy. *"Leptospirosis: diagnostic method and molecular characterization of leptospira"*.

## Field of expertise

---

Biotechnology, molecular biology, nanotechnology, bioconjugate chemistry, bioassay, microscopy (confocal and scanning electron).

## Publication and patent list

---

Cumbo, A.; Lorber, B.; Corvini, P. F.-X.; Meier, W.; Shahgaldian, P., A synthetic nanomaterial for virus recognition produced by surface imprinting. *Nat. Commun.*, **2013**, DOI: 10.1038/ncomms2529.

Cumbo, A.; Corvini, P. F.-X.; Shahgaldian, P., A novel synthetic virus recognition nanomaterial for diagnostic and environmental applications. *Chimia*, **2013**, 67, 9.

Tauran, Y.; Brioude, A.; Shahgaldian, P.; Cumbo, A.; Kim, B.; Perret, F.; Coleman, A.W.; Montasser, I., Calix-arene silver nanoparticles interactions with surfactants are charge, size and critical micellar concentration dependent. *Chem. Commun.*, **2012**, 48, 9483–9485.

Rullaud, V.; Siragusa, M.; Cumbo, A.; Gygax, D.; Shahgaldian, P., DNA surface coating of calixarene-based nanoparticles: a sequence-dependent binding mechanism. *Chem. Commun.*, **2012**, 48, 12186–12188.

Nault, L.; Cumbo, A.; Pretôt, R. F.; Sciotti, M. A.; Shahgaldian, P., Cell transfection using layer-by-layer (LbL) coated calixarene-based solid lipid nanoparticles (SLNs). *Chem. Commun.*, **2010**, 46, 5581–5583.

Shahgaldian, P.; Correro, M. R.; Corvini, P. F.-X.; Cumbo, A.; Dudal, Y., European Patent, **2013**, EP13178504.0. Biocatalytical composition.

Hommes, G.; Corvini, P. F.-X.; Cumbo, A.; Shahgaldian, P.; Dudal, Y.; European Patent, **2013**, EP13153276.4. Method of producing nanobiocatalysts.

Shahgaldian, P.; Corvini, P. F.-X.; Cumbo, A., European Patent, **2010**, PCT/EP2011065671. Preparation of a molecular recognition element.

## Conferences

---

Cumbo, A.; Lorber, B.; Corvini, P. F.-X.; Meier, W.; Dudal, Y.; Shahgaldian, P., Frontiers in Chemistry, 2013, Yerevan, Armenia. Silica-Based Virus Recognition Nanoparticles: a surface imprinting approach. **Poster presentation.**

Cumbo, A.; Shahgaldian, P., Molecularly imprinted polymers - MIP 2012, 2012, Paris, France. Virus-Imprinted Particles (VIPs): Synthetic nanomaterial for virus recognition produced by surface imprinting. **Oral contribution.**

Cumbo, A.; Shahgaldian, P., Supramolecular Chemistry in Water, 2012, Riccione, Italy. Design of Silica-Based Virus Recognition Nanoparticles. **Oral contribution.**

Cumbo, A.; Corvini, P. F.-X.; Meier, W.; Dudal, Y.; Shahgaldian, P., Affinity 2011, 2011, Tavira, Portugal. Design of Silica-Based Virus Recognition Nanoparticles. **Oral contribution.**

Cumbo, A.; Mittaud, P.; Ackermann, J.; Hen, R.; Hornung, J.-P., Federation of European Neuroscience Societies - FENS, 2008, Geneva, Switzerland. Changes in the dendritic arborisation of CA1 pyramidal neurons in absence of 5-HT1A receptors during development affect a specific intrahippocampal circuit in the mature hippocampus. **Poster presentation.**

## Awards

---

*Travel award* for PhD scientific accomplishments from the Swiss Academy of Sciences/Swiss Chemical Society, 2013, Switzerland.

*Young investigator award* for a poster presented at the Affinity 2011 conference, 2011, Portugal.

## Technical skills

---

### *Molecular biology*

Real time-polymerase chain reaction,  
Cloning and bacterial protein expression/purification,

### *Bioassay*

Enzyme-linked immunosorbent assay,  
Gel electrophoresis and capillary electrophoresis,  
Surface plasmon resonance,  
Amplified fragment length polymorphisms,  
Immunohistochemistry (DAB and fluorescence),  
Fast Protein Liquid Chromatography,

### *Microscopy*

Scanning electron microscopy,  
Confocal microscopy,

### *Chemistry*

Stöber synthesis (silica nanoparticles),  
Chemistry of organosilanes,  
Protein bioconjugate chemistry,

### *Mice Surgery*

Perfusion,  
Brain dissection,  
Brain sectioning (Vibratome, Cryotome).

## Languages

---

Italian (native speaker), English (fluent), French (beginner).

## Notes

---

During the course of the Ph.D. thesis, together with Dr. Y. Dudal, Prof. P. Shahgaldian and Prof. P. Corvini, I have been involved in the creation of a spin-off company that we named INOFEA. The spin-off, with competences in enzyme immobilization and nanomaterials manufacture, aims to the commercialization of a class of materials that find applications in the removal, detection and valorization of undesired compounds present in the environment or in industrial flow streams. The VIP technology developed within the framework of the present doctoral thesis, in addition to two other technologies, represents a product of the INOFEA portfolio.

# 8

## Acknowledgements

Intensive, long term research studies, as represented by my experimental PhD project, implicate the contributions of a number of people, with different levels of involvement and support from each. I extend a "*herzlichen danke*" to them all.

My special thanks go to Prof. Dr. Patrick Shahgaldian. With patience, coherence and farsightedness, Patrick guided, taught and helped me throughout this excellent life experience. I learned a lot from him and I'm especially thankful.

I would like to thank my "doctor father" at the University of Basel, Prof. Dr. Wolfgang Meier, and his research group. I thank him for his support and the freedom he allowed me.

I am thankful to Dr. Bernard Lorber, of the University of Strasbourg, for providing us with large quantities of pure virus samples. Without his contribution, the project would surely have been even more challenging.

I would like to thank also Prof. Dr. Philippe Corvini and his group, including Markus and Erik. I thank him for many scientific discussions and for granting me access to his laboratory facilities and instruments.

I would like to thank also Prof. Dr. Uwe Pieleles and his group, including Theo, Marcus, Jasmin, Lucy and Sina. I thank Uwe for continuously challenging me and constantly being critical toward the small and big achievements reached within the project.

Of course, a special place in these acknowledgments is dedicated to my "Chemical Brothers" (and sisters, as Negar would say!), with whom I spent long days in the last years. I thank them all for giving me the possibility of sharing the moments of joy and frustration, even if they have not always been prone to sharing the frustration! Thanks to Negar, Ludovico, Mohamed, Rita and Vanessa. I would like also to thank the FHNW life sciences bioanalytics department



members, including Peter and Daniela. Special thanks go to Anna Weston for helping me with the quantitative PCR development and for always being available for listening.

Special thanks go to Dr. Yves Dudal. With his charismatic and optimistic personality, he guided me in the start-up creation challenge. Thanks Yves.

The cover figure of the manuscript was coloured by Dr. Martin Oeggerli. He is gratefully acknowledged.

Last but not least, I acknowledge the financial supports from the Swiss Nano Science Institute (SNI), the Swiss Commission for Technology and Innovation (CTI) and the Swiss National Science Foundation (SNSF).

All seen together, this training period, with all the associated experiences, had a positive and relevant impact on my life. I am thankful for all the opportunities I had and I'm convinced that the competencies I gained will be a key asset for my future career.

Muttenz, September 2013

Alessandro Cumbo

